2004

FY2004 Annual Report of the Water Quality Monitoring Project for the Water Quality Protection Program of the Florida Keys National Marine Sanctuary

Joseph N. Boyer
Southeast Environmental Research Center, Florida International University, boyerj@fiu.edu

FY2004 ANNUAL REPORT OF THE WATER QUALITY MONITORING PROJECT

FOR THE WATER QUALITY PROTECTION PROGRAM

OF THE FLORIDA KEYS NATIONAL MARINE SANCTUARY

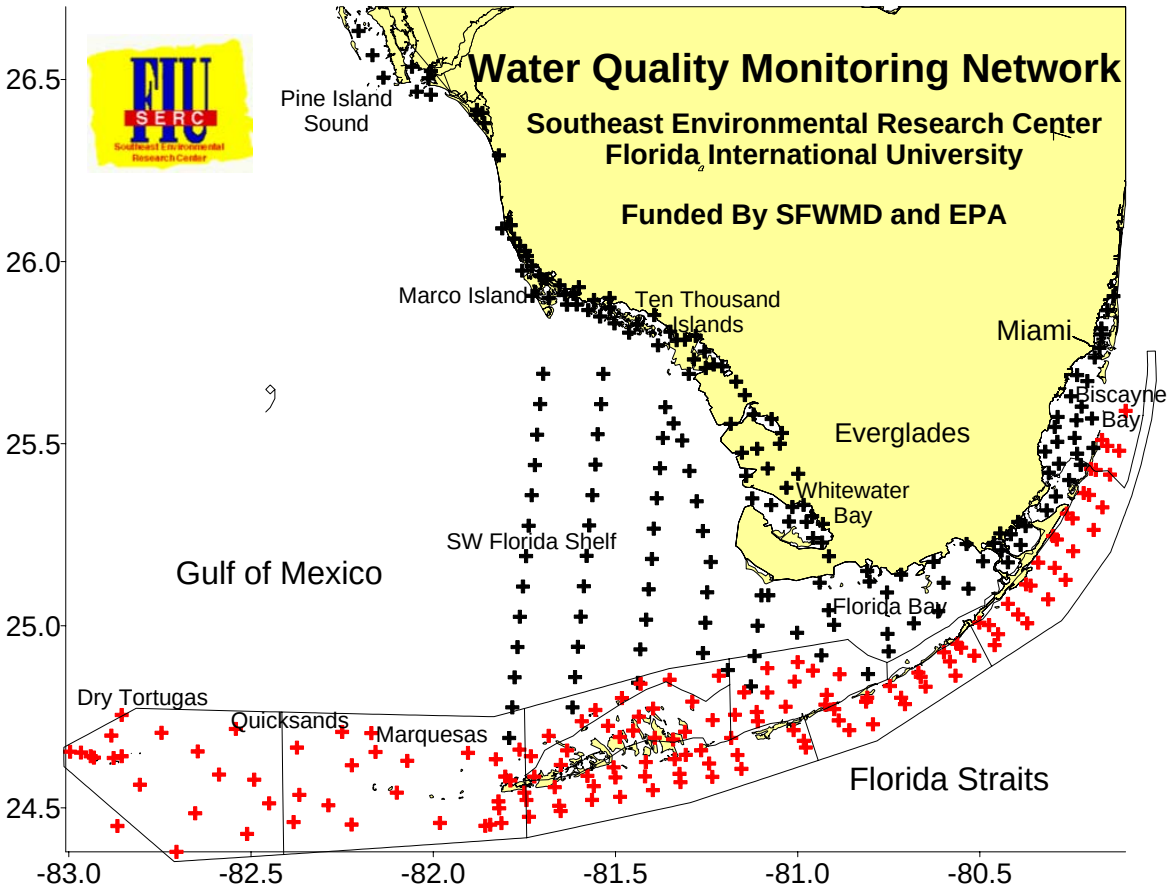

Joseph N. Boyer, Ph.D.

Southeast Environmental Research Center
Florida International University
Miami, FL 33199
http://serc.fiu.edu/wqmnetwork/

FY2004 ANNUAL REPORT OF THE WATER QUALITY MONITORING PROJECT

FOR THE WATER QUALITY PROTECTION PROGRAM

IN THE FLORIDA KEYS NATIONAL MARINE SANCTUARY

Principal Investigator

Joseph N. Boyer, Ph.D.

Southeast Environmental Research Center
Florida International University
Miami, FL 33199
http://serc.fiu.edu/wqmnetwork/

US EPA Agreement #X994621-94-0

This is Technical Report #T-259 of the Southeast Environmental Research Center,
Florida International University.

FY2004 ANNUAL REPORT OF THE WATER QUALITY MONITORING PROJECT FOR THE WATER QUALITY PROTECTION PROGRAM IN THE FLORIDA KEYS NATIONAL MARINE SANCTUARY

Joseph N. Boyer, Ph.D.
Southeast Environmental Research Center
Florida International University

Funded by the Environmental Protection Agency (X994621-94-0)

EXECUTIVE SUMMARY

This report serves as a summary of our efforts to date in the execution of the Water Quality Monitoring Project for the FKNMS as part of the Water Quality Protection Program. The period of record for this report is Mar. 1995 – Sept. 2004 and includes data from 37 quarterly sampling events at 154 stations within the FKNMS including the Dry Tortugas National Park.

Field parameters measured at each station include salinity (practical salinity scale), temperature (ºC), dissolved oxygen (DO, mg l^{-1}), turbidity (NTU), relative fluorescence, and light attenuation (K_d, m^{-1}). Water chemistry variables include the dissolved nutrients nitrate (NO_3^-), nitrite (NO_2^-), ammonium (NH_4^+), dissolved inorganic nitrogen (DIN), and soluble reactive phosphate (SRP). Total unfiltered concentrations of nitrogen (TN), organic nitrogen (TON), organic carbon (TOC), phosphorus (TP), and silicate ($Si(OH)_4$) were also measured. The biological parameters included in the study were chlorophyll *a* (CHLA, μg l^{-1}) and alkaline phosphatase activity (APA, μM h^{-1}).

Several important results have been realized from this monitoring project. First, is documentation of elevated DIN in the inshore waters of the Keys (Fig. 1). This result was evident from out first sampling event in 1995 and continues to be a characteristic of the ecosystem. Interestingly, this gradient was not observed in a comparison transect from the Tortugas. This type of distribution implies an inshore source which is diluted by low nutrient Atlantic Ocean waters. Presence of a similar gradient in TOC and decreased variability in salinity from land to reef also support this concept. There were no trends in either TP or CHLA with distance from land.

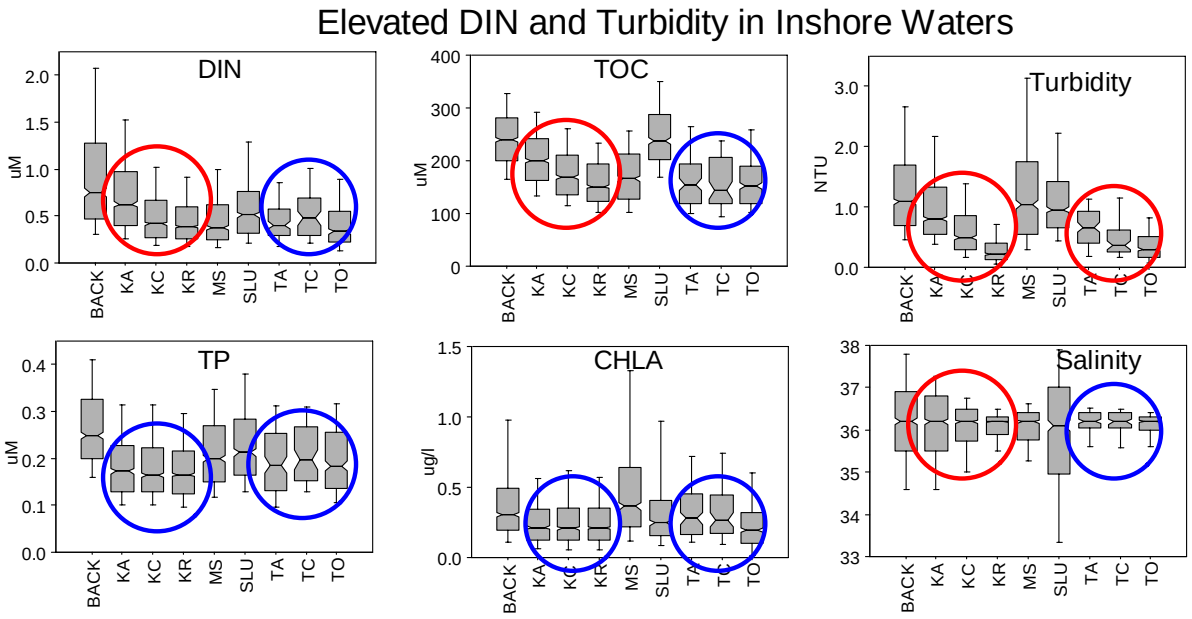

Figure 1.

Another observation is that the Backcountry exhibits elevated levels of DIN, TOC, turbidity, TP, and CHLA. I believe most of these distributions are driven by the SW Florida Shelf waters moving through this area (median DIN = 0.7 µM, TOC = 298 µM, Turbidity = 6.4 NTU, TP = 0.48 µM, and CHLA = 1.6 µg l^{-1}). In addition to Shelf influence, elevated NO_3^- is a regular feature of Backcountry waters, where some of the highest concentrations are observed in non-populated areas (Fig. 2). This is probably the result of the benthic flux of nutrients in this very shallow water column.

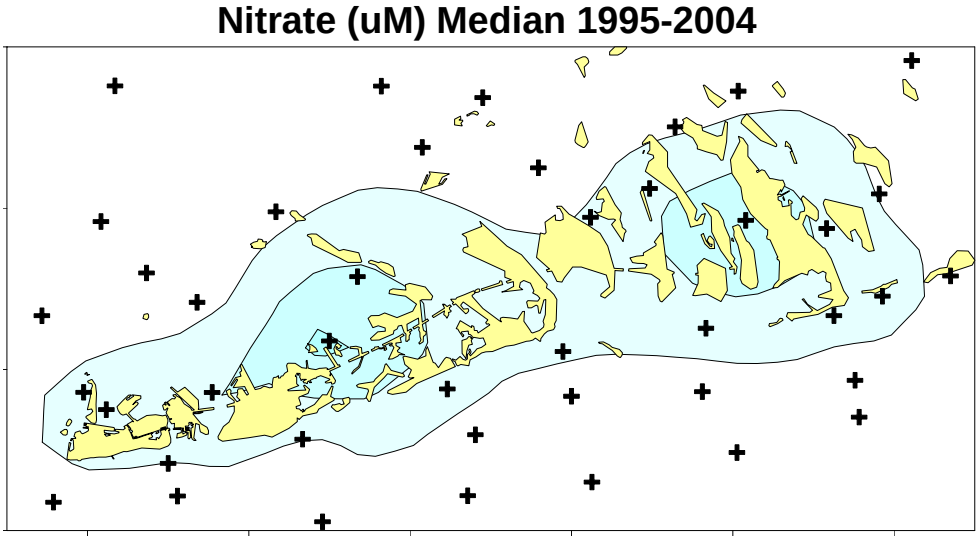

Figure 2.

The third important result is that highest CHLA concentrations occur on the Shelf and show a strong N-S gradient towards the Marquesas and Tortugas (Fig. 3). This is due to higher TP concentrations on the Shelf as a result of southward advection of Gulf of Mexico waters along the coast with entrainment of coastal rivers and runoff.

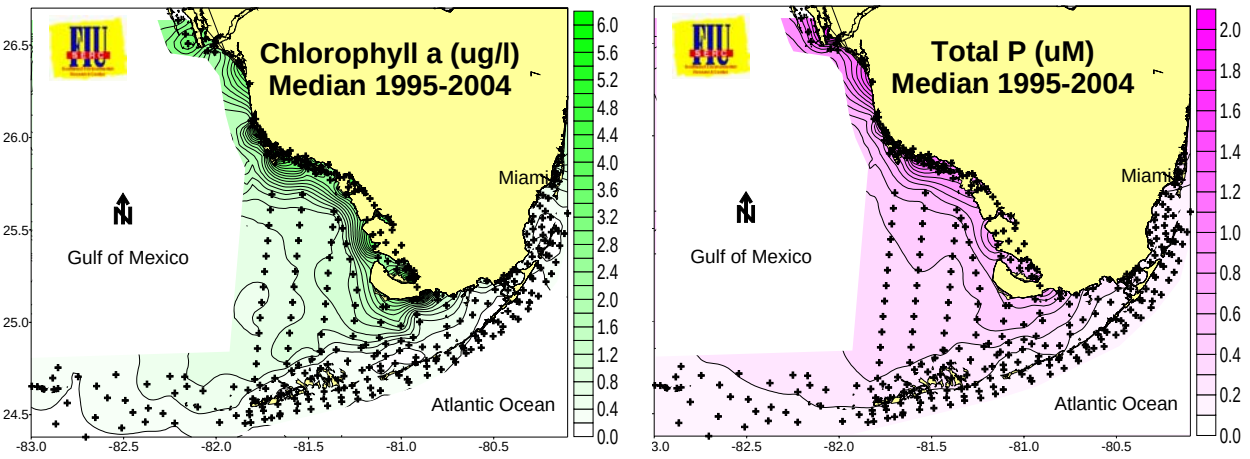

Figure 3.

The forth result is that trends in water quality showed most variables to relatively consistent from year to year, with some showing seasonal excursions. Overall, there were statistically significant **decreases** in DIN, TON (except for increases in Tortugas), TP, TOC, and DO throughout the region. This is contrary to some of the trend analysis reported last year. Clearly, there have been large changes in the FKNMS water quality over time, and some sustained monotonic trends have been observed, however, we must always keep in mind that trend analysis is limited to the window of observation. Trends may change, or even reverse, with additional data collection. This brings up another important point; when looking at what are perceived to be local trends, we find that they seem to occur across the whole region but at more damped amplitudes. This spatial autocorrelation in water quality is an inherent property of highly interconnected systems such as coastal and estuarine ecosystems driven by similar hydrological and climatological forcings. It is clear that trends observed inside the FKNMS are influenced by regional conditions outside the Sanctuary boundaries.

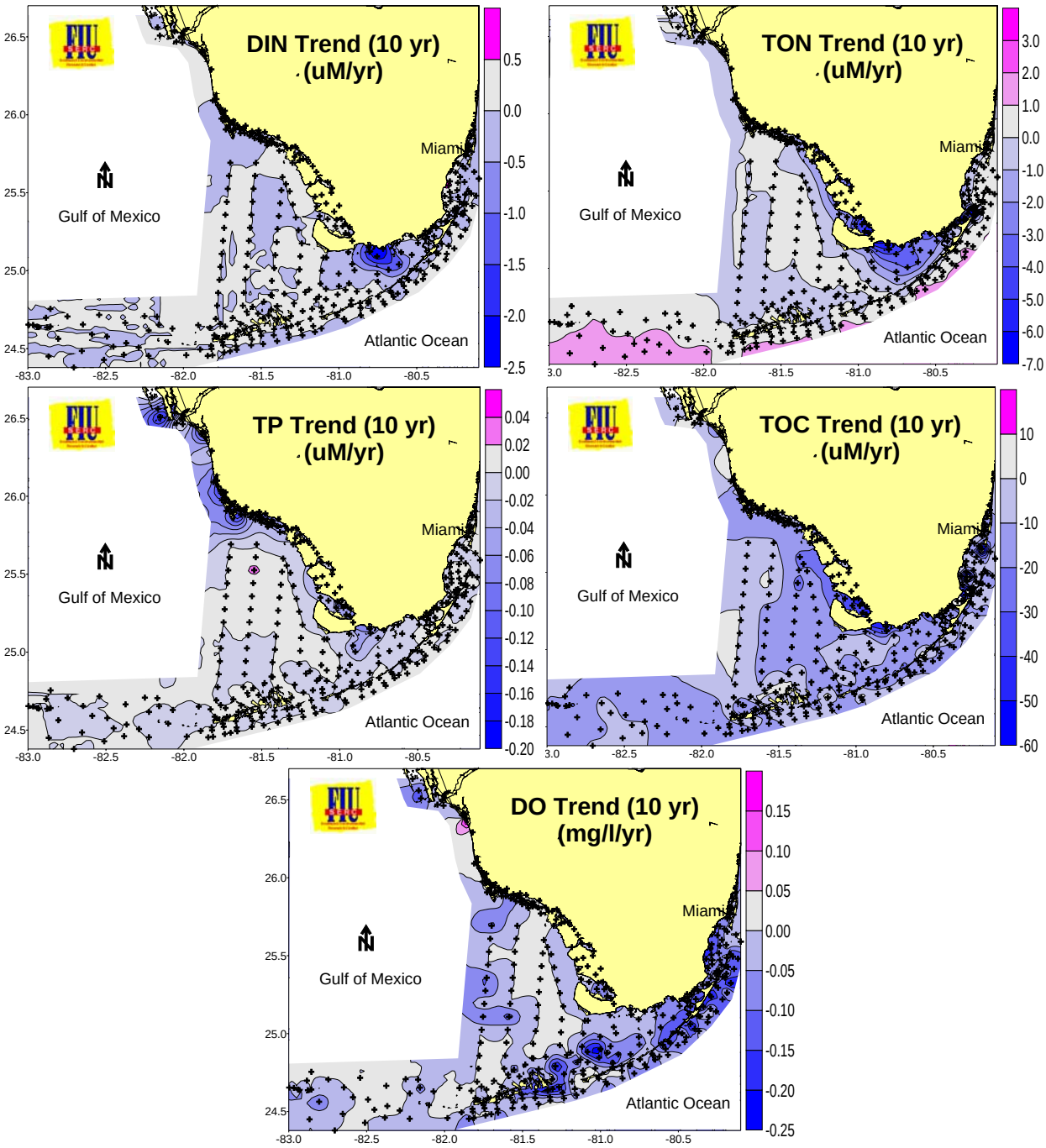

Figure 4.

The large scale of this monitoring program has allowed us to assemble a much more holistic view of broad physical/chemical/biological interactions occurring over the South Florida hydroscape. Much information has been gained by inference from this type of data collection program: major nutrient sources have be confirmed, relative differences in geographical determinants of water quality have been demonstrated, and large scale transport via circulation

pathways have been elucidated. In addition we have shown the importance of looking "outside the box" for questions asked within. Rather than thinking of water quality monitoring as being a static, non-scientific pursuit it should be viewed as a tool for answering management questions and developing new scientific hypotheses.

We continue to maintain a website (http://serc.fiu.edu/wqmnetwork/) where data from the FKNMS is integrated with the other parts of the SERC water quality network (Florida Bay, Whitewater Bay, Biscayne Bay, Ten Thousand Islands, and SW Florida Shelf) and displayed as downloadable contour maps, time series graphs, and interpretive reports.

Table of Contents

1. Project Background

The Florida Keys are a archipelago of sub-tropical islands of Pleistocene origin which extend in a NE to SW direction from Miami to Key West and out to the Dry Tortugas (Fig. 1). In 1990, President Bush signed into law the Florida Keys National Sanctuary and Protection Act (HR5909) which designated a boundary encompassing >2,800 square nautical miles of islands, coastal waters, and coral reef tract as the Florida Keys National Marine Sanctuary (FKNMS). The Comprehensive Management Plan (NOAA 1995) required the FKNMS to have a Water Quality Protection Plan (WQPP) thereafter developed by EPA and the State of Florida (EPA 1995). The contract for the water quality monitoring component of the WQPP was subsequently awarded to the Southeast Environmental Research Program at Florida International University and the field sampling program began in March 1995.

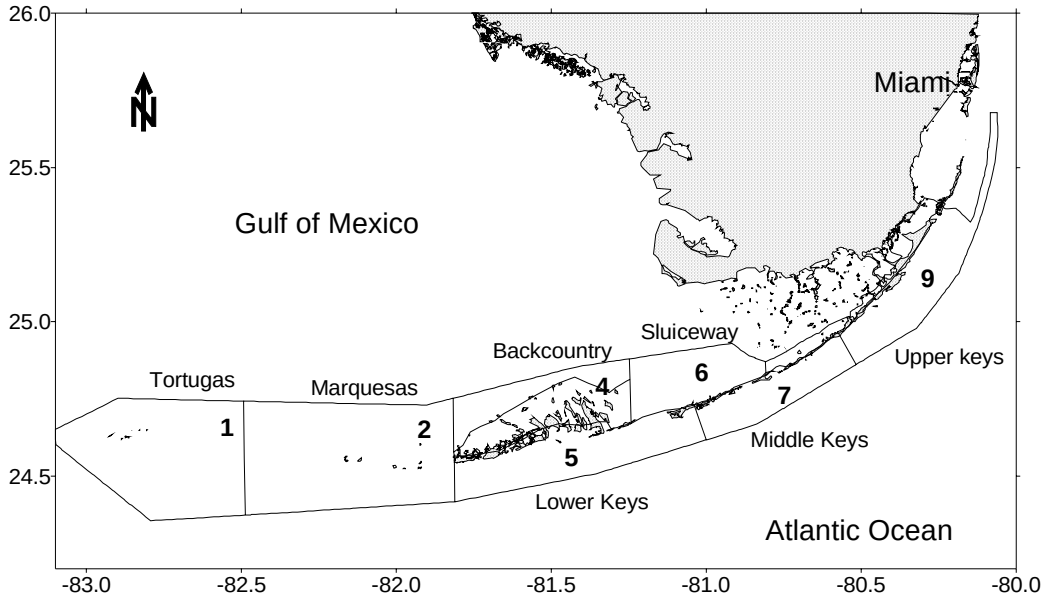

Figure 1. Map of South Florida showing FKNMS boundary, Segment numbers, and common names for Segments.

The waters of the FKNMS are characterized by complex water circulation patterns over both spatial and temporal scales with much of this variability due to seasonal influence in regional circulation regimes. The FKNMS is directly influenced by the Florida Current, the Gulf of Mexico Loop Current, inshore currents of the SW Florida Shelf (Shelf), discharge from the Everglades through the Shark River Slough, and by tidal exchange with both Florida Bay and Biscayne Bay (Lee et al. 1994, Lee et al. 2002). Advection from these external sources has significant effects on the physical, chemical, and biological composition of waters within the

FKNMS, as may internal nutrient loading and freshwater runoff from the Keys themselves. Water quality of the FKNMS may be directly affected both by external nutrient transport and internal nutrient loading sources. Therefore, the geographical extent of the FKNMS is one of political/regulatory definition and should not be thought of as an enclosed ecosystem.

A spatial framework for FKNMS water quality management was proposed on the basis of geographical variation of regional circulation patterns (Klein and Orlando, 1994). The final implementation plan (EPA, 1995) partitioned the FKNMS into 9 segments which was collapsed to 7 for routine sampling (Fig. 1). Station locations were developed using a stratified random design along onshore/offshore transects in Segment 5, 7, and 9 or within EMAP grid cells in Segment 1, 2, 4, and 6.

Segment 1 (Tortugas) includes the Dry Tortugas National Park (DTNP) and surrounding waters and is most influenced by the Loop Current and Dry Tortugas Gyre. Originally, there were no sampling sites located within the DTNP as it was outside the jurisdiction of NOAA. Upon request from the National Park Service, we initiated sampling at 5 sites within the DNTP boundary. Segment 2 (Marquesas) includes the Marquesas Keys and a shallow sandy area between the Marquesas and Tortugas called the Quicksands. Segment 4 (Backcountry) contains the shallow, hard-bottomed waters on the gulfside of the Lower Keys. Segments 2 and 4 are both influenced by water moving south along the SW Shelf. Segment 6 can be considered as part of western Florida Bay. This area is referred to as the Sluiceway as it strongly influenced by transport from Florida Bay, SW Shelf, and Shark River Slough (Smith, 1994). Segments 5 (Lower Keys), 7 (Middle Keys), and 9 (Upper Keys) include the inshore, Hawk Channel, and reef tract of the Atlantic side of the Florida Keys. The Lower Keys are most influenced by cyclonic gyres spun off of the Florida Current, the Middle Keys by exchange with Florida Bay, while the Upper Keys are influenced by the Florida Current frontal eddies and to a certain extent by exchange with Biscayne Bay. All three oceanside segments are also influenced by wind and tidally driven lateral Hawk Channel transport (Pitts, 1997).

We have found that water quality monitoring programs composed of many sampling stations situated across a diverse hydroscape are often difficult to interpret due to the "can't see the forest for the trees" problem (Boyer et al. 2000). At each site, the many measured variables are independently analyzed, individually graphed, and separately summarized in tables. This approach makes it difficult to see the larger, regional picture or to determine any associations

among sites. In order to gain a better understanding of the spatial patterns of water quality of the FKNMS, we attempted to reduce the complicated data matrix into fewer elements which would provide robust estimates of condition and connection. To this end we developed an objective classification analysis procedure which grouped stations according to water quality similarity.

Ongoing quarterly sampling of >200 stations in the FKNMS and Shelf, as well as monthly sampling of 100 stations in Florida Bay, Biscayne Bay, and the mangrove estuaries of the SW coast (Fig.2), has provided us with a unique opportunity to explore the spatial component of water quality variability. By stratifying the sampling stations according to depth, regional geography, distance from shore, proximity to tidal passes, and influence of Shelf waters we report some preliminary conclusions as to the relative importance of external vs. internal factors on the ambient water quality within the FKNMS.

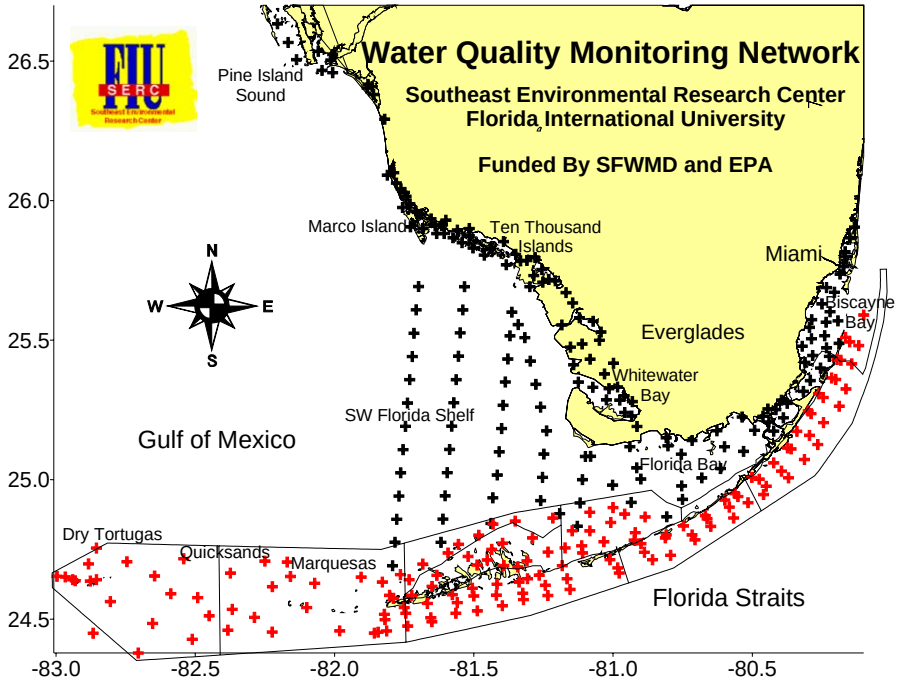

Figure 2. The SERC Water Quality Monitoring Network showing the distribution of fixed sampling stations (+) within the FKNMS, Florida Bay, Biscayne Bay, Whitewater Bay, Ten Thousand Islands, and Southwest Florida Shelf.

2. Methods

2.1.Field Sampling

The period of record of this study was from March 1995 to September 2004 which included 37 quarterly sampling events. For each event, field measurements and grab samples were collected from 154 fixed stations within the FKNMS boundary (Fig. 2). Depth profiles of temperature (°C), salinity (practical salinity scale), dissolved oxygen (DO, mg l^{-1}), photosynthetically active radiation (PAR, µE m^{-2} s^{-1}), *in situ* chlorophyll *a* specific fluorescence (FSU), optical backscatterance turbidity (OBS), depth as measured by pressure transducer (m), and density (σ_t, in kg m^{-3}) were measured by CTD casts (Seabird SBE 19). The CTD was equipped with internal RAM and operated in stand alone mode at a sampling rate of 0.5 sec. The vertical light attenuation coefficient (K_d, m^{-1}) was calculated at 0.5 m intervals from PAR and depth using the standard exponential equation (Kirk 1994) and averaged over the station depth. This was necessary due to periodic occurrence of optically distinct layers within the water column. During these events, K_d was reported for the upper layer. To determine the extent of stratification we calculated the difference between surface and bottom density as delta sigma-t ($\Delta\sigma_t$), where positive values denoted greater density of bottom water relative to the surface. A $\Delta\sigma_t$ >1 is weakly stratified, while anything >2 is considered strongly stratified.

In the Backcountry area (Seg. 4, Fig. 1) where it was too shallow to use a CTD, surface salinity and temperature were measured using a combination salinity-conductivity-temperature probe (Orion model 140). DO was measured using an oxygen electrode (Orion model 840) corrected for salinity and temperature. PAR was measured using a Li-Cor irradiance meter equipped with two 4π spherical sensors (LI-193SB) separated by 0.5 m in depth and oriented at 90° to each other. The light meter measured instantaneous difference between sensors which was then used to calculate K_d from in-air surface irradiance.

Water was collected from approximately 0.25 m below the surface and at approximately 1 m from the bottom with a teflon-lined Niskin bottle (General Oceanics) except in the Backcountry and Sluiceway where it was collected directly into sample bottles. Duplicate, unfiltered water samples were dispensed into 3x sample rinsed 120 ml HDPE bottles for analysis of total constituents. Duplicate water samples for dissolved nutrients were dispensed into 3x sample rinsed 150 ml syringes which were then filtered by hand through 25 mm glass fiber filters (Whatman GF/F) into 3x sample rinsed 60 ml HDPE bottles. The resulting wet filters, used for

chlorophyll *a* (CHLA) analysis, were placed in 1.8 ml plastic centrifuge tubes to which 1.5 ml of 90 % acetone/water was added (Strickland and Parsons 1972).

Unfiltered samples were kept at ambient temperature in the dark during transport to the laboratory. During shipboard collection in the Tortugas/Marquesas and overnight stays in the Keys, unfiltered samples were analyzed for APA and turbidity prior to refrigeration. Filtered samples and CHLA filters were kept on ice in the dark during transport. During shipboard collection in the Tortugas/Marquesas and overnight stays in the lower Keys, filtrates and filters were frozen until further analysis.

2.2. Laboratory Analysis

Unfiltered water samples were analyzed for total organic carbon (TOC), total nitrogen (TN), total phosphorus (TP), silicate ($Si(OH)_4$), alkaline phosphatase activity (APA), and turbidity. TOC was measured by direct injection onto hot platinum catalyst in a Shimadzu TOC-5000 after first acidifying to pH<2 and purging with CO_2-free air. TN was measured using an ANTEK 7000N Nitrogen Analyzer using O_2 as carrier gas to promote complete recovery of the nitrogen in the water samples (Frankovich and Jones 1998). TP was determined using a dry ashing, acid hydrolysis technique (Solórzano and Sharp 1980). $Si(OH)_4$ was measured using the molybdosilicate method (Strickland and Parsons 1972). The APA assay measures the activity of alkaline phosphatase, an enzyme used by bacteria and algae to mineralize orthophosphate from organic compounds. The assay is performed by adding a known concentration of methylfluorescein phosphate to an unfiltered water sample. Alkaline phosphatase in the water sample cleaves the orthophosphate, leaving methylfluorescein, a highly fluorescent compound. Fluorescence at initial and after 2 hr incubation were measured using a Gilford Fluoro IV Spectrofluorometer (excitation = 430 nm, emission = 507 nm) and subtracted to give APA in μM h^{-1} (Jones 1996). Turbidity was measured using an HF Scientific model DRT-15C turbidimeter and reported in NTU.

Filtrates were analyzed for nitrate+nitrite (NO_x^-), nitrite (NO_2^-), ammonium (NH_4^+), and soluble reactive phosphorus (SRP) by flow injection analysis (Alpkem model RFA 300). Filters for CHLA content (μg l^{-1}) were allowed to extract for a minimum of 2 days at -20° C before analysis. Extracts were analyzed using a Gilford Fluoro IV Spectrofluorometer (excitation = 435

nm, emission = 667 nm). All analyses were completed within 1 month after collection in accordance to SERC laboratory QA/QC guidelines.

Some parameters were not measured directly, but were calculated by difference. Nitrate (NO_3^-) was calculated as NO_X^- - NO_2^-, dissolved inorganic nitrogen (DIN) as NO_X^- + NH_4^+, and total organic nitrogen (TON) defined as TN - DIN. All concentrations are reported as μM unless noted. All elemental ratios discussed were calculated on a molar basis. DO saturation in the water column (DO_{sat} as %) was calculated using the equations of Garcia and Gordon (1992).

2.3. Objective Classification Analysis

Stations were stratified according to water quality characteristics (i.e. physical, chemical, and biological variables) using a statistical approach. Multivariate statistical techniques have been shown to be useful in reducing a large data sets into a smaller set of independent, synthetic variables that capture much of the original variance. The method we chose was a type of objective classification analysis (OCA) which uses principal component analysis (PCA) followed by k-means clustering algorithm to classify sites as to their overall water quality. This approach has been very useful in understanding the factors influencing nutrient biogeochemistry in Florida Bay (Boyer et al., 1997), Biscayne Bay, and the Ten Thousand Islands (Boyer and Jones, 1998). We have found that water quality at a specific site is the result of the interaction of a variety of driving forces including oceanic and freshwater inputs/outputs, sinks, and internal cycling.

Briefly, data were first standardized as Z-scores prior to analysis to reduce artifacts of differences in magnitude among variables. PCA was used to extract statistically significant composite variables (principal components) from the original data (Overland and Preisendorfer 1982). The PCA solution was rotated (using VARIMAX) in order to facilitate the interpretation of the principal components and the factor scores were saved for each data record. Both the mean and SD of the factor scores for each station over the entire period of record were then used as independent variables in a cluster analysis (k-means algorithm) in order to aggregate stations into groups of similar water quality. The purpose of this analysis was to collapse the 154 stations into a few groups which could then be analyzed in more detail.

2.4. Box and Whisker Plots

Typically, water quality data are skewed to the left (low concentrations and below detects) resulting in non-normal distributions. Therefore it is more appropriate to use the median as the measure of central tendency because the mean is inflated by high outliers (Christian et al. 1991). Data distributions of water quality variables are reported as box-and-whiskers plots. The box-and-whisker plot is a powerful statistic as it shows the median, range, the data distribution as well as serving as a graphical, nonparametric ANOVA. The center horizontal line of the box is the median of the data, the top and bottom of the box are the 25th and 75th percentiles (quartiles), and the ends of the whiskers are the 5th and 95th percentiles. The notch in the box is the 95% confidence interval of the median. When notches between boxes do not overlap, the medians are considered significantly different. Outliers (<5th and >95th percentiles) were excluded from the graphs to reduce visual compression. Differences in variables were also tested between groups using the Wilcoxon Ranked Sign test (comparable to a *t*-test) and among groups by the Kruskall-Wallace test (ANOVA) with significance set at $P<0.05$.

2.5. Contour Maps

In an effort to elucidate the contribution of external factors to the water quality of the FKNMS and to visualize gradients in water quality over the region, we combined data from other portions of our water quality monitoring network: Florida Bay, Biscayne Bay, Whitewater Bay, Ten Thousand Islands, SW Shelf, and Marco Island – Ft. Meyers (see example in Fig. 10 and http://serc.fiu.edu/wqmnetwork/CONTOUR%20MAPS/ContourMaps.htm for all other maps). Data from these 153 additional stations were collected during the same month as the FKNMS surveys and analyzed by the SERC laboratory using identical methods. Contour maps were produced using Surfer (Golden Software). The most important aspect of generating contour maps is the geostatistical algorithm used for interpolating the data values. Care should be taken in the selection of the algorithm because automated interpolation to a regular rectangular grid can produce artifacts, especially around the edges and when the area of interest is irregularly shaped. The kriging algorithm was used because it is designed to minimize the error variance while at the same time maintaining point pattern continuity (Isaaks & Srivastava, 1989). Kriging is a global approach which uses standard geostatistics to determine the "distance" of influence around each point and the "clustering" of similar samples sites

(autocorrelation). Therefore, unlike the inverse distance procedure, kriging will not produce valleys in the contour between neighboring points of similar value.

2.6. Time Series Analysis

Individual site data for the complete period of record were plotted as time series graphs (see http://serc.fiu.edu/wqmnetwork/CONTOUR%20MAPS/ContourMaps.htm) to illustrate any temporal trends that might have occurred. Temporal trends were quantified by simple regression with significance set at $P<0.05$. We originally planned to use a seasonal Kendall-τ analysis to test for monotonic trend (Hirsch et al. 1991) but found that it was not yet applicable to this short, quarterly sampled data set.

3. Results

3.1. General Water Quality of the FKNMS

Summary statistics for all water quality variables from all 37 sampling events are shown as median, minimum, maximum, and number of samples (Table 1). Overall, the region was warm and euhaline with a median temperature of 27.4°C and salinity of 36.2; oxygen saturation of the water column (DO_{sat}) was relatively high at 89.0%. On this coarse scale, the FKNMS exhibited very good water quality with median NO_3^-, NH_4^+, and TP concentrations of 0.09, 0.28, and 0.19 μM, respectively. NH_4^+ was the dominant DIN species in almost all of the samples (~70 %). However, DIN comprised a small fraction (4 %) of the TN pool with TON making up the bulk (median 11.2 μM). SRP concentrations were very low (median 0.02 μM) and comprised only 6 % of the TP pool. CHLA concentrations were also very low overall, 0.24 μg l^{-1}, but ranged from 0.01 to 15.2 μg l^{-1}. TOC was 183.6; a value higher than open ocean levels but consistent with coastal areas. Median turbidity was low (0.63 NTU) as reflected in a low K_d (0.213 m^{-1}). This resulted in a median photic depth (to 1 % incident PAR) of ~22 m. Molar ratios of N to P suggested a general P limitation of the water column (median TN:TP = 57, not shown) but this must be tempered by the fact that much of the TN is not bioavailable.

Table 1. Summary statistics for each water quality variable in the FKNMS for the period of record. Data are summarized as median (Median), minimum value (Min.), maximum value (Max.), and number of samples (*n*).

Variable	Depth	Median	Min.	Max.	*n*
NO_3^-	Surface	0.09	0.00	5.90	5765
(μM)	Bottom	0.08	0.00	5.01	3508
NO_2^-	Surface	0.04	0.00	0.71	5774
(μM)	Bottom	0.04	0.00	1.73	3515
NH_4^+	Surface	0.28	0.00	10.32	5772
(μM)	Bottom	0.26	0.00	3.88	3510
TN	Surface	11.82	0.92	213.21	5771
(μM)	Bottom	9.86	1.48	153.75	3483
TON	Surface	11.25	0.00	212.89	5748
(μM)	Bottom	9.31	0.00	153.43	3460
TP	Surface	0.19	0.00	1.78	5776
(μM)	Bottom	0.18	0.00	1.50	3495

Variable	Depth	Median	Min.	Max.	*n*
SRP	Surface	0.02	0.00	0.56	5759
(μM)	Bottom	0.02	0.00	0.39	3503
APA	Surface	0.06	0.00	5.62	5614
($\mu M\ h^{-1}$)	Bottom	0.05	0.00	0.49	3352
CHLA ($\mu g\ l^{-1}$)	Surface	0.24	0.01	15.24	5776
TOC	Surface	183.58	22.79	1653.5	5769
(μM)	Bottom	157.38	21.89	2135.8	3492
$Si(OH)_4$	Surface	0.67	0.00	127.11	5469
(μM)	Bottom	0.44	0.00	30.20	3317
Turbidity	Surface	0.63	0.00	37.00	5730
(NTU)	Bottom	0.51	0.00	16.90	3530
Salinity	Surface	36.2	26.7	40.9	5687
	Bottom	36.2	27.7	40.9	5658
Temperature	Surface	27.4	15.1	39.6	5694
(^oC)	Bottom	27.0	15.1	36.8	5665
DO	Surface	6.0	0.1	13.5	5660
($mg\ l^{-1}$)	Bottom	6.0	1.4	13.9	5613
K_d		0.213	0.001	4.084	3864
TN:TP	Surface	61.9	0.0	2591.2	5756
N:P	Surface	22.2	0.0	4111.0	4945
DIN:TP	Surface	2.5	0.0	71.3	5750
DO Saturation	Surface	89.0	1.2	191.6	5659
(%)	Bottom	89.2	19.3	207.0	5611
$\Delta\sigma_t$		0.01	-4.42	6.64	5639
Si:DIN	Surface	1.4	0.0	315.8	5451

3.2. Objective Classification Analysis

PCA identified five composite variables (hereafter called PC1, PC2, etc.) that passed the rule N for significance at $P<0.05$ (Overland and Preisendorfer 1982) indicating five separate modes of variation in the data (Table 2). These five principal components accounted for 63.2 % of the total variance of the original variables. PC1 had high factor loadings for NO_3^-, NO_2^-, NH_4^+, and SRP and was named the "Inorganic Nutrient" component. PC2 included TP, APA, CHLA, and turbidity and was designated as the "Phytoplankton" component. The covariance of TP with CHLA implies that, in many areas, phytoplankton biomass may be limited by phosphorus

availability. This is contrary to much of the literature on the subject which usually ascribes nitrogen as being the limiting factor for phytoplankton production in coastal oceans. TON and TOC were included in PC3 as the "Terrestrial Organic" component. Temperature and DO were inversely related in PC4. Finally, PC5 included salinity and TP, implying a source of TP from marine waters. Note that TP had two modes of variability as a function of its distribution.

Table 2. Results of principal component analysis are shown as factor loadings (correlations between the raw variables and the principal components) for the first four principal components after VARIMAX rotation. For clarity, loadings with a magnitude >0.450 are shown in boldface type.

Variable	PC1	PC2	PC3	PC4	PC5
NO_3^-	**0.707**	0.094	-0.121	0.100	0.004
NO_2^-	**0.608**	-0.082	0.354	0.057	0.111
NH_4^+	**0.691**	-0.124	0.200	0.001	-0.087
TON	0.001	0.071	**0.720**	-0.139	0.126
TP/TP	0.220	**0.449**	-0.047	-0.414	**0.499**
SRP	**0.550**	0.245	-0.413	-0.037	-0.112
APA	-0.066	**0.693**	0.214	0.394	0.041
CHLA	0.001	**0.789**	-0.135	0.006	-0.217
TOC	0.038	0.073	**0.696**	0.089	-0.185
Turbidity	0.036	**0.591**	0.190	-0.261	0.040
Salinity	-0.108	-0.141	-0.010	0.201	**0.820**
Temp.	-0.001	-0.001	0.141	**0.802**	0.074
DO	-0.122	0.052	0.109	**-0.737**	-0.024
%Variance Explained	19.0	16.2	10.6	9.5	7.9

Spatial distributions of the mean factor score for each station indicated how the average water quality varied over the study area. The "Inorganic Nutrient" component had two peaks: in the Backcountry and bayside of the Middle Keys. The "Phytoplankton" component described a N to S gradient in the Backcountry and Sluiceway which extended west across the northern Marquesas. The "Terrestrial Organic" component was highest in eastern Sluiceway extending into the Backcountry and was also distributed as a gradient away from land on the Atlantic side of the Keys. Temperature and DO showed a distribution heavily loaded in the oceanside.

Finally the salinity/TP component showed lower loadings in the alongshore Upper Keys and bayside Sluiceway extending through most Atlantic sites of the Middle and Lower Keys.

The k-means clustering algorithm used the mean and SD of the four factor scores of each station to classify all 150 sampling sites into 8 groups having robust correspondence in water quality (Fig. 3). The bulk of the stations fell into 6 large clusters (1, 3, 5, 6, 7, and 8) which described a gradient of water quality throughout the FKNMS. Although the differences among them were very subtle, they were statistically significant and allowed us to say that the overall nutrient gradient, from highest to lowest concentrations, was cluster 7, 8>1>5>6>3 (Table 3 in Appendix).

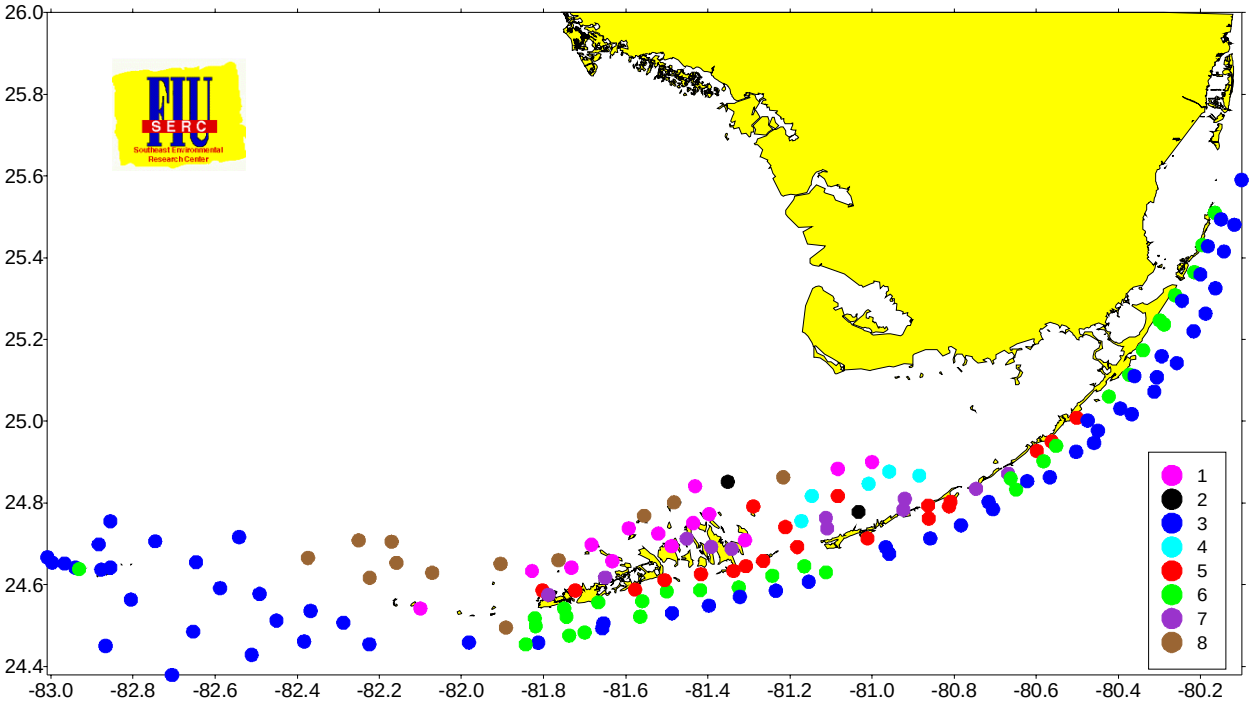

Figure 3. Results of objective analysis showing station membership in distinct water quality groups.

Cluster 7 (●) was composed primarily stations located inside the Backcountry, bayside Middle Keys, and the inshore sites off Lower Matecumbe Key. This group was highest in inorganic nutrients, especially NO_3^-, as well as TOC and TON (Fig. 4). We expect that there are different reasons for the distribution of these sites. In the shallow Backcountry sites we expect that benthic flux of nutrients might be very important, whereas elevated DIN at inshore Lower Matecumbe sites may be the result of anthropogenic loading.

Cluster 8 (●) included the northernmost sites in the Sluiceway, Backcountry and Marquesas. It had the highest TP, CHLA, and turbidity but was low in inorganic nutrients, DON, and DOC. We believe that the water quality in Cluster 8 was primarily driven by Shelf circulation patterns.

Cluster 1 (●) was composed of 2 sites in the northern Sluiceway and 12 sites in northern Backcountry extending out to the Marquesas. This group was high in TP, CHLA, and turbidity. The main distinction between Cluster 1 and 8 was higher in CHLA and lower in TOC. So Clusters 8 and 1 may be viewed as a gradient of high TP Shelf water being attenuated by uptake of nutrients within the Backcountry and/or mixing with Atlantic Ocean waters.

Clusters 5, 6, and 3 may be interpreted as representing an onshore-offshore nutrient gradient. Cluster 5 (●) included the most of the inshore sites of the Keys, excluding the northernmost and southernmost ones. They were elevated in DIN relative to the Hawk Channel and reef tract sites. Cluster 6 (●) was made up of sites in Hawk Channel of the Lower Keys and alongshore sites in the Upper Keys. This group was slightly lower in nutrients than Cluster 5. Cluster 3 (●) was made up of outer reef tract and Tortugas stations. These sites had lowest nutrients, CHLA, turbidity, and TOC of any in the FKNMS. A clear gradient of elevated DIN, TP, TOC, and turbidity from alongshore to offshore was observed in the Keys with the Upper Keys being lower than the Middle and Lower Keys. No significant onshore-offshore gradient was observed for CHLA.

Sites making up Cluster 4 (●) were located in the Sluiceway and were similar to other Sluiceway sites except that they had the greatest range in salinity. Cluster 2 (●) was composed of only 2 sites in the Sluiceway and will not be discussed.

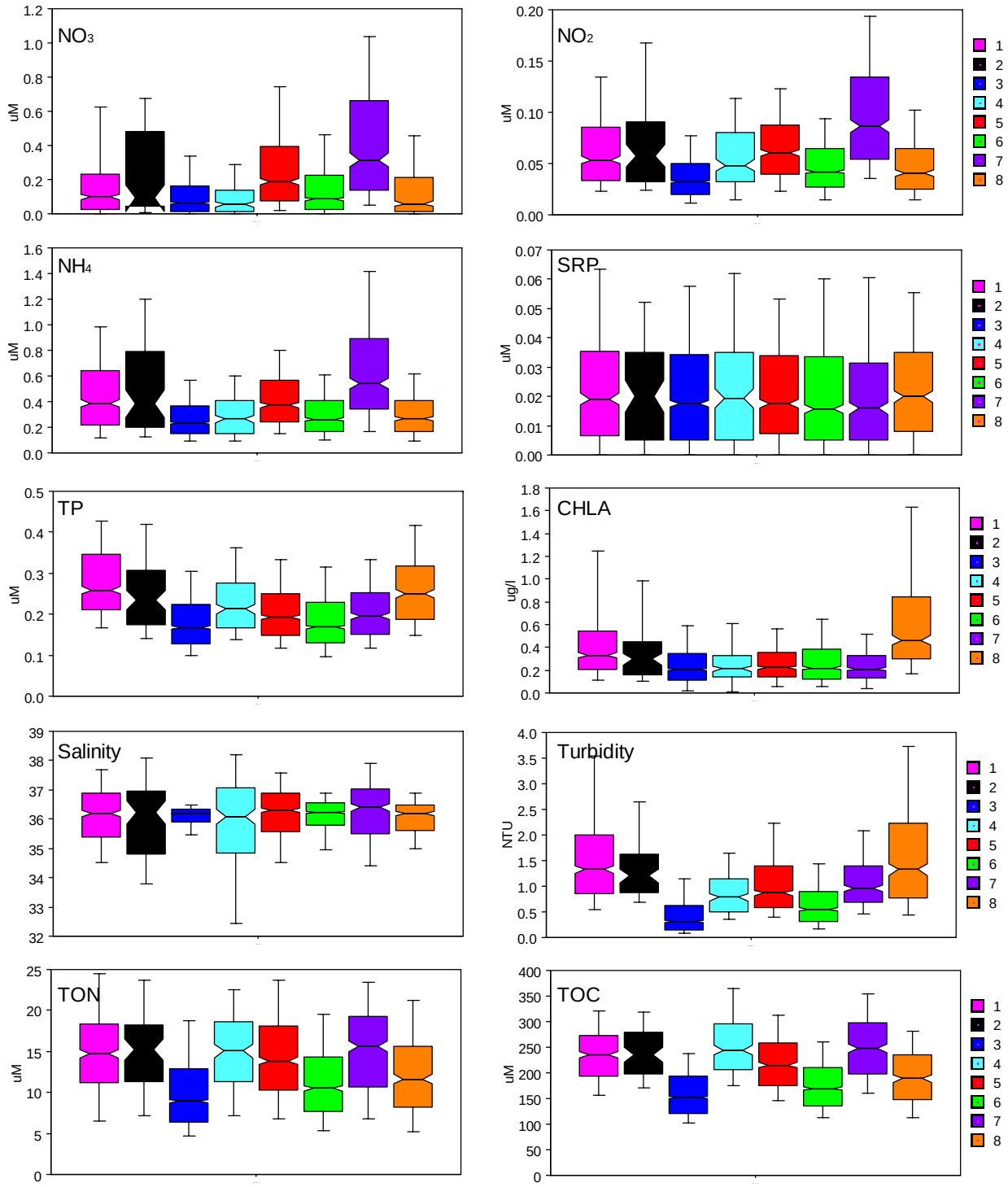

Figure 4. Box-and-whisker plots showing median and distribution of NO_3^-, NO_2^-, NH_4^+, SRP, TP, CHLA, salinity, turbidity, TP, TON, and TOC stratified by water quality cluster. Notches in the box that do not overlap with another are considered significantly different.

3.3. Contour Maps

All contour maps of combined data from EPA and SFWMD projects are archived on the website http://serc.fiu.edu/wqmnetwork/CONTOUR%20MAPS/ContourMaps.htm and are updated quarterly. An example of such (Fig. 5) shows the distribution of salinity across the region. Both freshwater sources and marine influences are visible using this approach. The major freshwater sources to the region are the Shark River/Slough system on the SW coast and the Taylor Slough/C-111 Basin in eastern Florida Bay. Southerly advection of water along the SW coast and Shelf may move through the Keys passes and can impact the reef tract.

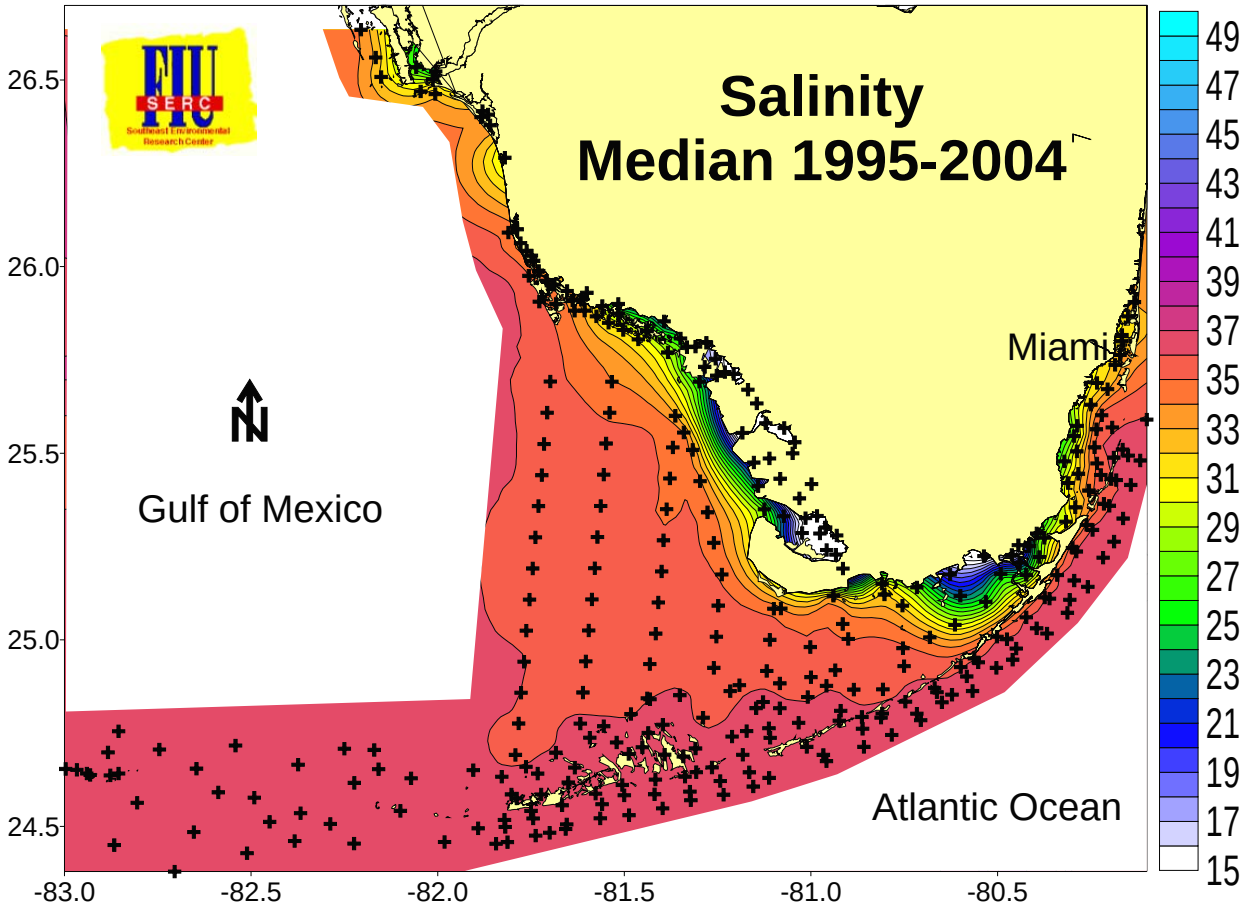

Figure 5. Example of contour map of salinity in the region showing freshwater inputs and marine influence.

The usual distribution of dissolved NO_3^- and NH_4^+ are very different than that for salinity (Fig. 6). This implies that there are other factors responsible for their distributions, such a phytoplankton and seagrass uptake as well as N_2 fixation and benthic remineralization.

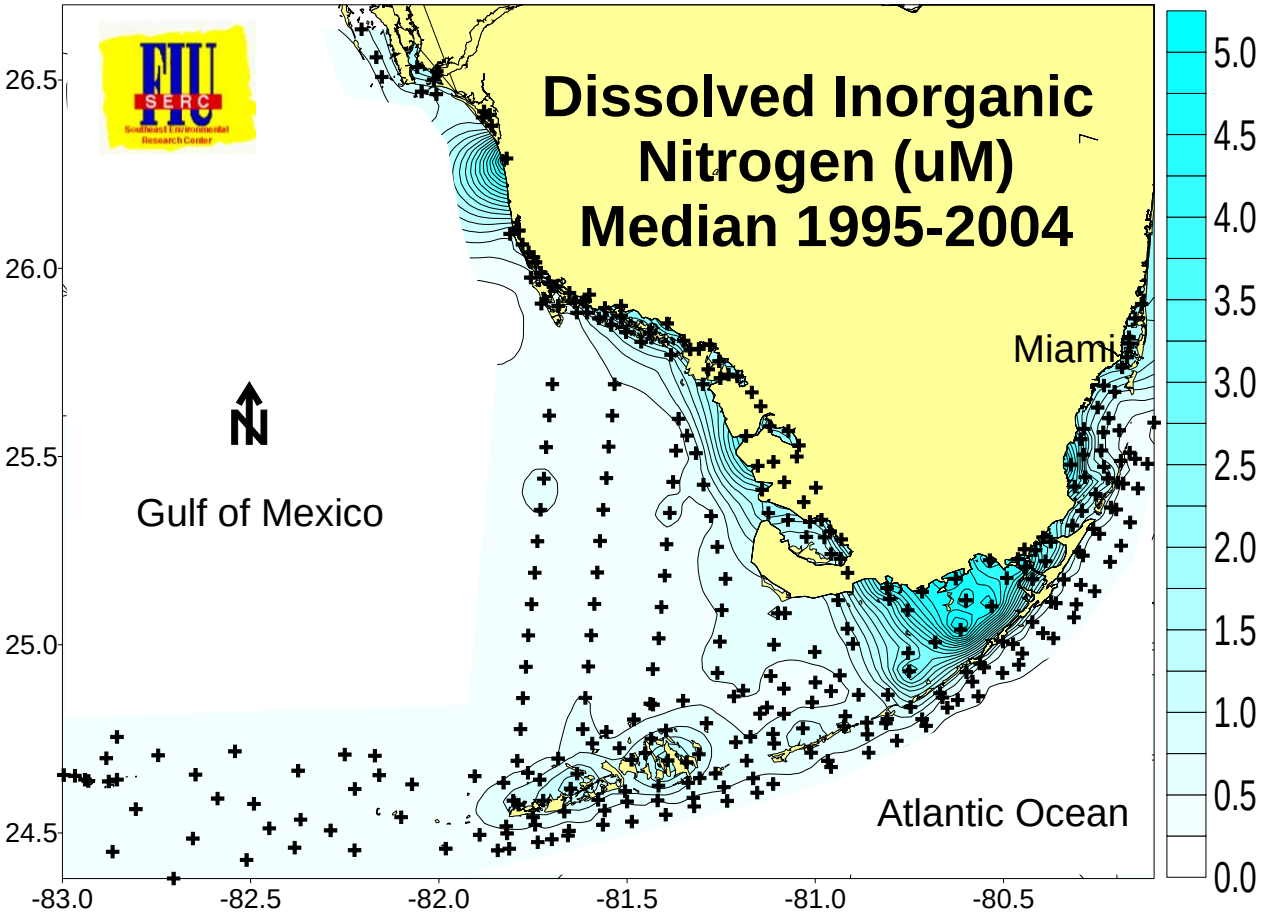

Figure 6. Example of contour map of nitrate in the region.

In contrast, total phosphorus distributions often are very similar to salinity patterns, but only on the west coast (Fig. 7).

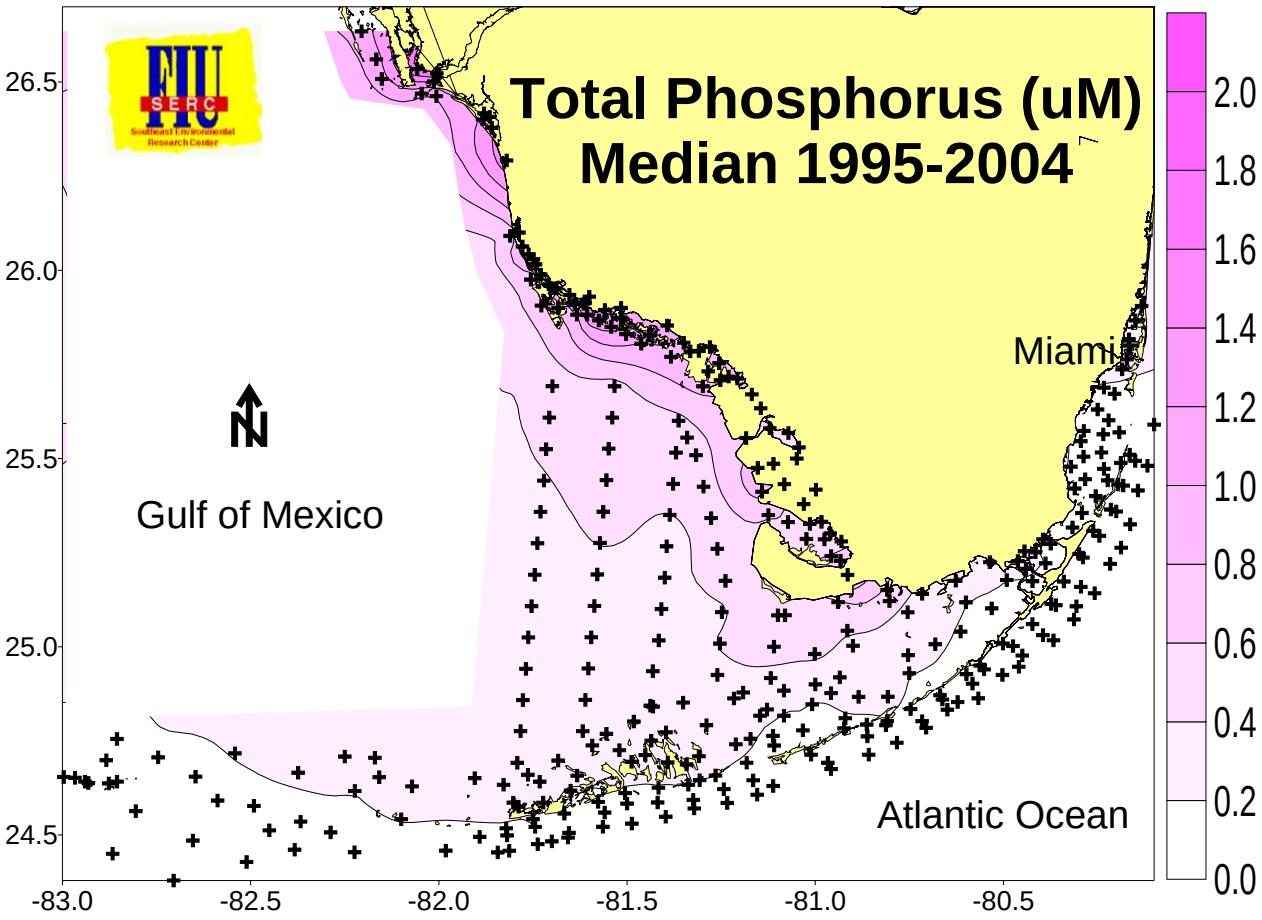

Figure 7. Example of contour map of total phosphorus in the region.

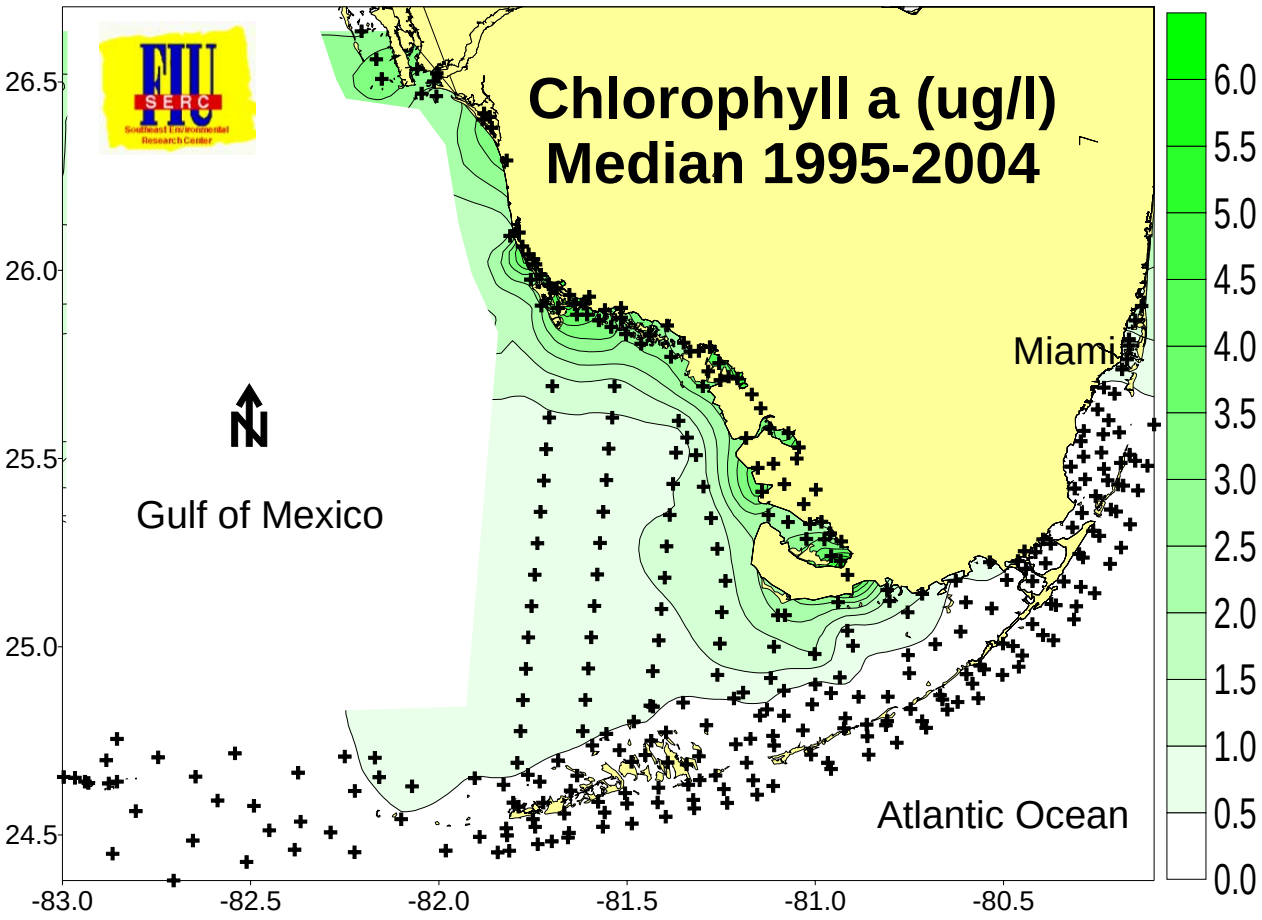

Figure 8. Example of contour map of salinity in the region showing freshwater source inputs and marine influences.

3.4. Time Series Analysis

Previously, we observed significant increasing trends in TP, NO_3^-, and decreasing TON (Jones and Boyer 2001). We ascribed these trends as being driven primarily by large scale circulation patterns. Since then, there have been trend reversals in some nutrient concentrations. Figures 9-14 show temporal trends in the median and range of the data (box-and-whisker plots) for each group by quarterly sampling event.

The outer reef tract/Tortugas sites (**Cluster 3**) showed large increases in NO_3^- and SRP during late 1999 through 2000 (Fig 9). Concurrent with these increases was an increase in CHLA and drop in DO_{sat}. These parameters have since returned to earlier levels. As reported previously, TP was increasing fairly consistently prior to 2001 but has since declined. An interesting aspect of this is that, more than the actual concentration, the variability of TP has increased dramatically. We observed an increased in TON values during 2002 which looks to have returned to previous levels. TOC shows interannual cycles with ~2 year period. Salinity is relatively constant except for low salinity excursions due to transport of Shelf waters through the Tortugas Channel and advective transport along the coast by regular gyre formations.

Cluster 6, the inshore Upper Keys/Hawk Channel Lower Keys, mirrored the patterns seen in **Cluster 3** except that the concentrations were higher for the nearshore sites (Fig. 10). This implies that the inorganic nutrients did not originate from offshore sources (upwelling). In fact, looking at all the data during this time period showed elevated NO_3^- concentrations occurred across the region (Fig. 9-14). This brings up an important point that, when looking at what are perceived to be local trends, we find that they may occur across the whole region at more subtle levels. This spatial autocorrelation in water quality is an inherent property of interconnected systems such as coastal and estuarine ecosystems which are driven by hydrological and climatological forcing.

Clearly, there have been large changes in the FKNMS water quality over time, but the only sustained monotonic trend that has been observed is a decline in TOC. We must always keep in mind that trend analysis is limited to the window of observation; trends may change with additional data collection.

Cluster 3 – Reef Tract/Tortugas

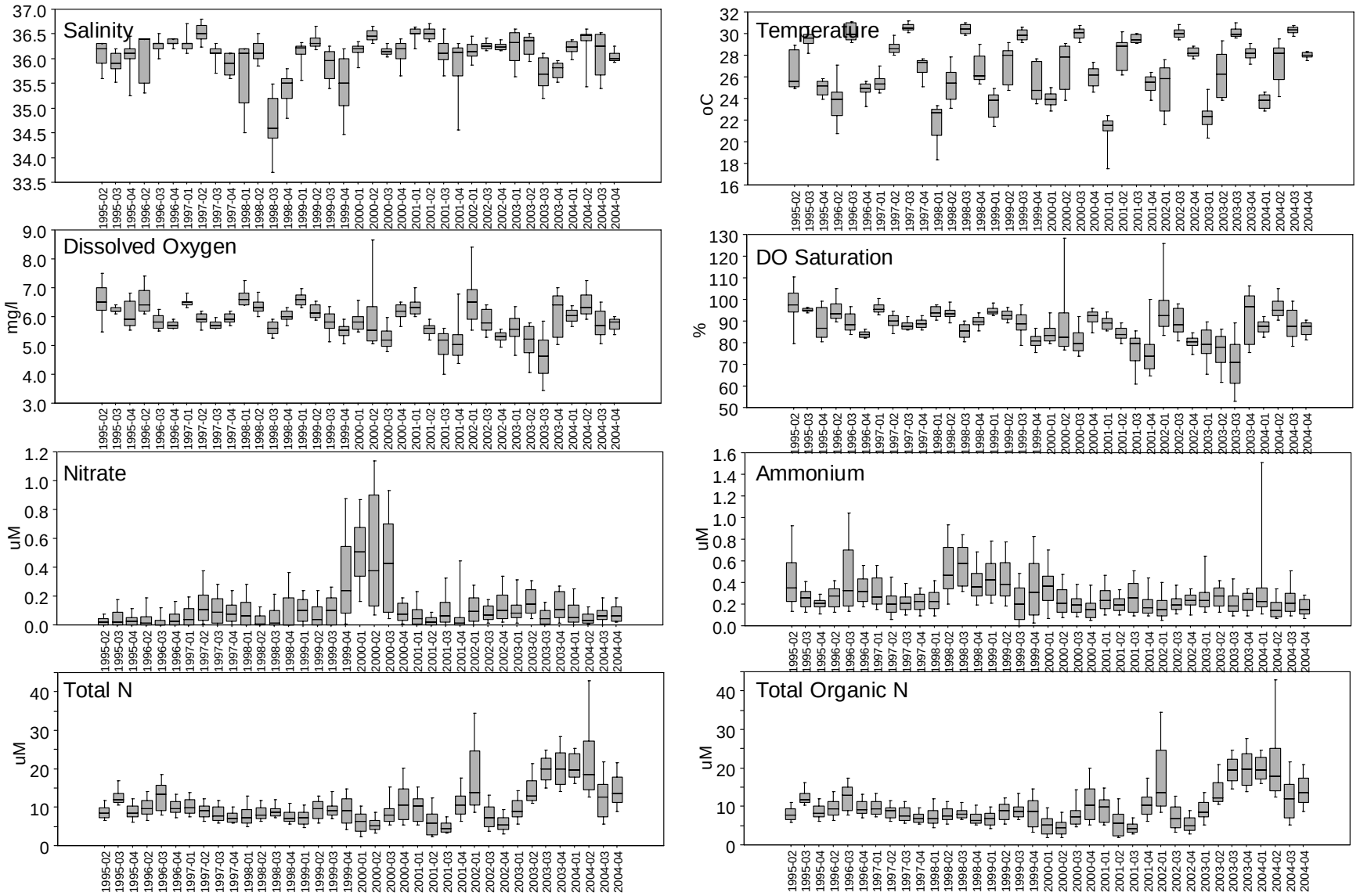

Cluster 3 – Reef Tract/Tortugas

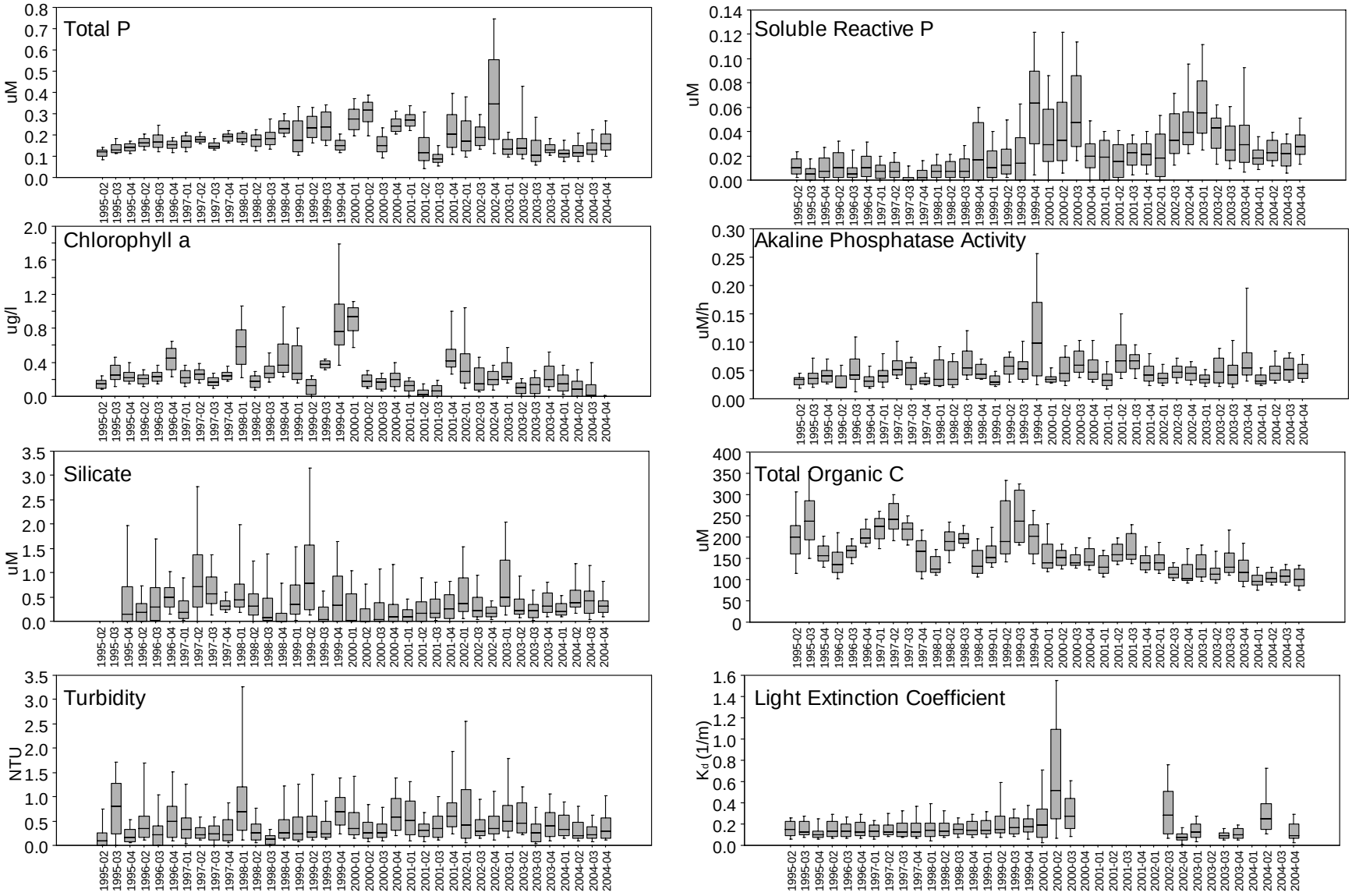

Figure 9

Cluster 6 – Inshore Upper Keys/Hawk Channel Lower Keys

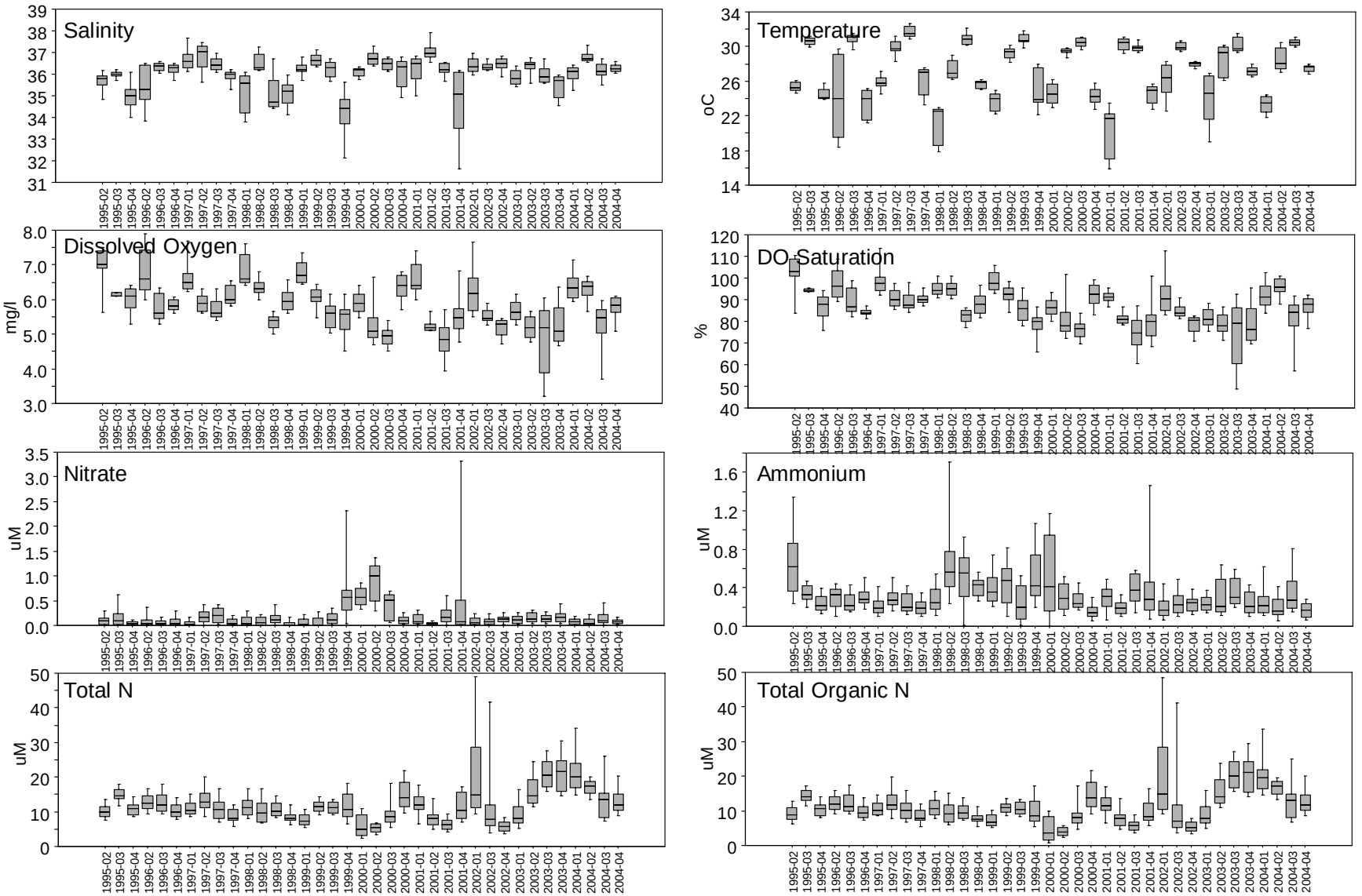

Cluster 6 – Inshore Upper Keys/Hawk Channel Lower Keys

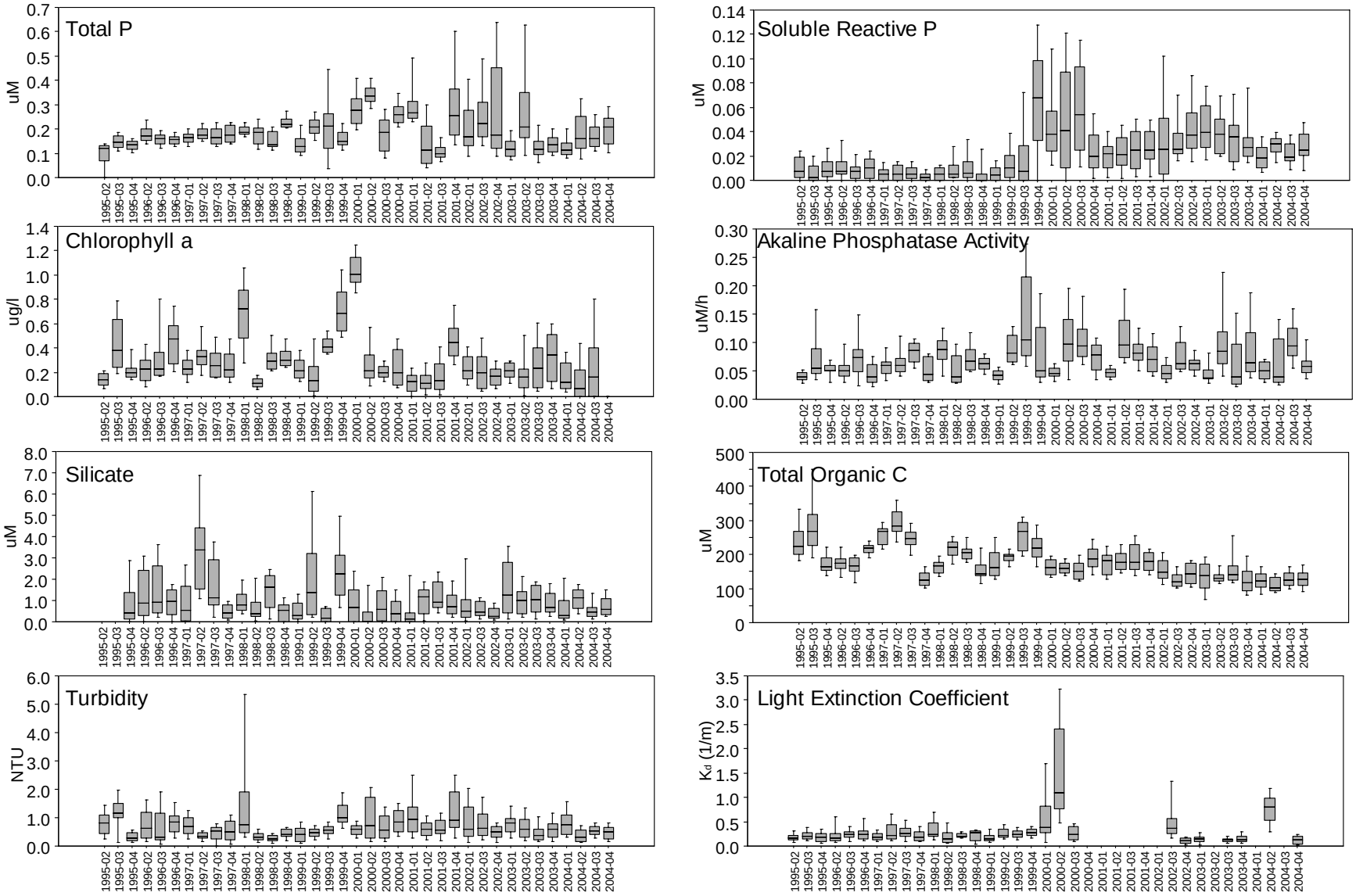

Figure 10

Cluster 5 – Inshore Middle and Lower Keys/Sluiceway

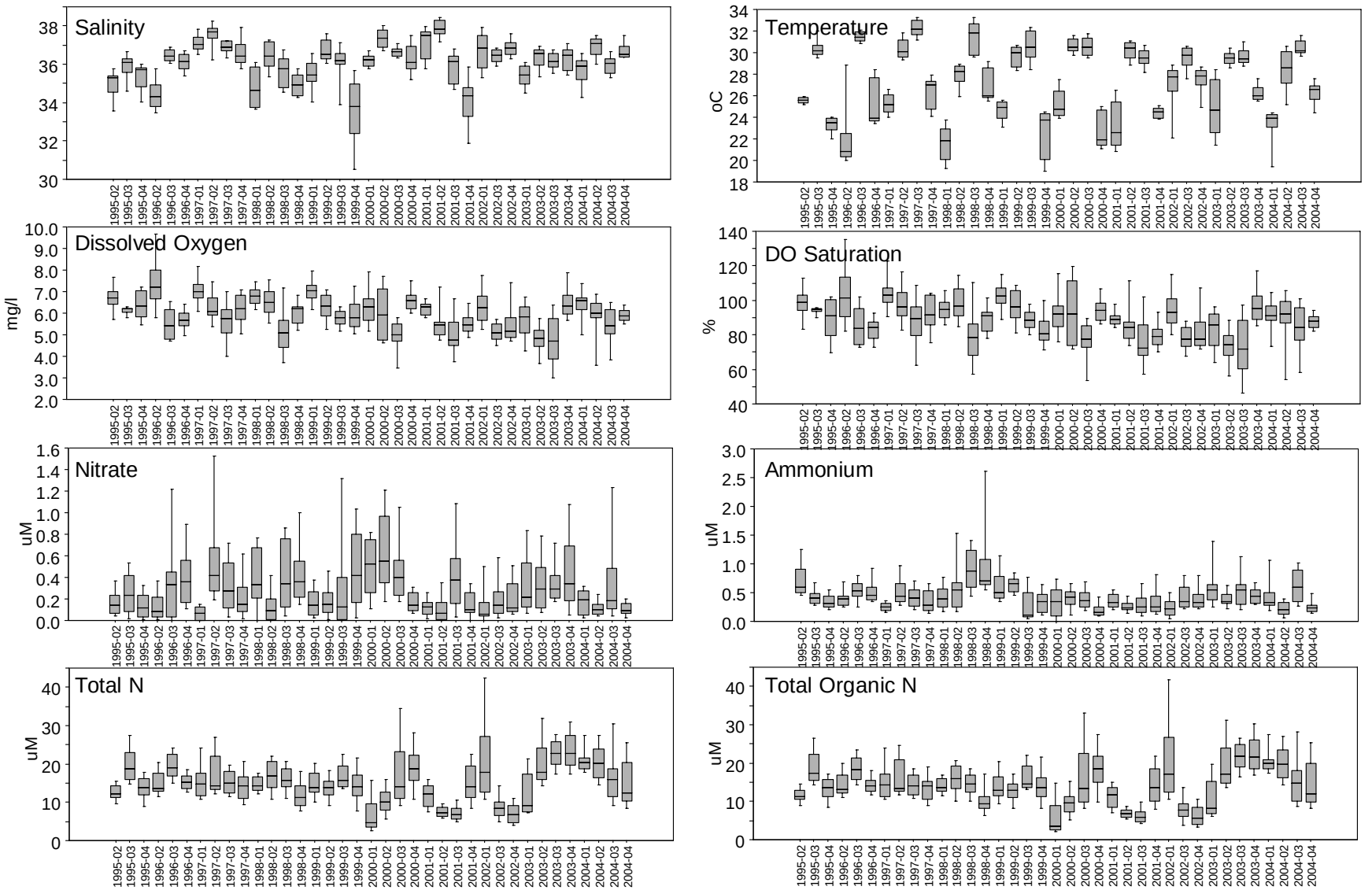

Cluster 5 – Inshore Middle and Lower Keys/Sluiceway

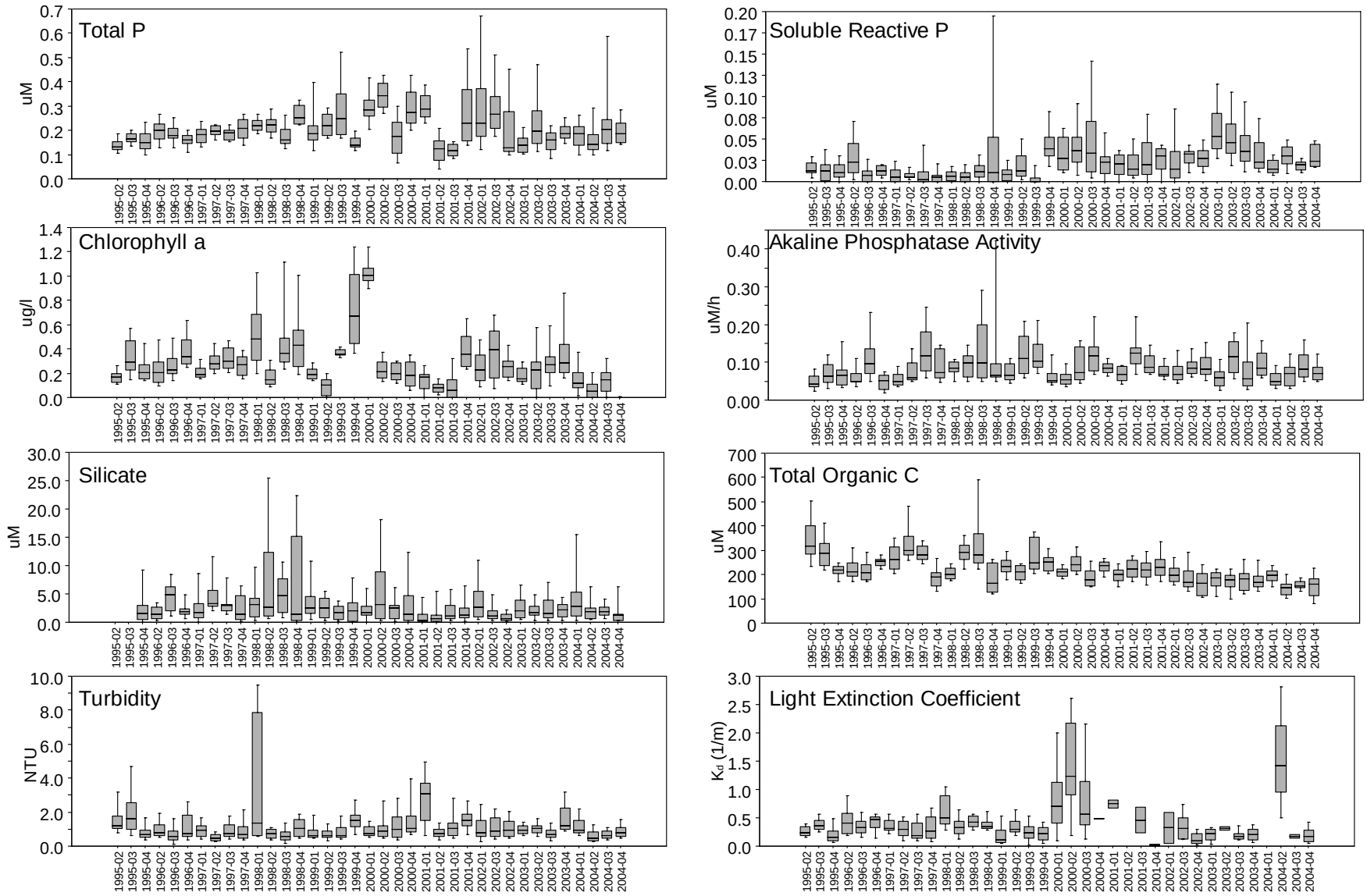

Figure 11

Cluster 7 – Bayside Middle Keys/Inside Backcountry/Inshore Long & Lower Matecumbe

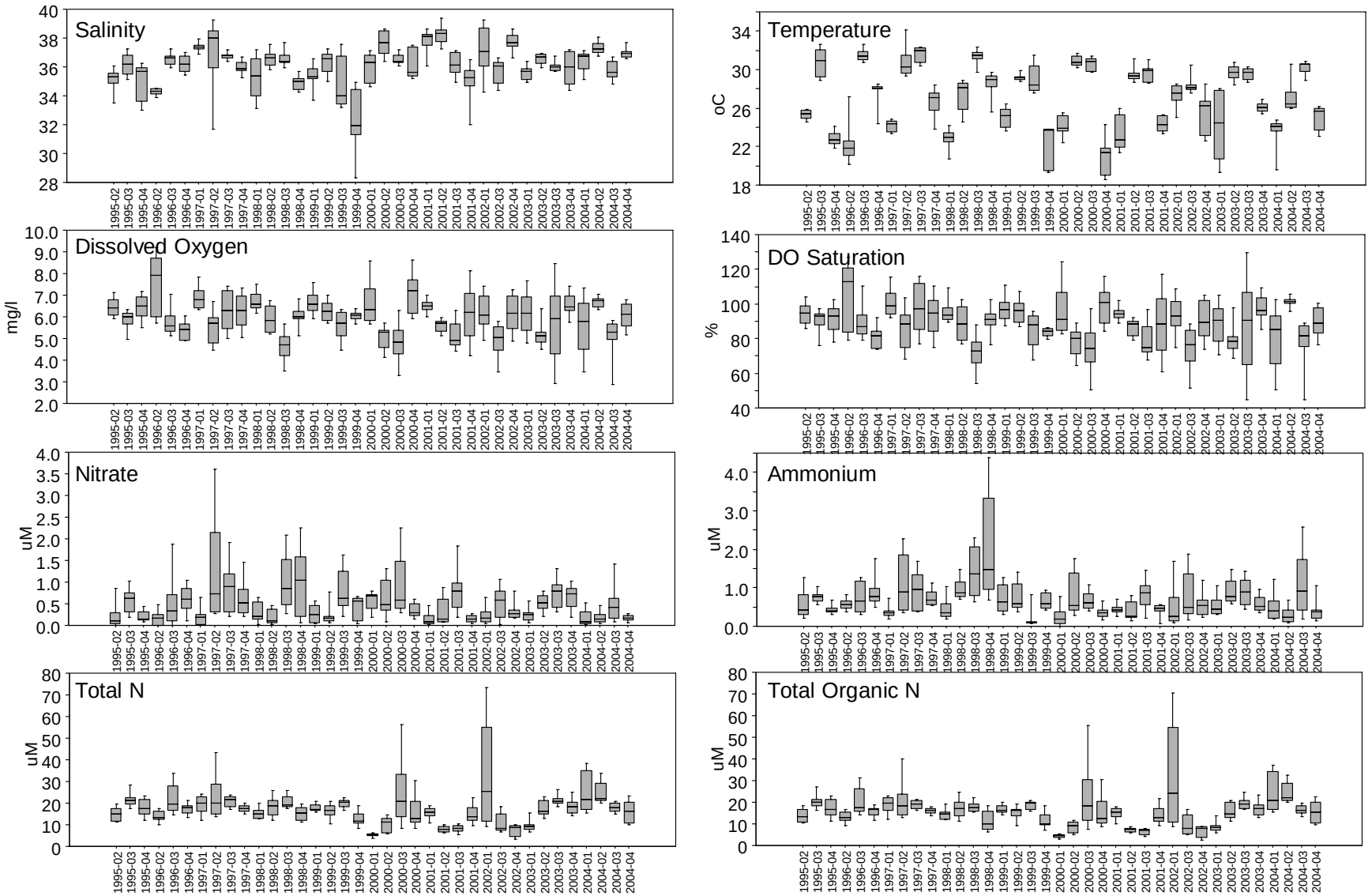

Cluster 7 – Bayside Middle Keys/Inside Backcountry/Inshore Long & Lower Matecumbe

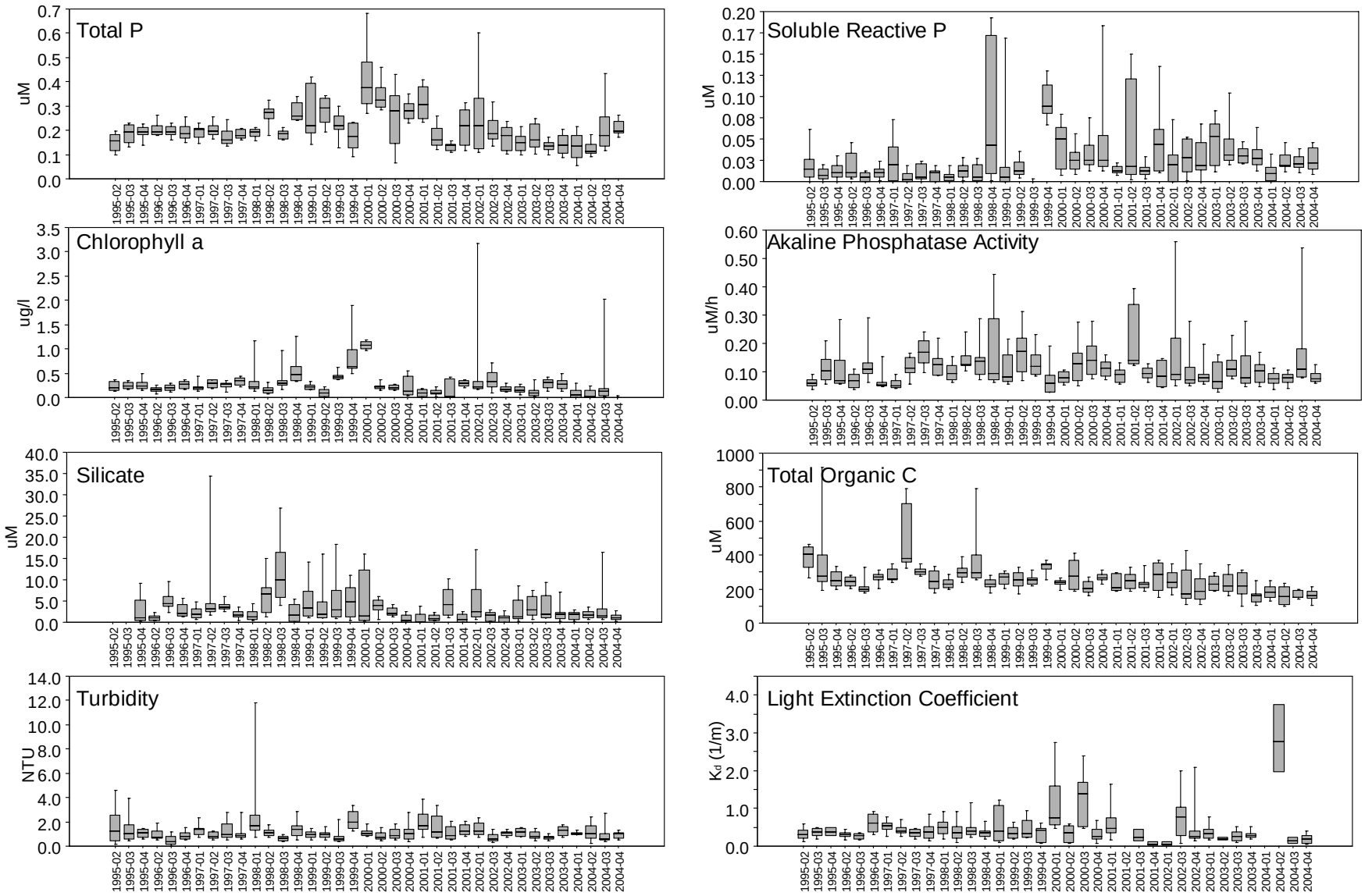

Figure 12

Cluster 1 – Backcountry/North Sluiceway

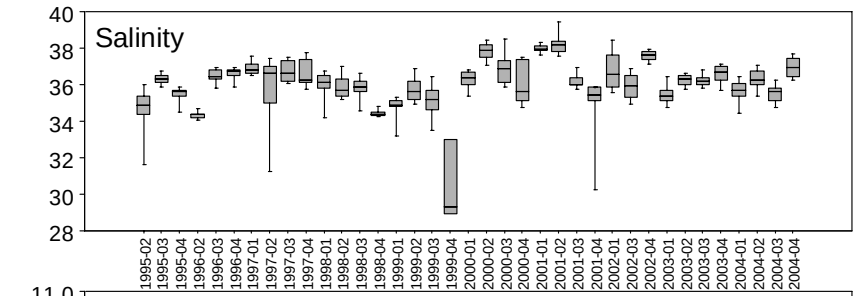

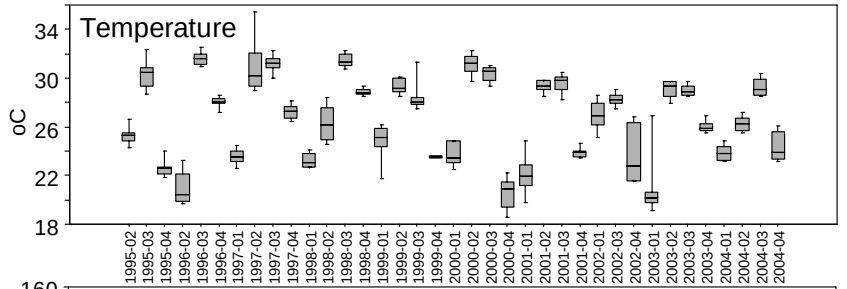

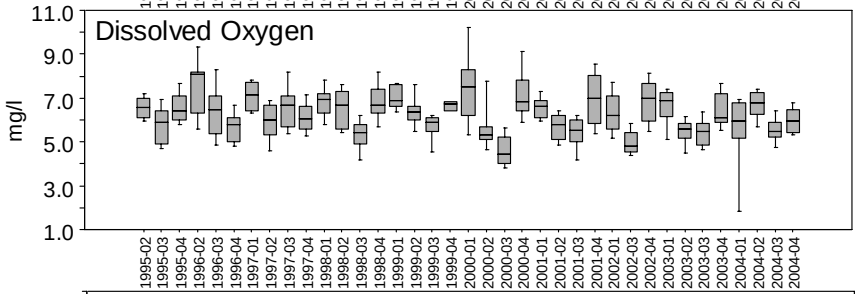

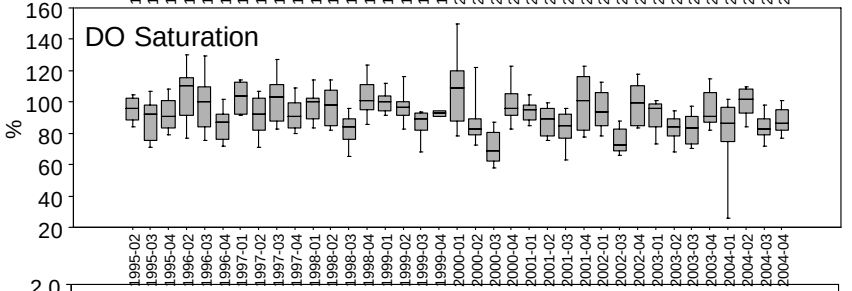

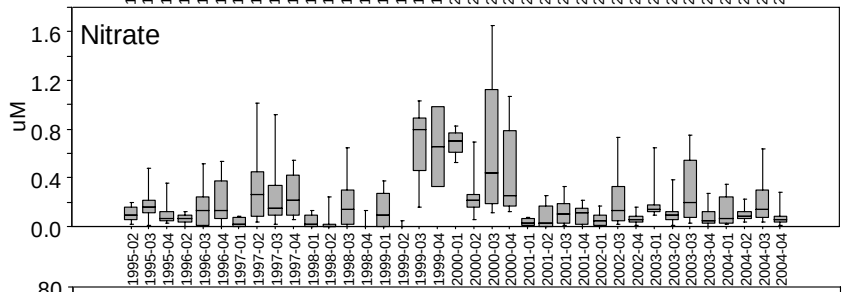

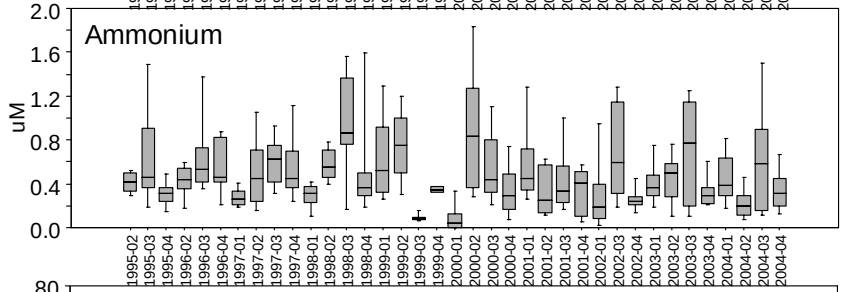

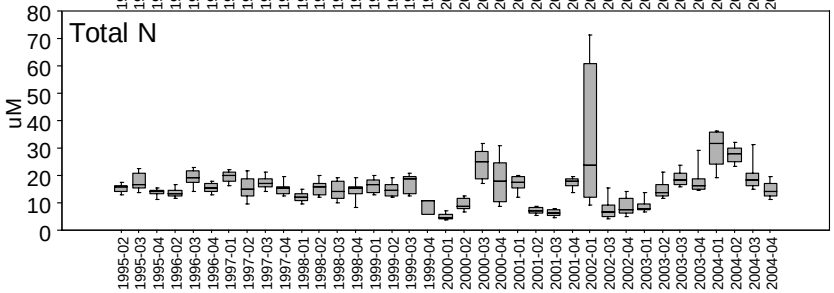

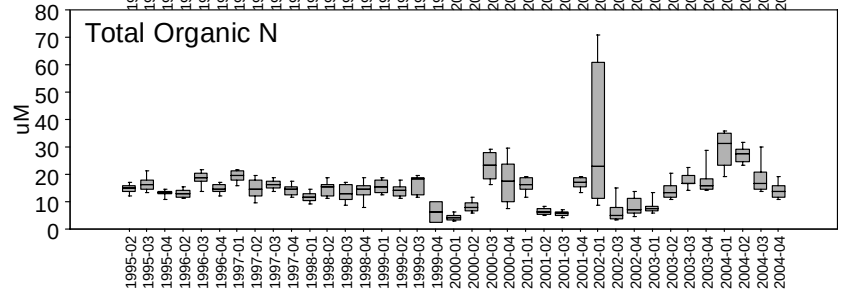

Cluster 1 – Backcountry/North Sluiceway

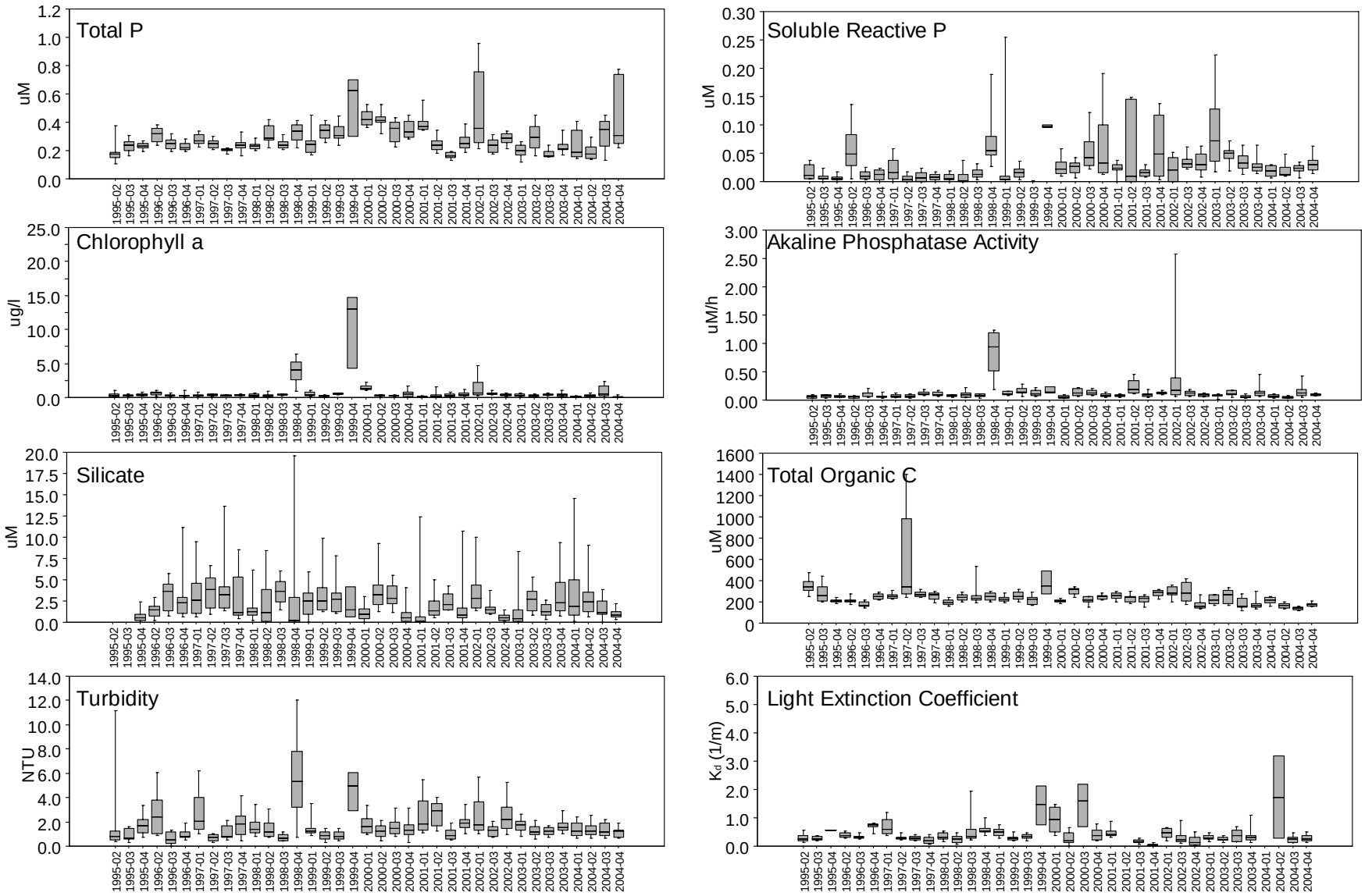

Figure 13

Cluster 8– North Marquesas/North Backcountry

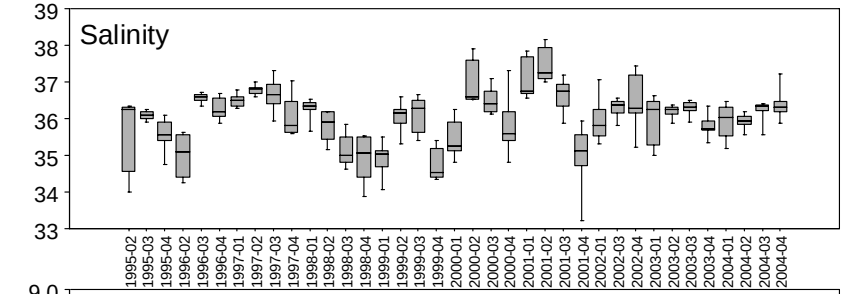

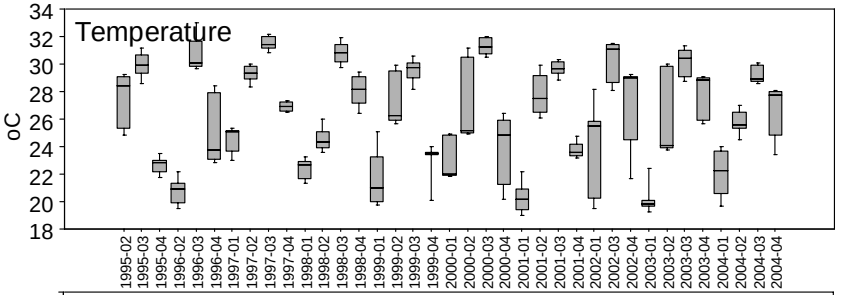

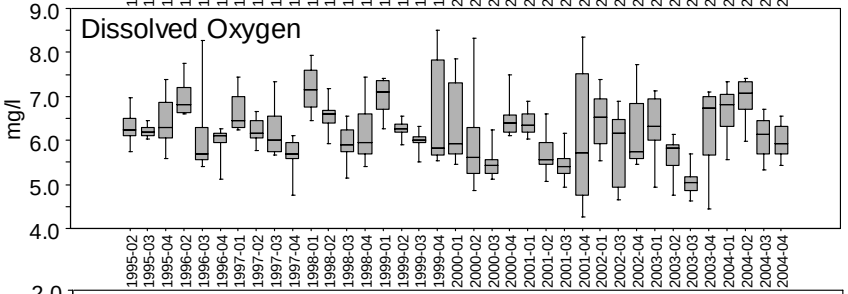

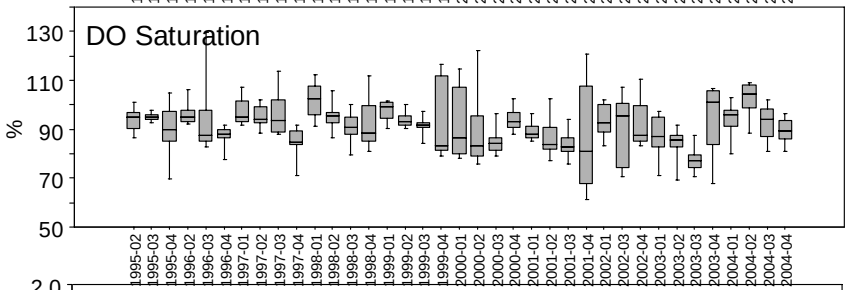

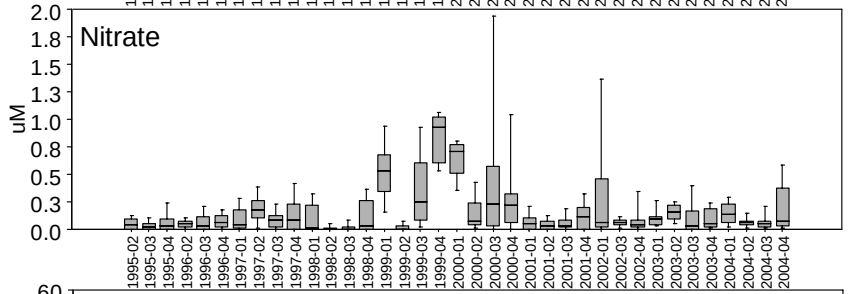

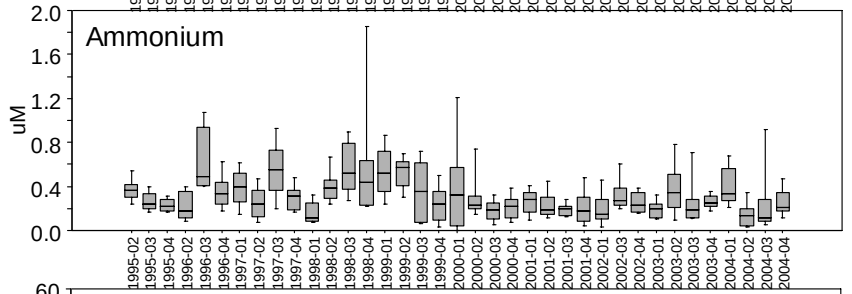

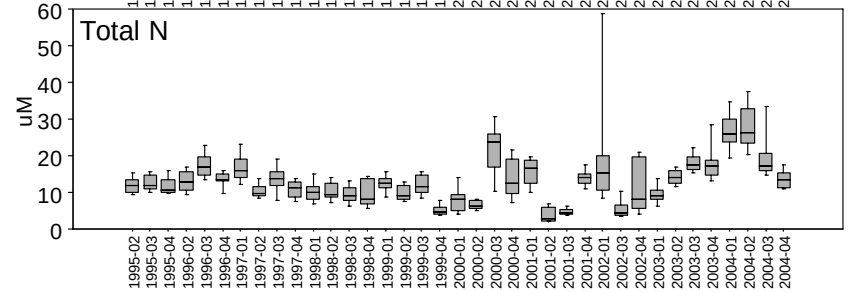

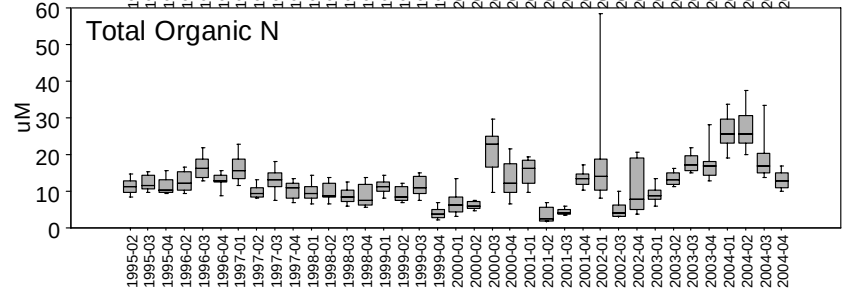

Cluster 8– North Marquesas/North Backcountry

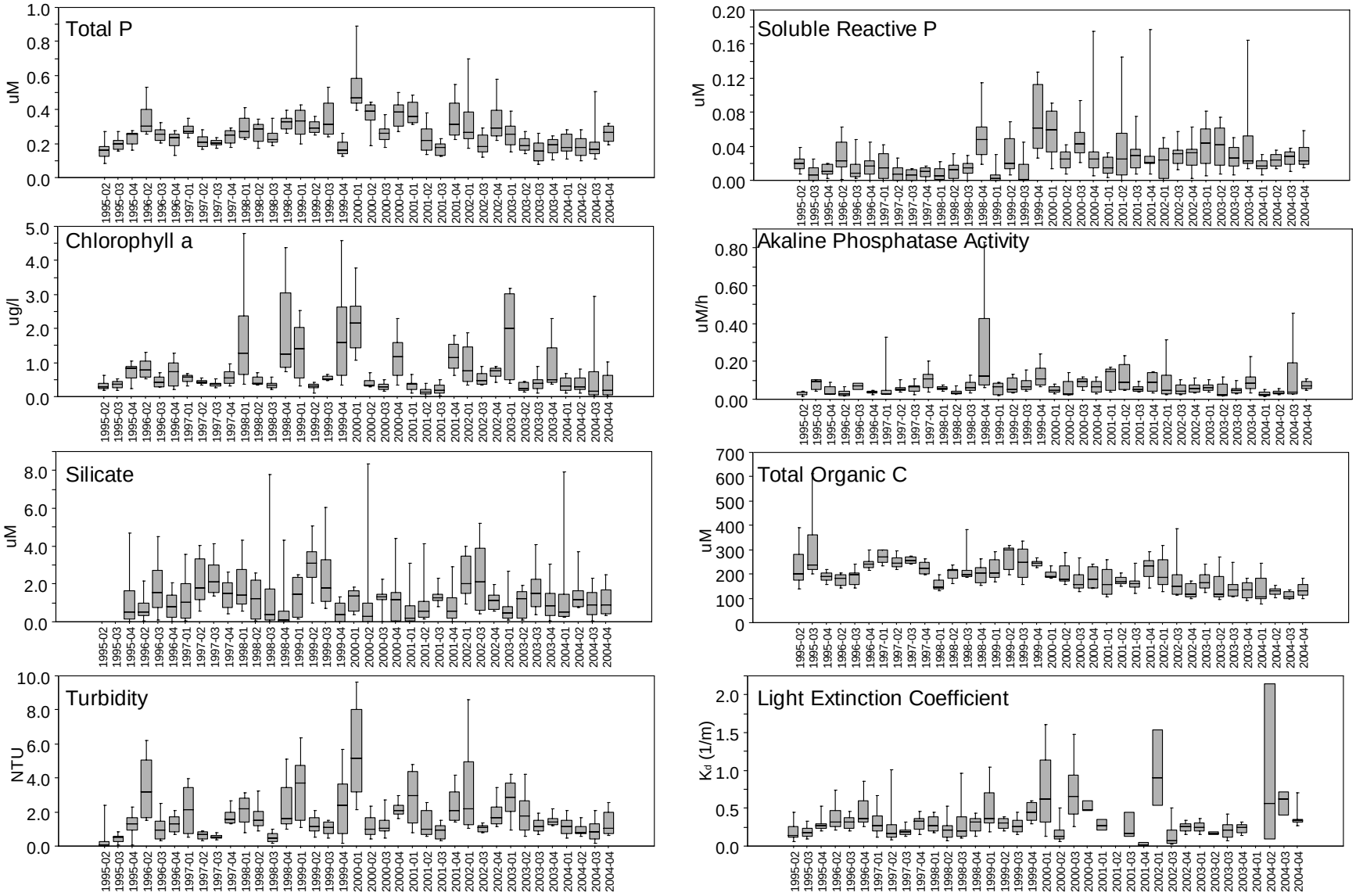

Figure 14

4. Overall Trends

Several important results have been realized from this monitoring project. The first is the documentation of elevated DIN in the nearshore zone of the Keys. This effect is not seen in a similar transect in the Tortugas which leaves landuse as the primary focus of attention.

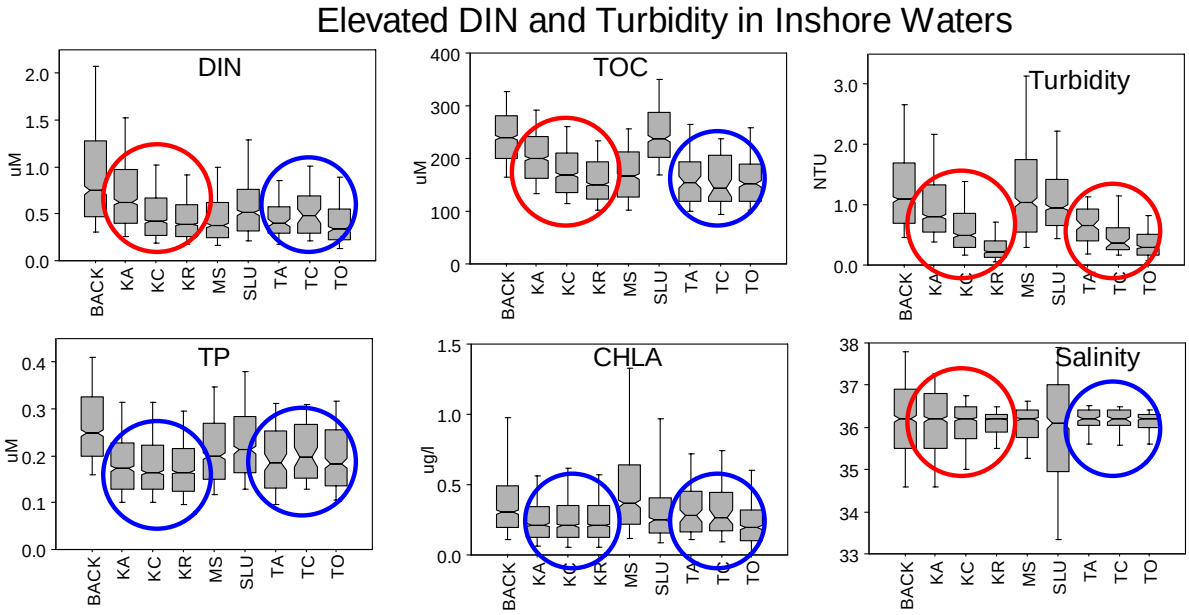

Figure 15

Second, highest CHLA concentrations are seen on the SW Florida Shelf with a strong gradient towards the Marquesas and Tortugas (Fig. 16). This is due to higher TP concentrations on the Shelf as a result of southerly advection of water along the coast (Fig. 17).

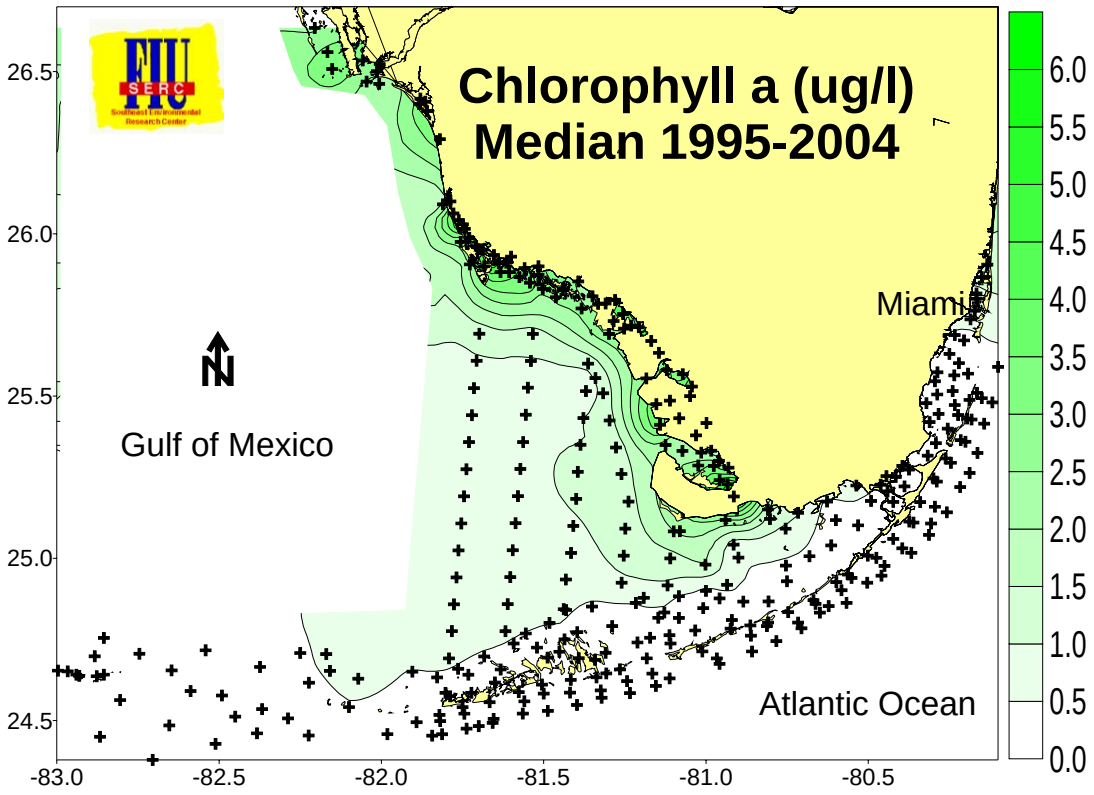

Figure 16

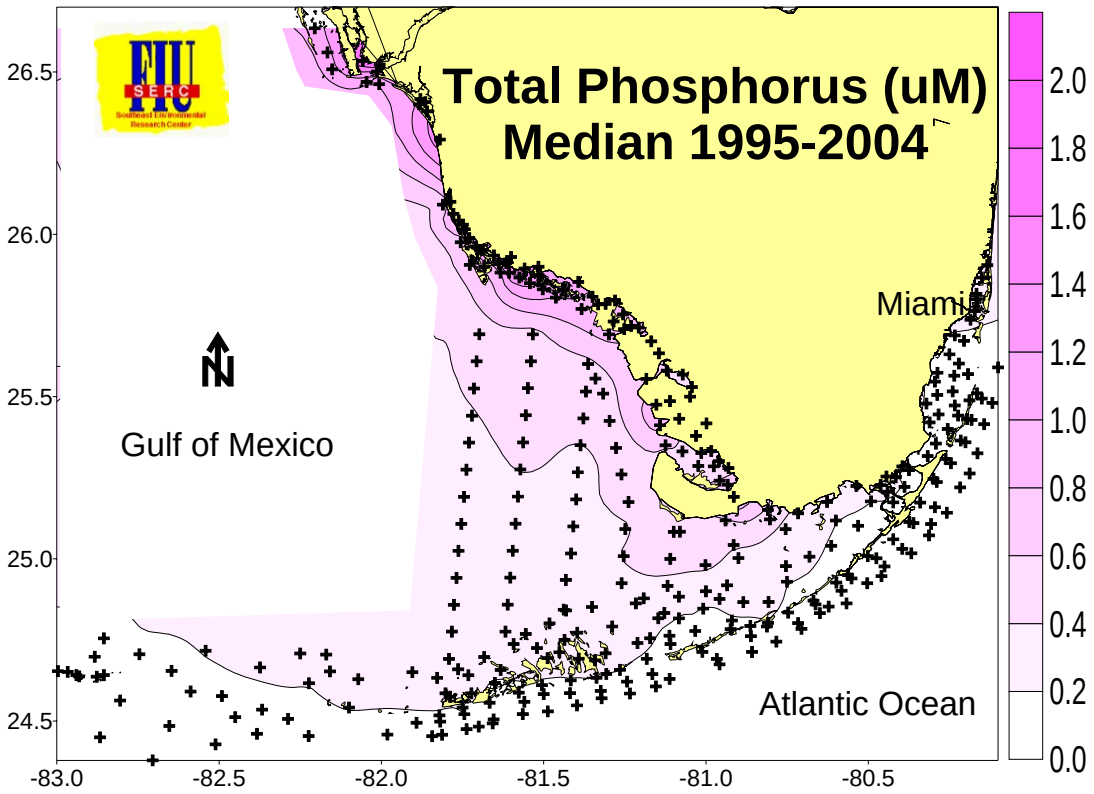

Figure 17

The third result is that trends in water quality showed most variables to relatively consistent from year to year, with some showing seasonal excursions. Overall, there were statistically significant **decreases** in DIN, TON (except for increases in Tortugas), TP, TOC, and DO throughout the region (Fig. 18). This is contrary to some of the trend analyses reported last year.

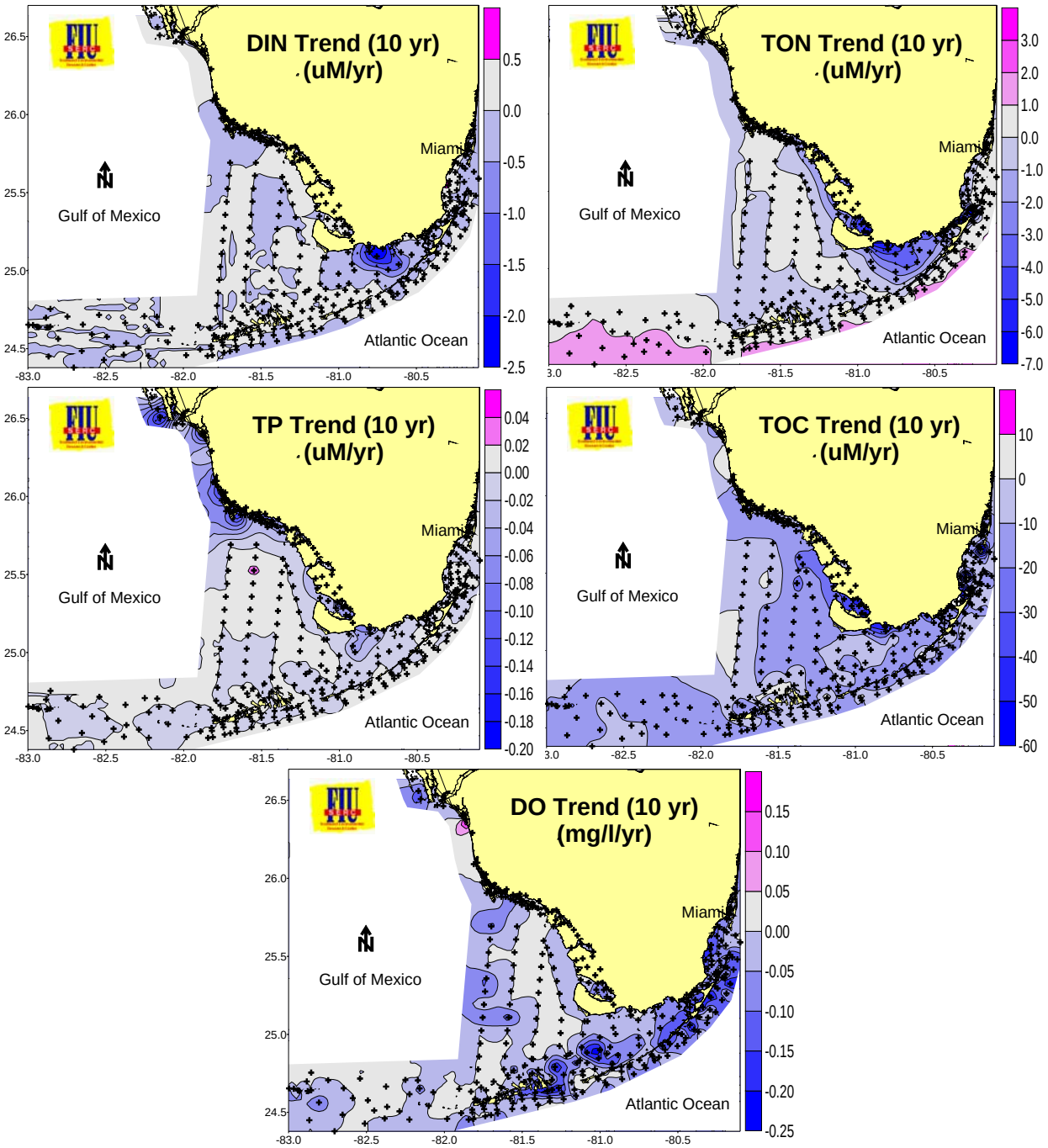

Figure 18

Clearly, there have been large changes in the FKNMS water quality over time, and some sustained monotonic trends have been observed, however, we must always keep in mind that trend analysis is limited to the window of observation. Trends may change, or even reverse, with additional data collection. This brings up another important point; when looking at what are perceived to be local trends, we find that they seem to occur across the whole region but at more damped amplitudes. This spatial autocorrelation in water quality is an inherent property of highly interconnected systems such as coastal and estuarine ecosystems driven by similar hydrological and climatological forcings. It is clear that trends observed inside the FKNMS are influenced by regional conditions outside the Sanctuary boundaries.

5. Discussion

Water quality is a subjective measure of ecosystem well being. Aside from the physical-chemical composition of the water there is also a human perceptual element which varies according to our intents for use (Kruczyinski and McManus 2002). Distinguishing internal from external sources of nutrients in the FKNMS is a difficult task. The finer discrimination of internal sources into natural and anthropogenic inputs is even more difficult. Most of the important anthropogenic inputs are regulated and most likely controlled by management activities, however, recent studies have shown that nutrients from shallow sewage injection wells may be leaking into nearshore surface waters (Corbett et al. 1999). Advective transport of nutrients through the FKNMS was not measured by the existing fixed sampling plan. However, nutrient distribution patterns may be compared to the regional circulation regimes in an effort to visualize the contribution of external sources and advective transport to internal water quality of the FKNMS.

Circulation in coastal South Florida is dominated by regional currents such as the Loop Current, Florida Current, and Tortugas Gyre and by local transport via Hawk Channel and along-shore Shelf movements (Klein and Orlando 1994). Regional currents may influence water quality over large areas by the advection of external surface water masses into and through the FKNMS (Lee et al. 1994, Lee et al. 2002) and by the intrusion of deep offshore ocean waters onto the reef tract as internal bores (Leichter et al. 1996). Local currents become more important in the mixing and transport of freshwater and nutrients from terrestrial sources (Smith 1994; Pitts 1997).

Spatial patterns of salinity in coastal South Florida show these major sources of freshwater to have more than just local impacts (Fig. 3 and http://serc.fiu.edu/wqmnetwork/CONTOUR%20MAPS/ContourMaps.htm). In Biscayne Bay, freshwater is released through the canal system operated by the South Florida Water Management District; the impact is clearly seen to affect northern Key Largo by causing episodic depressions in salinity at alongshore sites. Freshwater entering NE Florida Bay via overland flow from Taylor Slough and C-111 basin mix in a SW direction. The extent of influence of freshwater from Florida Bay on alongshore salinity in the Keys is less than that of Biscayne Bay but it is more episodic. Transport of low salinity water from Florida Bay does not affect the Middle Keys sites enough to depress the median salinity in this region but is

manifested as increased variability. On the west coast, the large influence of the Shark River Slough, which drains the bulk of the Everglades and exits through the Whitewater Bay - Ten Thousand Islands mangrove complex, is clearly seen to impact the Shelf waters. The mixing of Shelf waters with the Gulf of Mexico produces a salinity gradient in a SW direction which extends out to Key West. This freshwater source does not affect the Backcountry because of its shallow nature but instead follows a trajectory of entering western Florida Bay and exiting out through the channels in the Middle Keys (Smith 1994). This net transport of lower salinity water from mainland to reef in open channels through the Keys is observed as an increase in the range and variability of salinity rather than as a large depression in salinity.

In addition to surface currents there is evidence that internal tidal bores regularly impact the Key Largo reef tract (Leichter et al. 1996; Leichter and Miller 1999). Internal bores are episodes of higher density, deep water intrusion onto the shallower shelf or reef tract. Depending on their energy, internal tidal bores can promote stratification of the water column or cause complete vertical mixing as a breaking internal wave of sub-thermocline water. According to $\Delta\sigma_t$, the SW area of the Tortugas segment tends to experience the greatest frequency of stratification events. The decreased temperature and increased salinity in bottom waters from intrusion of deeper denser oceanic waters to this region may also account for increases in NO_3^-, TP, and SRP in these bottom waters as well.

Surface $Si(OH)_4$ concentrations exhibited a pattern similar to salinity. The source of $Si(OH)_4$ in this geologic area of carbonate rock and sediments is from siliceous periphyton (diatoms) growing in the Shark River Slough, Taylor Slough, and C-111 basin watersheds. Unlike the Mississippi River plume with CHLA concentrations of 76 $\mu g\ l^{-1}$ (Nelson and Dortch 1996), phytoplankton biomass on the Shelf (1-2 $\mu g\ l^{-1}$ CHLA) was not sufficient to account for the depletion of $Si(OH)_4$ in this area. Therefore, $Si(OH)_4$ concentrations on the Shelf were depleted by mixing alone allowing $Si(OH)_4$ to be used as a semi-conservative tracer of freshwater in this system (Ryther et al. 1967; Moore et al. 1986). Unlike Florida Bay and the west coast, there was very little $Si(OH)_4$ loading to southern Biscayne Bay, mostly because the source of freshwater to this system is from canals which drain agricultural and urban areas of Dade County.

In the Lower and Middle Keys, it is clear that the source of $Si(OH)_4$ to the nearshore Atlantic waters is through the Sluiceway and Backcountry (Fig. 19). $Si(OH)_4$ concentrations near the coast were elevated relative to the reef tract with much higher concentrations occurring in the

Lower and Middle Keys than the Upper Keys. There is an interesting peak in $Si(OH)_4$ concentration in an area of the Sluiceway which is densely covered with the seagrass, *Syringodium* (Fourqurean et al. 2002). We are unsure as to the source but postulate that it may be due to benthic flux.

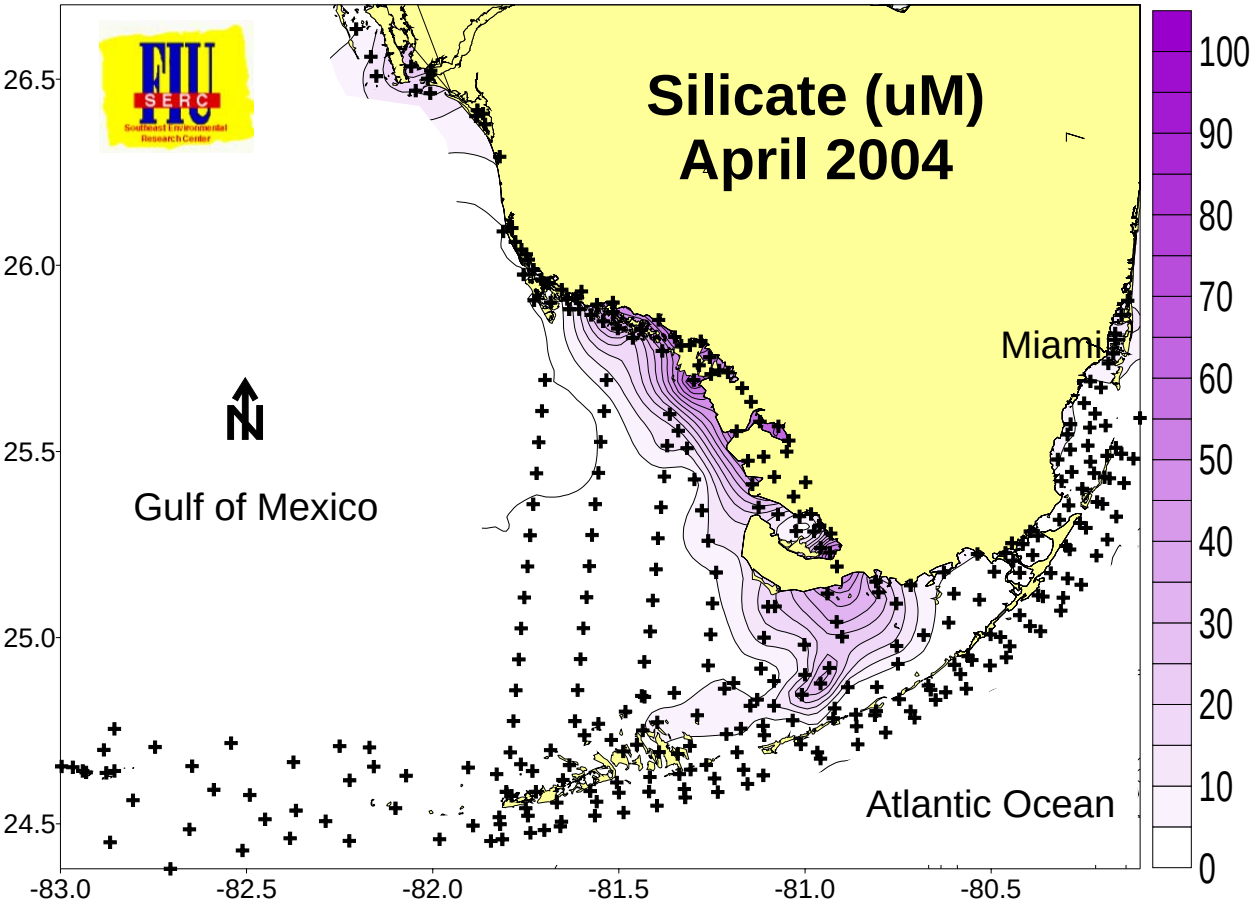

Figure 19. Example of silicate distributions across the region during spring 2004.

Visualization of spatial patterns of NO_3^- concentration over South Florida waters provide an extended view of source gradients over the region (see website). Biscayne Bay, Florida Bay, and the Shark River area of the west coast exhibited higher NO_3^- concentrations relative to the FKNMS and Shelf. Elevated NO_3^- in Biscayne Bay is the result of loading from both the canal drainage system and from inshore groundwater (Alleman et al. 1995, Meeder et al. 1997). The source of NO_3^- to Florida Bay is the Taylor Slough and C-111 basin (Boyer and Jones, 1999; Rudnick et al., 1999) while the Shark River Slough impacts the west coast mangrove rivers and out onto the Shelf (Rudnick et al., 1999). We speculate that in both cases, elevated NO_3^- concentrations are the result of N_2 fixation/nitrification within the mangroves (Pelegri and Twilley 1998). The oceanside transects off the uninhabited Upper Keys (off Biscayne Bay in

Seg. 9) exhibited the lowest alongshore NO_3^- compared to the Middle and Lower Keys. A similar pattern was observed in a previous transect survey from these areas (Szmant and Forrester 1996). They also showed an inshore elevation of NO_3^- relative to Hawk Channel and the reef tract which is also demonstrated in our analysis (Fig. 20). Interestingly, NO_3^- concentrations in all stations in the Tortugas transect were similar to those of reef tract sites in the mainland Keys; there was no inshore elevation of NO_3^- on the transect off uninhabited Loggerhead Key. We suggest this source of NO_3^- in the Keys is the due to human shoreline development.

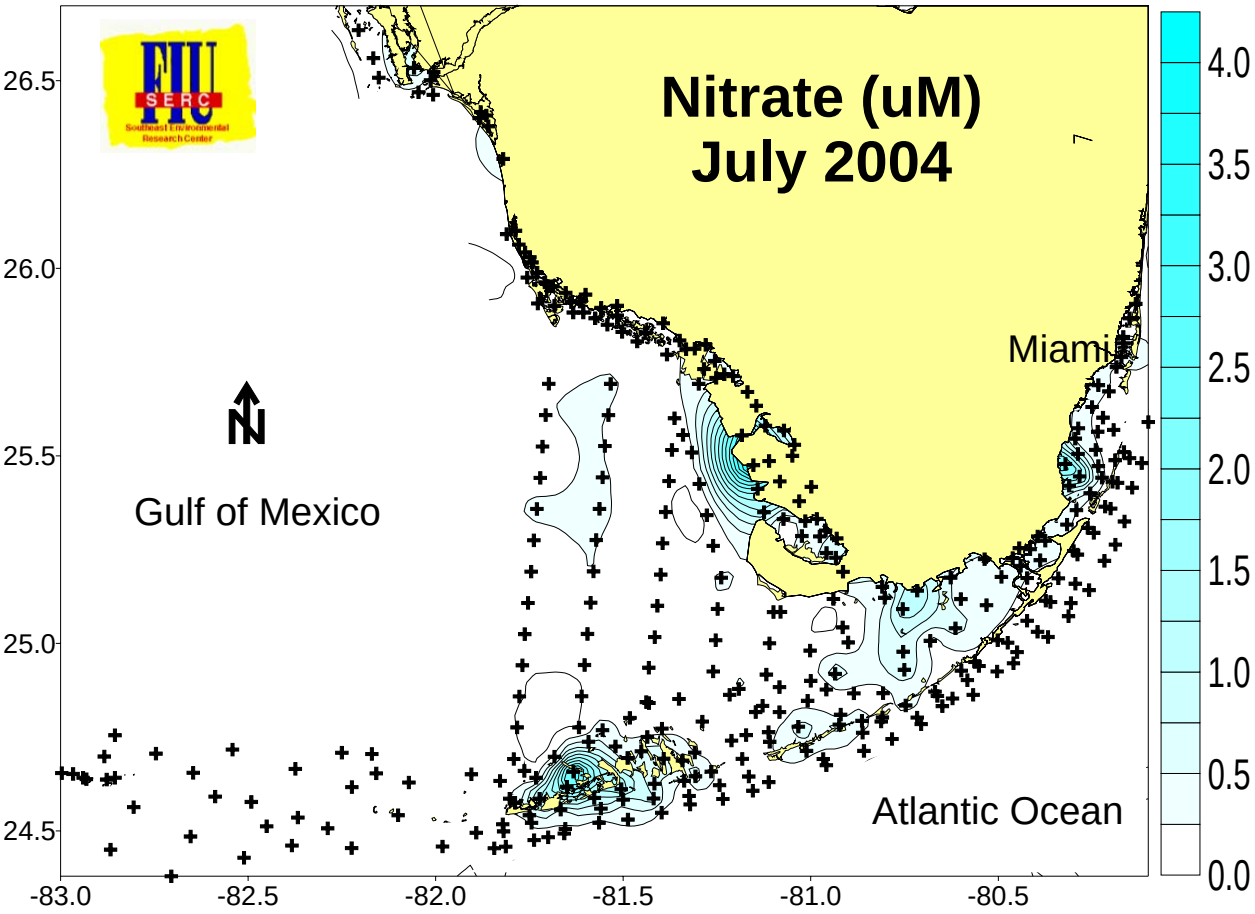

Figure 20. Example of nitrate distributions across the region during summer 2004.

Figure 20 also shows that a distinct intensification of NO_3^- occurs in the Backcountry region. Part of this increase may due to local sources of NO_3^-, i.e. septic systems and stormwater runoff around Big Pine Key (Lapointe and Clark 1992). However, there is another area, the Snipe Keys, that also exhibits high NO_3^- which is uninhabited by man, which rules out the premise of septic systems being the only source of NO_3^- in this area. It is important to note that the Backcountry area is very shallow (~0.5 m) and hydraulically isolated from the Shelf and Atlantic

which results in its having a relatively long water residence time. Elevated NO_3^- concentrations may be partially due to simple evaporative concentration as is seen in locally elevated salinity values. Another possibility is a contribution of benthic N_2 fixation/nitrification in this very shallow area.

NH_4^+ concentrations were distributed in a similar manner as NO_3^- with highest levels occurring in Florida Bay, the Ten Thousand Islands, and the Backcountry. NH_4^+ concentrations were very low in Biscayne Bay because it is not a major component of loading from the canal drainage system. NH_4^+ also showed similarities with NO_3^- in its spatial distribution, being lowest in the Upper Keys and highest inshore relative to offshore. There was no alongshore elevation of NH_4^+ concentrations in the Tortugas where levels were similar to those of reef tract sites in the mainland Keys. That the least developed portion of the Upper Keys in Biscayne National Park and uninhabited Loggerhead Key (Tortugas) exhibited lowest NO_3^- and NH_4^+ concentrations is evidence of a local anthropogenic source for both of these variables along the ocean side of the Upper, Middle, and Lower Keys. This pattern of decline offshore implies an onshore N source which is diluted with distance from land by low nutrient Atlantic Ocean waters.

Elevated DIN concentrations in the Backcountry, on the other hand, are not so easily explained. We postulate that the high concentrations found there are due to a combination of anthropogenic loading, physical entrapment, and benthic N_2 fixation. The relative contribution of these potential sources is unknown. Lapointe and Matzie (1996) have shown that stormwater and septic systems are responsible for increased DIN loading in and around Big Pine Key. The effect of increased water residence time in DIN concentration is probably small. Salinities in this area were only 1-2 higher than local seawater which resulted in a concentration effect of only 5-6%. Benthic N_2 fixation may potentially be very important in the N budget of the Backcountry. Measured rates of N_2 fixation in a *Thalassia* bed in Biscayne Bay, having very similar physical and chemical conditions, were 540 μmol N m^{-2} d^{-1} (Capone and Taylor 1980). Without the plant community N demand, one day of N_2 fixation has the potential to generate a water column concentration of >1 μM NH_4^+ (0.5 m deep). Much of this NH_4^+ is probably nitrified and may help account for the elevated NO_3^- concentrations observed in this area as well. Clearly, N_2 fixation may be a significant component of the N budget in the Backcountry and that it may be a exported as DIN to the FKNMS in general.

Spatial patterns in TP in South Florida coastal waters were strongly driven by the west coast sources (Fig. 21). A small gradient in TP extended from the inshore waters of Whitewater Bay - Ten Thousand Islands mangrove complex out onto the Shelf and Tortugas. A weak gradient also extended from north central Florida Bay to the Middle Keys. Brand (1997) has postulated that groundwater from a subterranean Miocene quartz sand channel, "the river of sand", containing high levels of phosphorus is the source of TP in this region. However, little evidence of this source exists to date and field data from Florida Bay does not indicate a subterranean source (Corbett et al. 1999; Boyer and Jones unpublished data). Finally, there was no evidence of a significant terrestrial source of TP to Biscayne Bay.

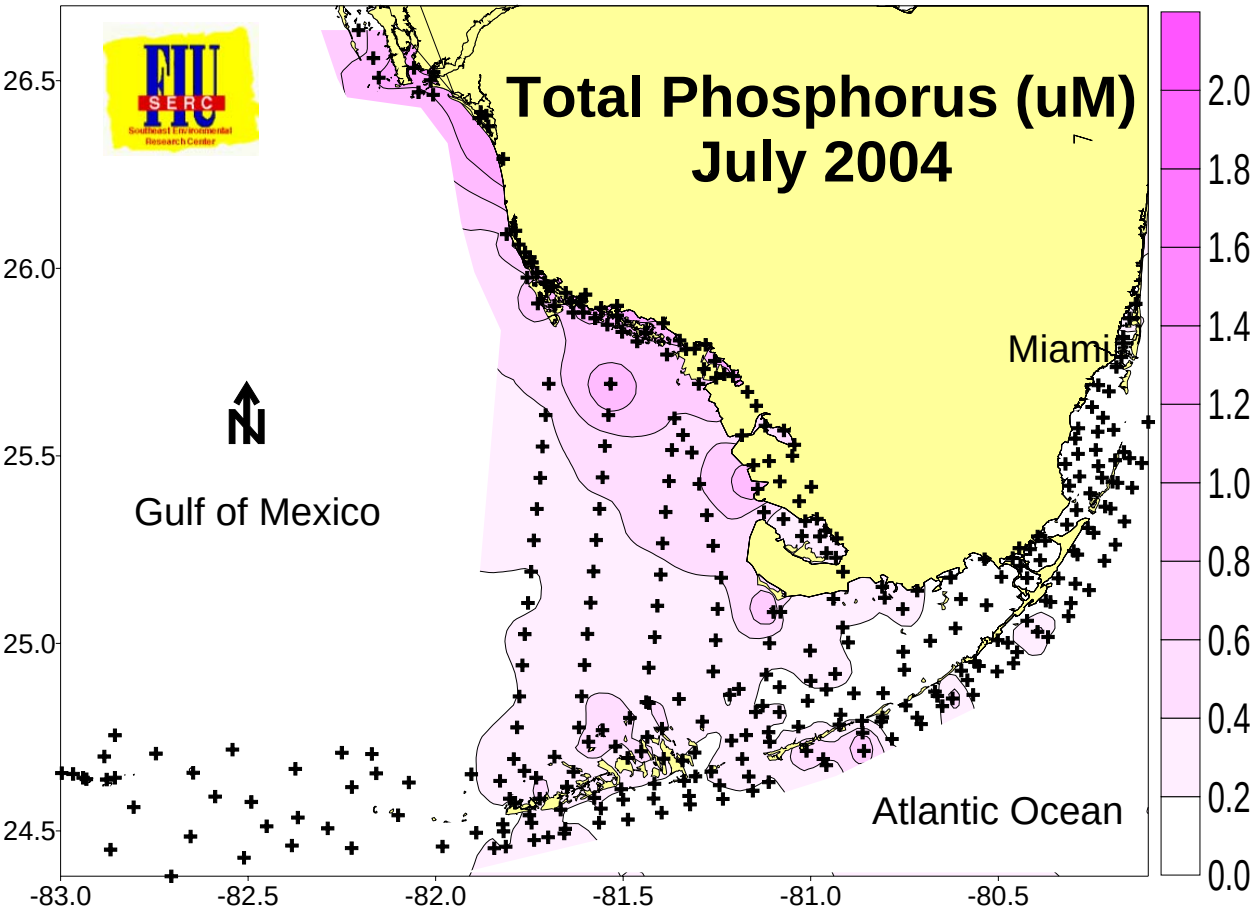

Figure 21. Example of total phosphorus distributions across the region during summer 2004.

In the Keys, there was evidence of elevated TP in alongshore stations of the Middle and Lower Keys but the differences were very small. The Upper Keys actually showed higher TP concentrations on the reef tract than inshore implying an offshore source. Interestingly, the Tortugas area had higher TP concentrations than the Upper Keys as a result of Shelf water advection. In South Florida coastal waters, very little of TP is found in the inorganic form

(SRP); most is organic P. The distribution of SRP on the west coast and Shelf was similar to that of TP with the general gradient from the west coast to Tortugas remaining (Appendix). However, the SRP distribution was distinctly different from that of TP in Florida Bay, Whitewater Bay, and Biscayne Bay. In central Florida Bay the N-S gradient previously observed for TP was highly diminished for SRP indicating that almost all the TP in central Florida Bay was in the form of organic P. It is unlikely that the source of TP to this region is from overland flow or groundwater as this is also the region that expresses highest salinity. Alternately, we hypothesize that the presence of the Flamingo channel, running parallel to the southern coastline of Cape Sable, acts as a tidal conduit for episodic advection of inshore Shelf water to enter north central Florida Bay. Subsequent trapping and evaporation then may act to concentrate TP in this region. The second difference in P distributions was that there was a significant SRP gradient present in NE Florida Bay that was not observed for TP. The sources of SRP to this area are the Taylor Slough and C-111 basin (W. Walker per. communication; Boyer and Jones, 1999; Rudnick et al., 1999). Whitewater Bay displayed an east-west gradient in SRP concentrations which increased with salinity leading us to conclude that the freshwater inputs from the Everglades were not a source of SRP to this area. Finally, there was evidence of a significant onshore-offshore SRP gradient in southern Biscayne Bay; most probably as a direct result of canal loading and groundwater seepage to this region (A. Lietz personal communication; Meeder et al. 1997).

Concentrations of TOC (Fig. 22) and TON (Appendix) are remarkably similar in pattern of distribution across the South Florida coastal hydroscape. The decreasing gradient from west coast to Tortugas was very similar to that of TP. A steep gradient with distance from land was also observed in Biscayne Bay. Both these gradients were most probably due to terrestrial loading. On the west coast, the source of TOC and TON was from the mangrove forests. Our data from this area shows that concentrations of TOC and TON increased from Everglades headwaters through the mangrove zone and then decrease with distance offshore. In Biscayne Bay, much of the TOC and TON is from agricultural land use. The high concentrations of TOC and TON found in Florida Bay were due to a combination of terrestrial loading (Boyer and Jones, 1999), in situ production by seagrass and phytoplankton, and evaporative concentration (Fourqurean et al. 1993).

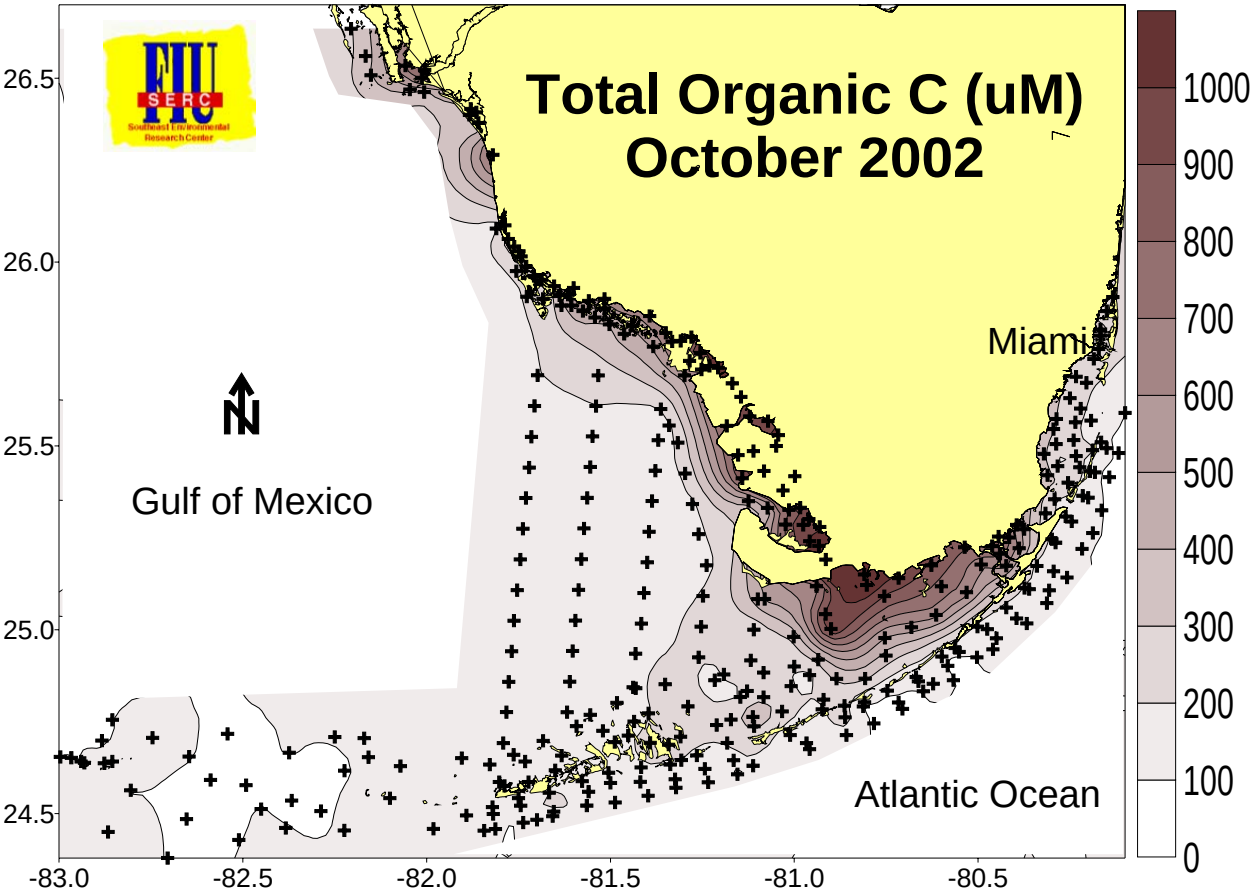

Figure 22. Example of total organic carbon distributions across the region during fall 2002.

Advection of Shelf and Florida Bay waters through the Sluiceway and passes accounted for this region and the inshore area of the Middle Keys as having highest TOC and TON of the FKNMS. Strong offshore gradients in TOC and TON existed for all mainland Keys segments but not for the Tortugas transect. Part of this difference may be explained by the absence of mangroves in the single Tortugas transect. The higher concentrations of TOC and TON in the inshore waters of the Keys implies a terrestrial source rather than simply benthic production and sediment resuspension. Main Keys reef tract concentrations of TOC and TON were similar to those found in the Tortugas.

Much emphasis has been placed on assessing the impact of episodic phytoplankton blooms in Florida Bay on the offshore reef tract environment. Spatial patterns of CHLA concentrations showed that NW Florida Bay, Whitewater Bay, and the Ten Thousand Islands exhibited high levels of CHLA relative to Biscayne Bay, Shelf, and FKNMS (Fig. 23). The highest CHLA concentrations were found in west coast mangrove estuaries (up to 45 $\mu g\ l^{-1}$ in Alligator Bay, TTI). CHLA is also routinely higher (~2 $\mu g\ l^{-1}$) in NW Florida Bay along the channel

connecting the Shelf to Flamingo. It is interesting that CHLA concentrations are higher in the Marquesas (0.36 µg l^{-1}) than in other areas of the FKNMS. When examined in context with the whole South Florida ecosystem, it is obvious that the Marquesas zone should be considered a continuum of the Shelf rather than a separate management entity. This shallow sandy area (often called the Quicksands) acts as a physical mixing zone between the Shelf and the Atlantic Ocean and is a highly productive area for other biota as well as it encompasses the historically rich Tortugas shrimping grounds. A CHLA concentration of 2 µg l^{-1} in the water column of a reef tract might be considered an indication of eutrophication. Conversely, a similar CHLA level in the Quicksands indicates a productive ecosystem which feeds a valuable shrimp fishery.

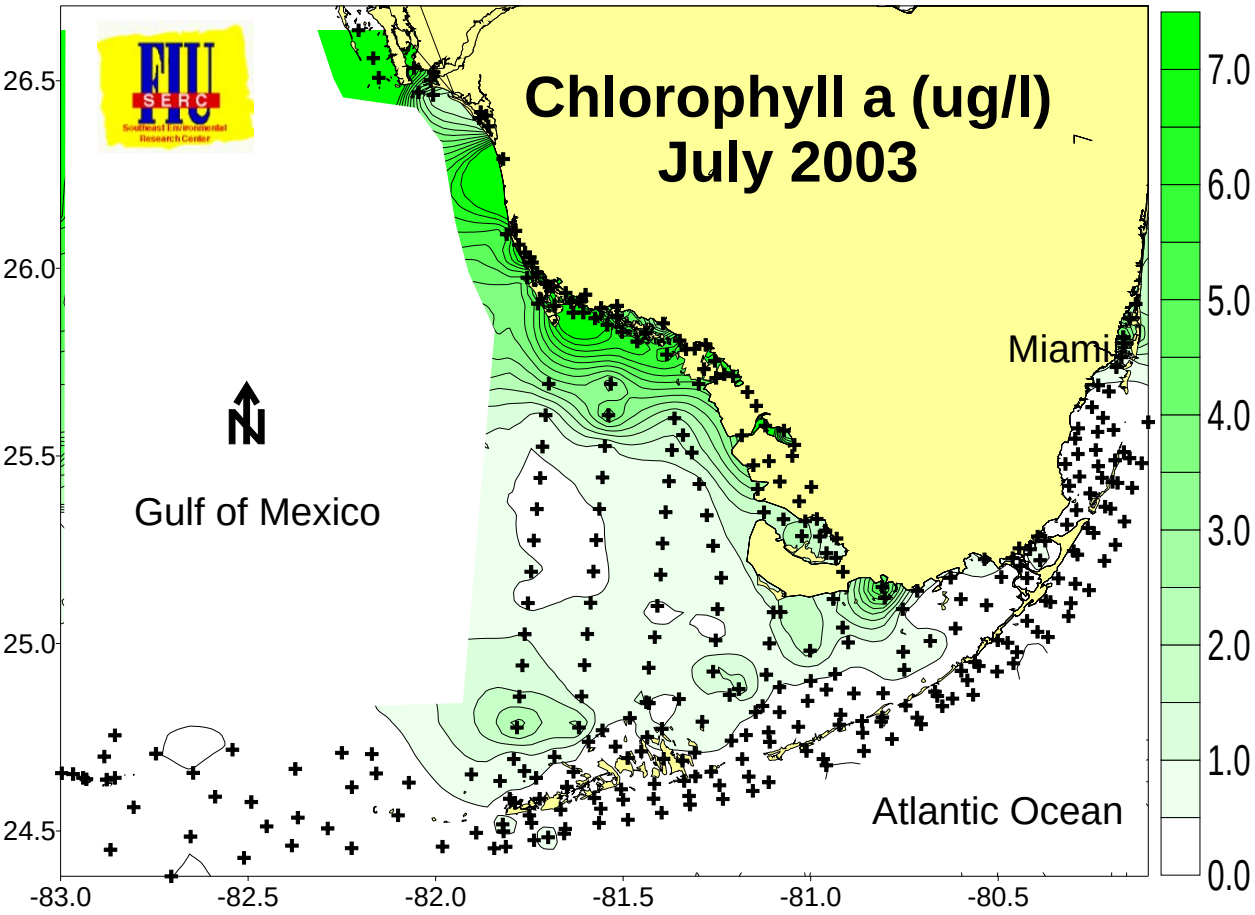

Figure 23. Example of chlorophyll a distributions across the region during summer 2003.

The oceanside transects in the Upper Keys exhibited the lowest overall CHLA concentrations of any zone in the FKNMS. Transects off the Middle and Lower Keys showed that a drop in CHLA occurred at reef tract sites; there was no linear decline with distance from shore. Interestingly, CHLA concentrations in the Tortugas transect showed a similar pattern as the

mainland Keys. Inshore and Hawk Channel CHLA concentrations among Middle Keys, Lower Keys and Tortugas sites were not significantly different. As inshore CHLA concentrations in the Tortugas were similar to those in the Middle and Lower Keys, we see no evidence of persistent phytoplankton bloom transport from Florida Bay.

Along with TP, turbidity is probably the second most important determinant of local ecosystem health (Fig. 24). The fine grained, low density carbonate sediments in this area are easily resuspended, rapidly transported, and have high light scattering potential. Sustained high turbidity of the water column indirectly affects benthic community structure by decreasing light penetration, promoting seagrass extinction.

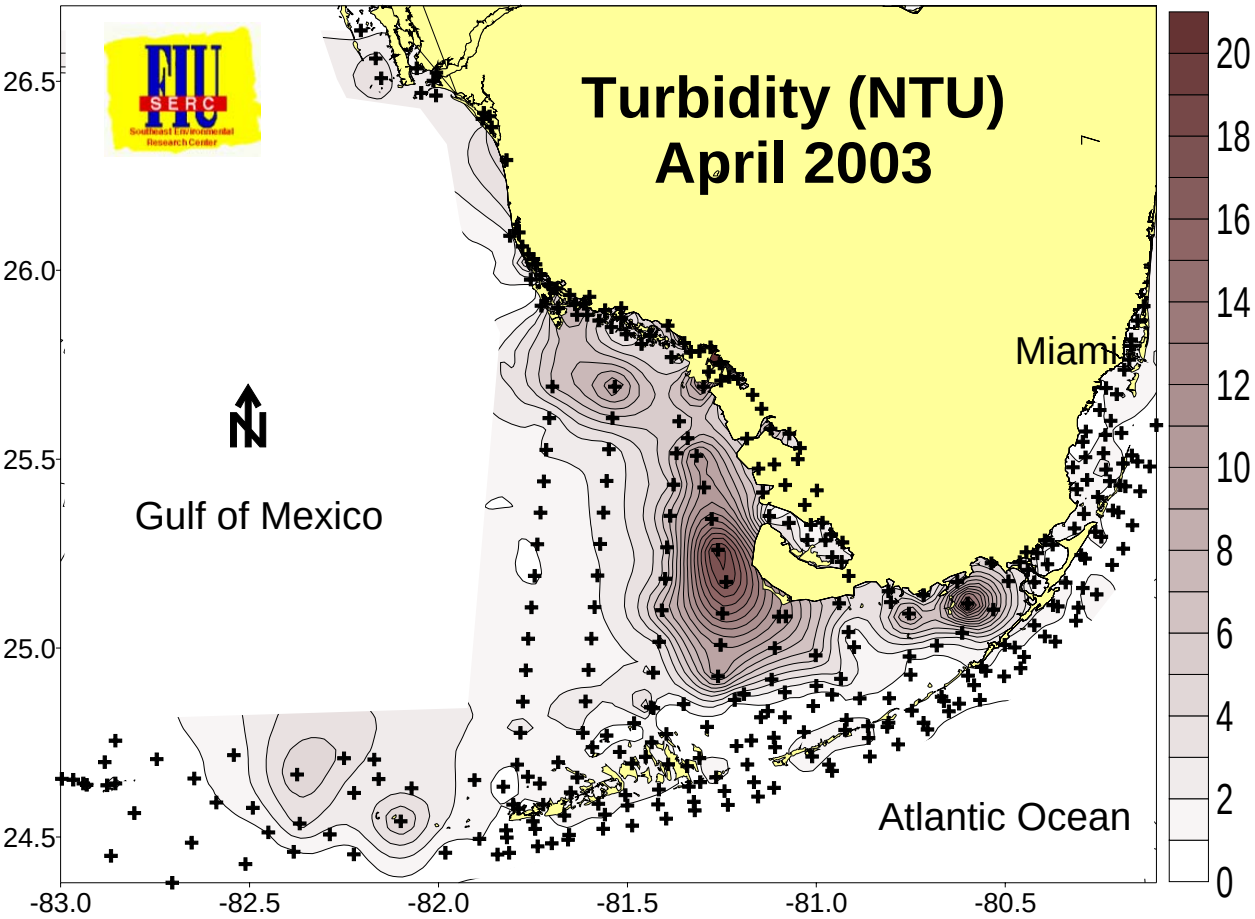

Figure 24. Example of turbidity distributions across the region during spring 2003.

Large scale observations of turbidity clearly show patterns of onshore-offshore gradients which extend out onto the Shelf to the Marquesas (Appendix; Stumpf et al. 1999). In the last seven years, turbidities in Florida Bay have increased dramatically in the NE and central regions (Boyer et al. 1998) potentially as a consequence of destabilization of the sediment from seagrass

die-off (Robblee et al. 1991). Strong turbidity gradients were observed for all Keys transects but reef tract levels were remarkably similar regardless of inshore levels. High alongshore turbidity is most probably due to the shallow water column being easily resuspended by wind and wave action. Light extinction (K_d) was highest alongshore and improved with distance from land. This trend was expected as light extinction is directly related to water turbidity.

Using the TN:TP ratio has been used as a relatively simple method of estimating potential nutrient limitation status of phytoplankton (Redfield 1967). Most of the South Florida hydroscape has TN:TP values >> 16:1, indicating the potential for phytoplankton to be limited by P at these sites. However, most of the TN is not available to phytoplankton while much of the TP is labile. Therefore, using the TN:TP ratio overestimates potential P limitation and should be recognized as such (Fig. 25).

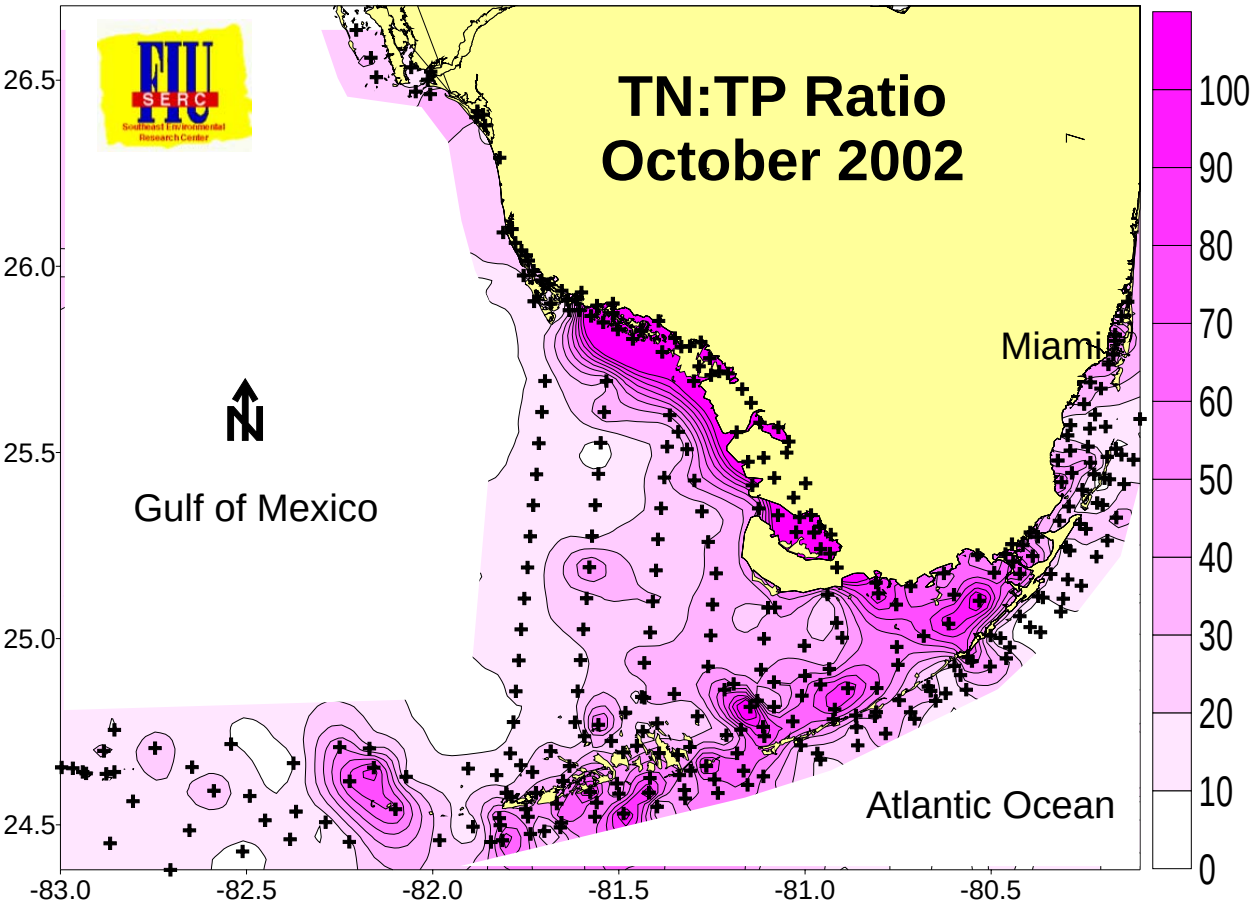

Figure 25. Example of DIN:TP ratio distribution across the region during fall 2002.

The bulk of Florida Bay and both southern and northern Biscayne Bay were severely P limited, mostly as a result of high DIN concentrations. Most of the FKNMS is routinely P

limited using this metric. Interestingly, the Shelf and Tortugas area was the least P limited of all zones and exhibited a significant regression between SRP and CHLA. Only in the northern Ten Thousand Islands and Shelf did N become the limiting nutrient. The south-north shift from P to N limitation observed in the west coast estuaries has been ascribed to changes in landuse and bedrock geochemistry of the watersheds (Boyer and Jones 1998). The west coast south of 25.4 N latitude is influenced by overland freshwater flow from the Everglades and Shark River Slough having very low P concentrations relative to N. Above 25.7 N latitude the bedrock geology of the watershed changes from carbonate to silicate based and landuse changes from relatively undeveloped wetland (Big Cypress Basin) to a highly urban/agricultural mix (Naples, FL).

This brings up an important point that, when looking at what are perceived to be local trends, we find that they seem to occur across the whole region but at more damped amplitudes. This spatial autocorrelation in water quality is an inherent property of highly interconnected systems such as coastal and estuarine ecosystems driven by similar hydrological and climatological forcings. Clearly, there have been large changes in the FKNMS water quality over time, and some sustained monotonic trends have been observed, however, we must always keep in mind that trend analysis is limited to the window of observation. Trends may change, or even reverse, with additional data collection.

The large scale of this monitoring program has allowed us to assemble a much more holistic view of broad physical/chemical/biological interactions occurring over the South Florida hydroscape. Much information has been gained by inference from this type of data collection program: major nutrient sources have be confirmed, relative differences in geographical determinants of water quality have been demonstrated, and large scale transport via circulation pathways have been elucidated. In addition we have shown the importance of looking "outside the box" for questions asked within. Rather than thinking of water quality monitoring as being a static, non-scientific pursuit it should be viewed as a tool for answering management questions and developing new scientific hypotheses.

We continue to maintain a website (http://serc.fiu.edu/wqmnetwork/) where data from the FKNMS is integrated with the other parts of the SERC water quality network (Florida Bay, Whitewater Bay, Biscayne Bay, Ten Thousand Islands, and SW Florida Shelf) and displayed as downloadable contour maps, time series graphs, and interpretive reports.

5.1. Acknowledgments

I thank all the field and laboratory technicians involved with this project, especially Pete Lorenzo, John Fulop, George Meichel, Ruth Justiniano, Pura Rodriguez de la Vega, Pierre Sterling, and Frank Tam. Special thanks to Danielle Mir-Gonzalez for help with time series analysis. We also thank the captains and crew of the R/V Bellows of the Florida Institute of Oceanography for their professional support of the monitoring program. This project was possible due to continued funding by the US-EPA (Agreement #X994621-94-0) and the South Florida Water Management District (Contract #C-15397). This is Technical Report #T-259 of the Southeast Environmental Research Center at Florida International University.

6. References

ALLEMAN, R. W., ET AL. 1995. Biscayne Bay surface water improvement and management. Technical supporting document. South Florida Water Management District.

BOYER, J. N., J. W. FOURQUREAN, AND R. D. JONES. 1997. Spatial characterization of water quality in Florida Bay and Whitewater Bay by multivariate analysis: Zones of similar influence (ZSI). Estuaries 20: 743-758.

BOYER, J. N., J. W. FOURQUREAN, AND R. D. JONES. 1999. Seasonal and long term trends in the water quality of Florida Bay (1989 - 1997). Estuaries 22: 417-430.

BOYER, J. N., AND R. D. JONES. 1998. Influence of coastal morphology and watershed characteristics on the water quality of mangrove estuaries in the Ten Thousand Islands - Whitewater Bay complex. Proceedings of the 1998 Florida Bay Science Conference. University of Florida Sea Grant.

BOYER, J. N., AND R. D. JONES. 1999. Effects of freshwater inputs and loading of phosphorus and nitrogen on the water quality of Eastern Florida Bay, p. 545-561. *In* K. R. Reddy, G. A. O'Connor, and C. L. Schelske (eds.) Phosphorus biogeochemistry in sub-tropical ecosystems. CRC/Lewis Publishers, Boca Raton, Florida.

BOYER, J. N., AND R. D. JONES. 2002. A view from the bridge: External and internal forces affecting the ambient water quality of the Florida Keys National Marine Sanctuary, p. 609-628. *In* J. W. Porter and K. G. Porter (eds.), The Everglades, Florida Bay, and Coral Reefs of the Florida Keys: An Ecosystem Sourcebook. CRC Press.

BOYER, J. N., P. STERLING, AND R. D. JONES. 2000. Maximizing information from a water quality monitoring network through visualization techniques. Estuarine, Coastal and Shelf Science 50: 39-48.

BRAND, L. 1998. The role of groundwater in the Florida Bay ecosystem. Proceedings of the 1998 Florida Bay Science Conference. University of Florida Sea Grant.

CAPONE, D. G., AND B. F. TAYLOR. 1980. Microbial nitrogen cycling in a seagrass community, p. 153-161. *In* V. S. Kennedy (ed.), Estuarine Perspectives. Academic.

CHRISTIAN, R. R., J. N. BOYER, D. W. STANLEY, AND W. M. RIZZO. 1991. Multi-year distribution patterns of nutrients in the Neuse River Estuary, North Carolina. Marine Ecology Progress Series 71:259-274.

ENVIRONMENTAL PROTECTION AGENCY. 1995. Water quality protection program for the Florida Keys National Marine Sanctuary: Phase III report. Final report submitted to the Environmental Protection Agency under Work Assignment 1, Contract No. 68-C2-0134. Battelle Ocean Sciences, Duxbury, MA and Continental Shelf Associates, Inc., Jupiter FL.

FOURQUREAN, J.W., M.D. DURAKO, M.O. HALL AND L.N. HEFTY. 2002. Seagrass distribution in south Florida: a multi-agency coordinated monitoring program, p. 497-522. *In* J. W. Porter and K. G. Porter (eds.), The Everglades, Florida Bay, and Coral Reefs of the Florida Keys: An Ecosystem Sourcebook. CRC Press.

HIRSCH, R. M., R. B. ALEXANDER, AND R. A. SMITH. 1991. Selection of methods for the detection and estimation of trends in water quality. Water Resources Research 27:803-813.

ISAAKS, E. H., AND R. M. SRIVASTAVA. 1989. An Introduction to Applied Geostatistics. Oxford Press, 561 pp.

JONES, R. D., AND J. N. BOYER 2001. 2000 Annual Report of the Water Quality Monitoring Project for the Florida Keys National Marine Sanctuary. SERC Technical Report #T151.

KLEIN, C. J., AND S. P. ORLANDO JR. 1994. A spatial framework for water-quality management in the Florida Keys National Marine Sanctuary. Bulletin of Marine Science 54: 1036-1044.

LAPOINTE, B. E., AND M. W. CLARK. 1992. Nutrient inputs from the watershed and coastal eutrophication in the Florida Keys. Estuaries 15: 465-476.

LAPOINTE, B. E., AND W. R. MATZIE. 1996. Effects of stormwater nutrient discharges on eutrophication processes in nearshore waters of the Florida Keys. Estuaries 19: 422-435.

LEE, T. N., M. E. CLARKE, E. WILLIAMS, A. F. SZMANT, AND T. BERGER. 1994. Evolution of the Tortugas gyre and its influence on recruitment in the Florida Keys. Bulletin of Marine Science 54: 621-646.

LEE, T. N., E. WILLIAMS, E. JOHNS, D. WILSON, AND N. P. SMITH. 2002. Transport processes linking South Florida ecosystems, p. 309-342. *In* J. W. Porter and K. G. Porter (eds.), The Everglades, Florida Bay, and Coral Reefs of the Florida Keys: An Ecosystem Sourcebook. CRC Press.

LEICHTER, J. J., S. R. WING, S. L. MILLER, AND M. W. DENNY. 1996. Pulsed delivery of subthermocline water to Conch Reef (Florida Keys) by internal tidal bores. Limnology and Oceanography 41: 1490-1501.

LEICHTER, J. J. , AND S. L. MILLER. 1999. Predicting high-frequency upwelling: Spatial and temporal patterns of temperature anomalies on a Florida coral reef. Continental Shelf Research 19: 911-928

MEEDER, J. F., J. ALVORD, M. BYRNE, M. S. ROSS, AND A. RENSHAW. 1997. Distribution of benthic nearshore communities and their relationship to groundwater nutrient loading. Final report to Biscayne National Park.

MOORE, W. S., J. L. SARMIENTO, AND R. M. KEY. 1986. Tracing the Amazon component of surface Atlantic water using ^{228}Ra, salinity, and silica. Journal of Geophysical Research 91: 2574-2580.

NELSON, D. M., AND Q. DORTCH. 1996. Silicic acid depletion and silicon limitation in the plume of the Mississippi River: evidence from kinetic studies in spring and summer. Marine Ecology Progress Series 136: 163-178.

NATIONAL OCEANIC AND ATMOSPHERIC ADMINISTRATION. 1995. Florida Keys National Marine Sanctuary Draft Management Plan/Environmental Impact Statement.

OVERLAND, J. E. AND R. W. PREISENDORFER. 1982. A significance test for principal components applied to cyclone climatology. Monthly Weather Review 110:1-4.

PITTS, P. A. 1997. An investigation of tidal and nontidal current patterns in Western Hawk Channel, Florida Keys. Continental Shelf Research 17: 1679-1687.

REDFIELD, A. C. 1958. The biological control of chemical factors in the environment. American Scientist 46: 205-222.

ROBBLEE, M. B., T. B. BARBER, P. R. CARLSON JR., M. J. DURAKO, J. W. FOURQUREAN, L. M. MUEHLSTEIN, D. PORTER, L. A. YABRO, R. T. ZIEMAN, AND J. C. ZIEMAN. 1991. Mass mortality of the tropical seagrass *Thallassia testudinum* in Florida Bay (USA). Marine Ecology Progress Series 71: 297-299.

RUDNICK, D., Z. CHEN, D. CHILDERS, T. FONTAINE, AND J. N. BOYER. 1999. Phosphorus and nitrogen inputs to Florida Bay: the importance of the Everglades watershed. Estuaries 22: 398-416.

RYTHER, J. H., D. W. MENZE, AND N. CORWIN. 1967. Influence of the Amazon River outflow on the ecology of the western tropical Atlantic, I. Hydrography and nutrient chemistry. Journal of Marine Research 25: 69-83.

SMITH, N. P. 1994. Long-term Gulf-to-Atlantic transport through tidal channels in the Florida Keys. Bulletin of Marine Science 54: 602-609.

STUMPF, R. P., M. L. FRAYER, M. J. DURAKO, AND J. C. BROCK. 1999. Variations in water clarity and bottom albedo in Florida Bay from 1985-1997. Estuaries 22: 431-444.

SZMANT, A. M., AND A. FORRESTER. 1996. Water column and sediment nitrogen and phosphorus distribution patterns in the Florida Keys, USA. Coral Reefs 15: 21-41.

7. Appendices

7.1. Appendix 1

Color contour maps of water quality variables by sampling event may be viewed and downloaded at http://serc.fiu.edu/wqmnetwork/CONTOUR%20MAPS/ContourMaps.htm. These maps encompass all 354 stations of the SERC Water Quality Monitoring Network which includes the FKNMS, Biscayne Bay, Florida Bay, Whitewater Bay, Ten Thousand Islands, and Southwest Florida Shelf. The data was collected over a period of a month so care should be taken in interpreting these maps as they are not truly synoptic.

7.2.Appendix 2

Table 3. Statistical summary of water quality in zones for the period of record. Data are summarized as median, minimum (Min.), maximum value (Max.), and number of samples (*n*).

Variable	Cluster	Median	Min.	Max.	*n*
Surface	1	0.10	0.00	2.18	474
NO_3^-	2	0.10	0.00	1.33	66
(μM)	3	0.06	0.00	2.30	2031
	4	0.06	0.00	0.81	169
	5	0.20	0.00	2.11	662
	6	0.09	0.00	5.90	982
	7	0.35	0.00	4.42	371
	8	0.06	0.00	2.11	405
Bottom	1	0.04	0.00	1.33	35
NO_3^-	2				
(μM)	3	0.08	0.00	4.46	1907
	4				
	5	0.13	0.00	1.17	112
	6	0.10	0.00	5.01	818
	7	0.06	0.01	0.39	3
	8	0.06	0.00	1.94	270
Surface	1	0.05	0.00	0.35	474
NO_2^-	2	0.06	0.00	0.25	66
(μM)	3	0.03	0.00	0.71	2039
	4	0.05	0.00	0.35	169
	5	0.06	0.00	0.25	664
	6	0.04	0.00	0.42	983
	7	0.09	0.00	0.40	371
	8	0.04	0.00	0.34	405
Bottom	1	0.04	0.02	0.17	35
NO_2^-	2				
(μM)	3	0.04	0.00	1.73	1912
	4				
	5	0.06	0.00	0.18	113
	6	0.04	0.00	0.36	818
	7	0.06	0.04	0.10	4
	8	0.04	0.00	0.32	270

Variable	Cluster	Median	Min.	Max.	*n*
Surface	1	0.39	0.00	1.84	473
NH_4^+	2	0.40	0.08	10.32	66
(μM)	3	0.24	0.00	2.30	2039
	4	0.29	0.00	3.17	169
	5	0.39	0.00	4.03	664
	6	0.27	0.00	5.03	982
	7	0.57	0.00	4.62	371
	8	0.27	0.00	2.21	405
Bottom	1	0.27	0.00	0.95	35
NH_4^+	2				
(μM)	3	0.25	0.00	2.90	1908
	4				
	5	0.36	0.04	2.49	113
	6	0.28	0.00	3.88	817
	7	0.44	0.30	0.64	4
	8	0.28	0.00	1.26	270
Surface	1	14.95	2.46	71.94	475
TN	2	15.17	3.90	63.44	66
(μM)	3	8.94	1.71	67.85	2036
	4	15.16	4.22	69.95	169
	5	14.32	0.92	86.60	661
	6	10.62	1.81	213.21	980
	7	16.31	2.54	73.72	372
	8	11.72	2.18	70.17	405
Bottom	1	11.29	2.47	32.62	35
TN	2				
(μM)	3	8.58	1.48	52.66	1901
	4				
	5	14.09	3.01	52.83	108
	6	10.72	2.37	153.75	804
	7	17.78	15.53	21.80	3
	8	10.34	2.30	29.39	270
Surface	1	14.34	1.97	71.65	473
TON	2	14.24	3.41	62.91	66
(μM)	3	8.49	0.00	67.72	2028
	4	14.69	3.03	69.19	169
	5	13.61	0.51	85.88	657
	6	10.08	0.39	212.89	976
	7	15.23	1.77	73.23	371
	8	11.17	1.55	70.00	405

Variable	Cluster	Median	Min.	Max.	*n*
Bottom	1	10.94	2.21	30.89	35
TON	2				
(μM)	3	8.06	0.00	51.94	1886
	4				
	5	13.25	2.47	52.67	108
	6	10.21	0.00	153.43	798
	7	15.91	15.14	16.68	2
	8	9.78	1.90	27.80	269
Surface	1	0.26	0.09	1.09	473
TP	2	0.24	0.11	0.83	66
(μM)	3	0.17	0.00	1.22	2037
	4	0.22	0.07	0.46	169
	5	0.19	0.02	1.39	665
	6	0.17	0.00	1.78	984
	7	0.20	0.03	0.84	372
	8	0.26	0.05	1.35	403
Bottom	1	0.21	0.10	0.45	34
TP	2				
(μM)	3	0.18	0.00	1.50	1906
	4				
	5	0.19	0.02	0.61	108
	6	0.18	0.00	1.02	812
	7	0.18	0.14	0.39	3
	8	0.24	0.05	0.67	269
Surface	1	0.02	0.00	0.30	474
SRP	2	0.02	0.00	0.22	66
(μM)	3	0.02	0.00	0.23	2028
	4	0.02	0.00	0.26	169
	5	0.02	0.00	0.56	661
	6	0.02	0.00	0.21	982
	7	0.02	0.00	0.20	371
	8	0.02	0.00	0.20	405
Bottom	1	0.02	0.00	0.17	35
SRP	2				
(μM)	3	0.02	0.00	0.39	1903
	4				
	5	0.02	0.00	0.15	113
	6	0.02	0.00	0.36	814
	7	0.01	0.01	0.11	5
	8	0.02	0.00	0.16	270

Variable	Cluster	Median	Min.	Max.	*n*
Surface	1	0.09	0.01	5.62	471
APA	2	0.09	0.02	0.55	66
(μM hr^{-1})	3	0.04	0.01	0.79	1922
	4	0.08	0.01	0.52	169
	5	0.08	0.01	2.52	659
	6	0.06	0.00	0.45	973
	7	0.10	0.02	1.43	372
	8	0.06	0.02	3.03	375
Bottom	1	0.06	0.02	0.46	31
APA	2				
(μM hr^{-1})	3	0.04	0.00	0.43	1792
	4				
	5	0.07	0.00	0.49	111
	6	0.06	0.01	0.43	812
	7	0.05	0.05	0.05	2
	8	0.05	0.02	0.34	241
Surface	1	0.34	0.00	15.24	475
Chl *a*	2	0.31	0.00	4.95	66
(μg l^{-1})	3	0.22	0.00	2.98	2035
	4	0.23	0.00	7.35	168
	5	0.24	0.00	2.79	665
	6	0.23	0.00	1.45	984
	7	0.22	0.00	6.20	371
	8	0.49	0.00	6.81	405
Surface	1	242.3	88.5	1435.4	474
TOC	2	243.6	137.3	505.5	66
(μM)	3	159.0	30.6	1054.8	2036
	4	245.0	150.9	702.5	169
	5	220.9	28.8	670.3	663
	6	178.0	22.8	805.3	979
	7	255.3	85.0	1653.5	371
	8	198.1	89.1	950.4	405
Bottom	1	197.8	88.1	446.0	35
TOC	2				
(μM)	3	155.8	0.0	883.1	1900
	4				
	5	214.5	99.9	392.6	112
	6	173.6	21.7	760.8	810
	7	225.9	147.4	281.7	3
	8	175.5	88.1	847.7	271

Variable	Cluster	Median	Min.	Max.	*n*
Surface	1	1.59	0.00	89.00	446
$Si(OH)_4$	2	4.86	0.00	55.16	62
(μM)	3	0.26	0.00	17.90	1916
	4	6.57	0.30	88.53	159
	5	1.81	0.00	127.11	624
	6	0.69	0.00	18.95	928
	7	2.11	0.00	37.36	348
	8	1.17	0.00	20.75	381
Bottom	1	1.09	0.00	3.93	32
$Si(OH)_4$	2				
(μM)	3	0.30	0.00	17.89	1796
	4				
	5	1.67	0.00	30.20	106
	6	0.78	0.00	18.35	767
	7	0.32	0.30	0.34	2
	8	1.10	0.00	9.71	254
Surface	1	1.34	0.00	37.00	469
Turbidity	2	1.21	0.20	5.55	66
(NTU)	3	0.33	0.00	9.30	2010
	4	0.79	0.00	7.70	168
	5	0.89	0.00	16.20	661
	6	0.55	0.00	8.80	982
	7	0.96	0.00	17.35	370
	8	1.38	0.00	11.84	397
Bottom	1	1.67	0.00	9.10	44
Turbidity	2	1.11	1.01	1.21	2
(NTU)	3	0.37	0.00	11.18	1885
	4	1.04	1.01	2.60	5
	5	0.80	0.00	16.90	131
	6	0.58	0.00	7.95	821
	7	0.72	0.00	4.89	12
	8	1.59	0.00	15.96	267
Surface	1	36.2	28.8	39.6	474
Salinity	2	36.2	29.6	40.3	66
	3	36.2	26.7	37.8	2014
	4	36.0	27.7	40.9	168
	5	36.3	29.5	40.0	642
	6	36.2	29.5	38.5	961
	7	36.3	28.0	40.4	365
	8	36.2	30.4	38.5	398

Variable	Cluster	Median	Min.	Max.	*n*
Bottom Salinity	1	36.2	28.8	39.7	474
	2	36.2	29.6	40.2	65
	3	36.2	32.6	37.8	2003
	4	36.0	27.7	40.9	168
	5	36.3	29.5	40.0	638
	6	36.2	30.5	38.5	953
	7	36.3	28.0	40.4	362
	8	36.2	30.4	38.5	397
Surface Temperature (^{o}C)	1	27.5	17.6	36.1	475
	2	27.8	21.2	32.1	66
	3	27.0	16.3	32.2	2015
	4	28.0	20.9	34.6	168
	5	27.9	15.1	39.6	643
	6	27.6	15.4	33.0	964
	7	28.0	18.4	35.0	365
	8	26.4	18.4	34.5	399
Bottom Temperature (^{o}C)	1	27.6	17.6	33.4	474
	2	27.8	21.2	32.1	65
	3	26.2	16.3	32.0	2004
	4	28.0	20.3	32.7	168
	5	27.9	15.1	33.4	641
	6	27.4	15.4	32.6	955
	7	28.0	18.4	36.8	362
	8	26.3	17.7	34.5	398
Surface DO (mg l^{-1})	1	6.2	2.8	11.3	475
	2	6.0	4.4	7.7	66
	3	5.9	4.4	13.5	1993
	4	6.1	4.1	10.5	168
	5	6.0	2.6	10.8	637
	6	5.8	2.5	10.5	959
	7	6.0	2.5	9.7	365
	8	6.2	2.3	10.8	398
Bottom DO (mg l^{-1})	1	6.2	2.7	11.4	474
	2	6.0	4.3	8.1	65
	3	5.9	1.4	13.9	1966
	4	6.2	4.3	10.6	168
	5	6.0	2.8	10.3	637
	6	5.9	3.2	9.8	947
	7	6.0	2.1	9.8	362
	8	6.2	3.0	10.9	396

Variable	Cluster	Median	Min.	Max.	*n*
K_d	1	0.326	0.004	2.562	373
(m^{-1})	2	0.304	0.021	1.856	40
	3	0.136	0.001	2.747	1479
	4	0.370	0.042	3.274	83
	5	0.313	0.005	3.137	406
	6	0.204	0.002	3.410	697
	7	0.356	0.011	2.983	257
	8	0.262	0.011	2.056	302
Surface	1	92.5	43.1	165.5	475
DO_{sat}	2	89.8	65.4	118.9	66
(%)	3	88.3	43.4	191.6	1993
	4	92.9	62.0	148.2	168
	5	89.0	40.8	153.3	637
	6	86.9	38.1	158.5	958
	7	90.2	38.6	134.8	365
	8	91.3	31.2	169.9	398
Bottom	1	92.5	41.6	166.9	474
DO_{sat}	2	90.2	65.4	125.1	65
(%)	3	88.0	19.3	207.0	1966
	4	94.3	65.2	149.6	168
	5	89.8	42.9	152.2	637
	6	88.0	46.7	144.0	946
	7	90.0	32.4	132.0	362
	8	91.6	41.2	171.4	396
$\Delta\sigma_t$	1	0.000	-0.743	6.528	473
	2	0.000	-0.222	0.371	65
	3	0.040	-3.185	6.640	1993
	4	0.000	-0.370	1.344	168
	5	0.000	-1.440	4.762	634
	6	0.032	-3.047	4.439	949
	7	0.000	-4.424	4.355	362
	8	0.003	-0.743	3.737	398

7.3.Appendix 3

Tables of time series analysis results - linear regressions and statistical significance for each variable by station

	Nitrate						Nitrite						Ammonium					
	Surface			*Bottom*			*Surface*			*Bottom*			*Surface*			*Bottom*		
Station	R^2	p-value	slope	R^2	p-value	slope	R^2	p-value	slope	R^2	p-value	slope	R^2	p-value	slope	R^2	p-value	slope
200	0.006	0.636	0.0049	0.001	0.873	0.0022	0.001	0.837	-0.0004	0.051	0.206	-0.0029	0.015	0.464	-0.0056	0.057	0.181	-0.0140
201	0.000	0.908	0.0034	0.001	0.871	0.0049	0.000	0.994	0.0000	0.000	0.929	-0.0003	0.003	0.748	-0.0042	0.046	0.228	-0.0200
202	0.015	0.464	0.0150	0.015	0.463	0.0141	0.000	0.979	0.0001	0.000	0.912	0.0003	0.013	0.497	-0.0054	0.070	0.114	-0.0130
203	0.007	0.611	0.0047	N/A	N/A	N/A	0.011	0.546	-0.0012	N/A	N/A	N/A	0.024	0.357	-0.1080	N/A	N/A	N/A
204	0.000	0.983	0.0050	0.006	0.662	0.0090	0.011	0.531	0.0018	0.006	0.647	0.0011	0.029	0.315	-0.0163	0.006	0.661	-0.0059
205	0.006	0.662	0.0102	0.023	0.369	0.0136	0.001	0.859	0.0005	0.040	0.237	0.0030	0.005	0.682	-0.0067	0.005	0.693	-0.0043
206	0.024	0.363	0.0178	0.047	0.195	0.0230	0.043	0.217	0.0037	0.063	0.133	0.0048	0.032	0.293	-0.0110	0.000	0.900	0.0013
207	0.001	0.845	0.0039	N/A	N/A	N/A	0.020	0.400	0.0025	N/A	N/A	N/A	0.017	0.449	-0.0096	N/A	N/A	N/A
208	0.006	0.652	0.0072	0.005	0.681	0.0076	0.010	0.550	0.0017	0.047	0.197	0.0037	0.003	0.746	-0.0038	0.000	0.945	-0.0009
209	0.000	0.958	-0.0019	N/A	N/A	N/A	0.100	0.057	0.0050	N/A	N/A	N/A	0.000	0.937	0.0015	N/A	N/A	N/A
210	0.001	0.820	0.0045	0.006	0.652	0.0097	0.019	0.417	0.0020	0.067	0.123	0.0032	0.012	0.525	0.0103	0.003	0.738	-0.0051
211	0.013	0.496	0.4340	0.015	0.484	0.0390	0.014	0.481	0.0024	0.004	0.698	0.0013	0.004	0.719	0.0114	0.002	0.796	0.0075
212	0.017	0.442	0.0171	0.027	0.335	0.0164	0.006	0.656	0.0008	0.007	0.619	0.0010	0.010	0.547	-0.0058	0.034	0.277	-0.0118
213	0.060	0.650	0.0079	0.001	0.871	0.0035	0.000	0.916	0.0002	0.001	0.835	0.0003	0.002	0.772	0.0030	0.057	0.153	-0.0137
214	0.034	0.273	0.0461	N/A	N/A	N/A	0.040	0.234	0.0029	N/A	N/A	N/A	0.001	0.831	0.0040	N/A	N/A	N/A
215	0.020	0.406	0.0297	0.180	0.401	0.0100	0.050	0.182	0.0031	0.886	0.005	0.0191	0.020	0.801	-0.0049	0.381	0.192	-0.0228
216	0.020	0.700	0.0125	0.010	0.794	0.0097	0.073	0.107	0.0024	0.266	0.156	0.0098	0.001	0.887	-0.0180	0.501	0.049	-0.0646
217	0.015	0.476	0.0251	N/A	N/A	N/A	0.038	0.251	0.0027	N/A	N/A	N/A	0.000	0.991	-0.0060	N/A	N/A	N/A
218	0.023	0.373	0.0208	0.022	0.851	-0.0176	0.045	0.206	0.0024	0.692	0.168	-0.0092	0.058	0.151	-0.0270	0.838	0.085	-0.0769
219	0.005	0.665	0.0040	0.000	0.953	0.0007	0.016	0.453	0.0011	0.030	0.308	0.0015	0.024	0.358	-0.0207	0.152	0.017	-0.0324
220	0.000	0.909	-0.0015	0.011	0.532	0.0105	0.025	0.348	0.0020	0.045	0.208	0.0021	0.049	0.190	-0.0137	0.071	0.111	-0.0183
221	0.011	0.529	0.0090	0.015	0.475	0.0119	0.017	0.438	0.0014	0.102	0.054	0.0035	0.083	0.084	-0.0176	0.192	0.007	-0.0245
222	0.018	0.440	0.0107	0.003	0.735	-0.0054	0.024	0.370	-0.0014	0.003	0.737	-0.0007	0.080	0.094	-0.0131	0.091	0.070	-0.0228
223	0.002	0.772	0.0052	N/A	N/A	N/A	0.011	0.538	0.0012	N/A	N/A	N/A	0.041	0.228	-0.0161	N/A	N/A	N/A
224	0.000	0.991	-0.0001	0.010	0.902	0.0076	0.007	0.612	0.0008	0.503	0.291	0.0053	0.053	0.169	-0.0162	0.008	0.912	-0.0036
225	0.021	0.392	0.0126	0.007	0.632	0.0053	0.020	0.401	0.0011	0.020	0.398	0.0017	0.057	0.156	-0.0192	0.031	0.297	-0.0163
226	0.004	0.707	-0.0065	N/A	N/A	N/A	0.004	0.708	-0.0009	N/A	N/A	N/A	0.057	0.154	-0.0307	N/A	N/A	N/A
227	0.001	0.833	-0.0020	0.006	0.641	0.0038	0.000	0.982	0.0000	0.027	0.338	-0.0016	0.042	0.225	-0.0169	0.073	0.111	-0.0162
228	0.024	0.360	-0.0073	0.036	0.259	-0.0106	0.004	0.702	-0.0008	0.022	0.384	-0.0017	0.045	0.205	-0.0279	0.128	0.030	-0.0381
229	0.014	0.482	-0.0086	N/A	N/A	N/A	0.049	0.186	-0.0036	N/A	N/A	N/A	0.066	0.125	-0.0374	N/A	N/A	N/A
230	0.005	0.673	-0.0042	0.000	0.963	-0.0005	0.006	0.654	-0.0008	0.003	0.738	0.0006	0.068	0.119	-0.0340	0.017	0.444	-0.0164
231	0.053	0.169	0.0123	0.020	0.407	0.0099	0.014	0.479	0.0008	0.001	0.823	-0.0003	0.011	0.539	-0.0137	0.039	0.240	-0.0224
232	0.008	0.597	0.0065	N/A	N/A	N/A	0.086	0.078	-0.0049	0.000	0.960	-0.0001	0.064	0.130	-0.0371	N/A	N/A	N/A
233	0.016	0.459	0.0079	0.009	0.570	0.0059	0.028	0.319	-0.0019	0.014	0.478	-0.0054	0.001	0.838	-0.0041	0.036	0.262	-0.0213
234	0.018	0.428	0.0087	0.005	0.668	-0.0120	0.002	0.799	0.0005	N/A	N/A	N/A	0.010	0.850	-0.0019	0.019	0.419	-0.0087
235	0.001	0.858	-0.0026	N/A	N/A	N/A	0.097	0.060	-0.0062	N/A	N/A	N/A	0.085	0.080	-0.4920	N/A	N/A	N/A
236	0.001	0.890	0.0016	0.000	0.921	0.0009	0.011	0.551	-0.0018	0.001	0.890	-0.0005	0.011	0.543	-0.0097	0.022	0.391	-0.0124
237	0.000	0.950	-0.0006	0.008	0.608	0.0058	0.005	0.671	-0.0012	N/A	N/A	N/A	0.064	0.131	-0.0202	0.066	0.124	-0.0284
238	0.018	0.433	-0.0191	N/A	N/A	N/A	0.038	0.247	-0.0043	0.007	0.613	0.0013	0.095	0.063	-0.0570	N/A	N/A	N/A
239	0.013	0.504	0.0079	0.080	0.090	0.0153	0.003	0.737	0.0011	0.015	0.473	0.0019	0.310	0.297	0.0256	0.003	0.754	0.0065
240	0.057	0.156	0.0127	0.042	0.226	0.0104	0.000	0.943	0.0002	N/A	N/A	N/A	0.003	0.733	-0.0066	0.011	0.534	-0.0135
241	0.003	0.735	0.0040	N/A	N/A	N/A	0.001	0.862	0.0005	0.010	0.558	0.0017	0.001	0.848	-0.0031	N/A	N/A	N/A
242	0.010	0.823	-0.0042	0.000	0.941	-0.0013	0.003	0.761	-0.0009	0.000	0.900	-0.0003	0.003	0.736	0.0062	0.001	0.821	-0.0038
243	0.021	0.389	0.0100	0.013	0.507	0.0080	0.006	0.641	0.0014	0.024	0.386	-0.0021	0.061	0.140	0.0318	0.002	0.791	0.0058
244	0.000	0.942	-0.0010	0.004	0.715	-0.0067	0.083	0.088	-0.0035	0.000	0.943	-0.0001	0.047	0.202	-0.0223	0.001	0.886	-0.0042
245	0.016	0.420	-0.0114	0.002	0.822	0.0032	0.051	0.184	-0.0027	0.014	0.495	-0.0012	0.028	0.332	-0.0161	0.037	0.266	-0.0128
246	0.004	0.734	0.0045	0.005	0.698	0.0038	0.025	0.361	-0.0016	1.000		-0.0238	0.034	0.283	-0.0133	0.147	0.021	-0.0226
247	0.003	0.750	-0.0098	N/A	N/A	N/A	0.000	0.993	0.0000	0.006	0.668	0.0005	0.012	0.530	-0.0097	N/A	N/A	N/A
248	0.071	0.121	0.0121	0.031	0.316	0.0127	0.002	0.795	-0.0003	0.023	0.377	-0.0012	0.038	0.252	-0.0162	0.006	0.670	-0.0062
249	0.033	0.294	0.0088	0.012	0.538	0.0083	0.019	0.420	-0.0015	N/A	N/A	N/A	0.041	0.237	-0.0133	0.114	0.044	-0.0227
250	0.021	0.414	0.0154	N/A	N/A	N/A	0.012	0.539	-0.0012	0.025	0.356	-0.0017	0.157	0.019	-0.0280	N/A	N/A	N/A

	Nitrate						Nitrite						Ammonium					
	Surface			*Bottom*			*Surface*			*Bottom*			*Surface*			*Bottom*		
Station	R^2	p-value	slope	R^2	p-value	slope	R^2	p-value	slope	R^2	p-value	slope	R^2	p-value	slope	R^2	p-value	slope
251	0.002	0.793	0.0036	0.007	0.635	0.0068	0.129	0.031	-0.0040	0.000	0.971	-0.0001	0.233	0.003	-0.0393	0.213	0.005	-0.0336
252	0.030	0.324	0.0134	0.021	0.407	0.0216	0.023	0.377	-0.0014	N/A	N/A	N/A	0.200	0.006	-0.0287	0.161	0.015	-0.0311
253	0.016	0.464	0.0156	N/A	N/A	N/A	0.008	0.615	0.0010	N/A	N/A	N/A	0.007	0.118	-0.0214	N/A	N/A	N/A
254	0.047	0.203	0.0204	N/A	N/A	N/A	0.011	0.539	0.0010	N/A	N/A	N/A	0.770	0.120	-0.0168	N/A	N/A	N/A
255	0.020	0.413	0.0135	0.041	0.238	0.0131	0.023	0.372	0.0028	0.063	0.144	0.0035	0.029	0.318	-0.0106	0.076	0.103	-0.0237
256	0.004	0.722	0.0056	0.000	0.940	-0.0018	0.000	0.937	-0.0002	N/A	N/A	N/A	0.101	0.058	-0.0260	0.026	0.354	-0.0129
257	0.006	0.646	0.0095	N/A	N/A	N/A	0.000	0.937	-0.0002	N/A	N/A	N/A	0.070	0.118	-0.0169	N/A	N/A	N/A
258	0.045	0.213	0.0131	0.002	0.819	-0.0028	0.011	0.539	0.0014	0.031	0.307	0.0025	0.050	0.188	-0.0235	0.141	0.024	-0.0390
259	0.003	0.745	0.0050	0.034	0.281	-0.0151	0.002	0.806	0.0006	N/A	N/A	N/A	0.101	0.059	-0.0284	0.062	0.143	-0.0172
260	0.018	0.444	0.0170	N/A	N/A	N/A	0.133	0.034	0.0052	N/A	N/A	N/A	0.003	0.741	0.0077	N/A	N/A	N/A
261	0.010	0.890	0.0070	0.002	0.776	-0.0088	0.010	0.568	0.0011	0.002	0.781	0.0006	0.000	0.899	-0.0024	0.016	0.474	-0.0251
262	0.000	0.973	-0.0005	0.008	0.605	-0.0069	0.094	0.069	0.0053	0.074	0.108	0.0044	0.009	0.577	-0.0096	0.004	0.707	0.0091
263	0.005	0.688	-0.0035	0.033	0.294	-0.0133	0.031	0.303	0.0014	0.015	0.482	0.0011	0.201	0.006	-0.0460	0.211	0.005	-0.0415
264	0.010	0.866	0.0021	0.007	0.627	0.0044	0.083	0.093	-0.0022	0.022	0.404	-0.0011	0.127	0.036	-0.0383	0.087	0.090	-0.0303
265	0.004	0.710	-0.0066	N/A	N/A	N/A	0.001	0.846	-0.0007	N/A	N/A	N/A	0.009	0.586	-0.0227	N/A	N/A	N/A
266	0.000	0.982	-0.0005	N/A	N/A	N/A	0.004	0.714	0.0007	N/A	N/A	N/A	0.065	0.139	-0.0320	N/A	N/A	N/A
267	0.006	0.663	0.0074	0.002	0.786	-0.0043	0.010	0.574	0.0007	0.000	0.929	0.0001	0.039	0.253	-0.0181	0.073	0.116	-0.0313
268	0.016	0.461	-0.0150	0.738	0.342	-0.0719	0.003	0.750	-0.0007	0.829	0.272	-0.0406	0.007	0.619	-0.0092	0.685	0.379	-0.6466
269	0.008	0.613	0.0085	0.000	0.972	0.0006	0.013	0.512	0.0012	0.010	0.565	0.0011	0.031	0.302	-0.0140	0.071	0.115	-0.0373
270	0.006	0.656	0.0075	0.004	0.709	0.0053	0.002	0.787	0.0009	0.002	0.774	-0.0004	0.008	0.598	-0.0147	0.046	0.209	-0.0187
271	0.000	0.932	0.0013	0.018	0.434	-0.0118	0.018	0.429	0.0012	0.037	0.259	0.0021	0.003	0.743	-0.0049	0.017	0.451	-0.0089
272	0.014	0.494	0.0087	0.022	0.393	0.0122	0.088	0.079	0.0027	0.111	0.051	0.0031	0.005	0.694	-0.0043	0.015	0.490	-0.0093
273	0.005	0.672	0.0067	0.014	0.485	0.0097	0.003	0.742	-0.0005	0.002	0.793	-0.0004	0.035	0.275	-0.0178	0.021	0.402	-0.0254
274	0.057	0.160	0.0213	0.064	0.138	0.0205	0.007	0.622	0.0009	0.012	0.521	0.0013	0.012	0.518	-0.0184	0.019	0.420	-0.0187
275	0.008	0.605	0.0088	0.007	0.637	0.0067	0.004	0.698	0.0008	0.000	0.976	-0.0001	0.004	0.701	-0.0068	0.036	0.265	-0.0179
276	0.015	0.473	0.0107	0.000	0.928	-0.0016	0.007	0.633	0.0025	0.001	0.879	-0.0002	0.012	0.529	-0.0112	0.032	0.295	-0.0151
277	0.018	0.437	-0.0144	0.027	0.334	-0.0171	0.003	0.765	-0.0007	0.018	0.431	-0.0017	0.080	0.094	-0.0250	0.023	0.373	-0.0261
278	0.001	0.858	-0.0032	0.000	0.907	-0.0020	0.000	0.936	0.0001	0.002	0.794	-0.0004	0.026	0.345	-0.0125	0.024	0.370	-0.0125
279	0.005	0.687	0.0048	0.002	0.801	0.0048	0.008	0.603	-0.0009	0.004	0.715	-0.0009	0.038	0.257	-0.0144	0.070	0.119	-0.0287
280	0.008	0.605	0.0081	0.002	0.809	-0.0053	0.003	0.766	-0.0004	0.007	0.624	-0.0011	0.005	0.177	-0.0190	0.015	0.474	-0.0274
281	0.000	0.990	-0.0001	0.068	0.130	-0.0271	0.000	0.915	-0.0002	0.036	0.272	-0.0022	0.106	0.052	-0.0370	0.136	0.029	-0.0328
282	0.054	0.174	0.0149	N/A	N/A	N/A	0.001	0.846	-0.0008	N/A	N/A	N/A	0.002	0.120	0.0080	N/A	N/A	N/A
283	0.003	0.766	0.0023	N/A	N/A	N/A	0.040	0.251	-0.0027	N/A	N/A	N/A	0.007	0.642	-0.0480	N/A	N/A	N/A
284	0.006	0.639	0.0050	N/A	N/A	N/A	0.024	0.356	-0.0022	N/A	N/A	N/A	0.200	0.409	-0.0093	N/A	N/A	N/A
285	0.001	0.844	0.0047	N/A	N/A	N/A	0.009	0.575	-0.0021	N/A	N/A	N/A	0.016	0.469	-0.0314	N/A	N/A	N/A
286	0.004	0.714	0.0069	N/A	N/A	N/A	0.001	0.833	-0.0007	N/A	N/A	N/A	0.008	0.607	-0.0246	N/A	N/A	N/A
287	0.008	0.590	0.0380	N/A	N/A	N/A	0.006	0.656	-0.0010	N/A	N/A	N/A	0.007	0.635	-0.0051	N/A	N/A	N/A
288	0.001	0.878	0.0013	N/A	N/A	N/A	0.013	0.508	-0.0014	N/A	N/A	N/A	0.013	0.504	-0.0074	N/A	N/A	N/A
289	0.090	0.071	0.0429	N/A	N/A	N/A	0.008	0.601	0.0022	N/A	N/A	N/A	0.000	0.991	0.0011	N/A	N/A	N/A
290	0.000	0.932	-0.0008	N/A	N/A	N/A	0.009	0.598	-0.0013	N/A	N/A	N/A	0.018	0.447	-0.0168	N/A	N/A	N/A
291	0.028	0.323	0.0088	N/A	N/A	N/A	0.001	0.867	0.0003	N/A	N/A	N/A	0.000	0.910	-0.0017	N/A	N/A	N/A
292	0.016	0.457	0.0143	N/A	N/A	N/A	0.001	0.855	0.0007	N/A	N/A	N/A	0.008	0.610	-0.0173	N/A	N/A	N/A
293	0.000	0.920	-0.0032	N/A	N/A	N/A	0.002	0.773	-0.0009	N/A	N/A	N/A	0.022	0.376	-0.0249	N/A	N/A	N/A
294	0.048	0.193	0.0167	N/A	N/A	N/A	0.006	0.646	-0.0009	N/A	N/A	N/A	0.020	0.403	-0.0093	N/A	N/A	N/A
295	0.024	0.377	0.0084	N/A	N/A	N/A	0.000	0.997	0.0000	N/A	N/A	N/A	0.008	0.607	-0.0473	N/A	N/A	N/A
296	0.000	0.976	-0.0003	N/A	N/A	N/A	0.019	0.424	-0.0023	N/A	N/A	N/A	0.000	0.951	0.0008	N/A	N/A	N/A
297	0.013	0.499	0.0097	N/A	N/A	N/A	0.021	0.390	0.0024	N/A	N/A	N/A	0.030	0.308	0.0177	N/A	N/A	N/A
298	0.003	0.762	-0.0053	N/A	N/A	N/A	0.000	0.916	0.0002	N/A	N/A	N/A	0.040	0.233	-0.0145	N/A	N/A	N/A
299	0.002	0.782	-0.0073	N/A	N/A	N/A	0.047	0.198	0.0075	N/A	N/A	N/A	0.019	0.411	0.0293	N/A	N/A	N/A
300	0.004	0.700	0.0046	N/A	N/A	N/A	0.067	0.120	0.0046	N/A	N/A	N/A	0.005	0.668	-0.0060	N/A	N/A	N/A
301	0.000	0.998	0.0000	N/A	N/A	N/A	0.033	0.281	0.0035	N/A	N/A	N/A	0.026	0.343	-0.0168	N/A	N/A	N/A

	Nitrate						Nitrite						Ammonium					
	Surface			*Bottom*			*Surface*			*Bottom*			*Surface*			*Bottom*		
Station	R^2	p-value	slope	R^2	p-value	slope	R^2	p-value	slope	R^2	p-value	slope	R^2	p-value	slope	R^2	p-value	slope
302	0.000	0.994	0.0001	N/A	N/A	N/A	0.102	0.054	-0.0031	N/A	N/A	N/A	0.119	0.037	-0.0246	N/A	N/A	N/A
303	0.044	0.211	-0.0425	N/A	N/A	N/A	0.017	0.443	0.0035	N/A	N/A	N/A	0.007	0.618	0.0188	N/A	N/A	N/A
304	0.000	0.989	-0.0004	N/A	N/A	N/A	0.001	0.841	0.0007	N/A	N/A	N/A	0.018	0.427	-0.0177	N/A	N/A	N/A
305	0.021	0.397	0.0114	N/A	N/A	N/A	0.050	0.185	0.0030	N/A	N/A	N/A	0.001	0.838	0.0028	N/A	N/A	N/A
306	0.000	0.948	0.0011	N/A	N/A	N/A	0.002	0.798	0.0010	N/A	N/A	N/A	0.005	0.666	-0.0092	N/A	N/A	N/A
307	0.010	0.565	0.0123	N/A	N/A	N/A	0.015	0.464	0.0034	N/A	N/A	N/A	0.009	0.574	-0.0102	N/A	N/A	N/A
308	0.000	0.971	-0.0007	N/A	N/A	N/A	0.008	0.596	0.0013	N/A	N/A	N/A	0.002	0.814	0.0054	N/A	N/A	N/A
309	0.012	0.524	-0.0089	N/A	N/A	N/A	0.029	0.317	0.0022	N/A	N/A	N/A	0.012	0.527	-0.0068	N/A	N/A	N/A
310	0.007	0.625	-0.0221	N/A	N/A	N/A	0.055	0.161	0.0054	N/A	N/A	N/A	0.069	0.117	0.0783	N/A	N/A	N/A
311	0.028	0.333	-0.0576	N/A	N/A	N/A	0.001	0.835	-0.0005	N/A	N/A	N/A	0.000	0.925	0.0028	N/A	N/A	N/A
312	0.000	0.930	0.0012	N/A	N/A	N/A	0.002	0.812	0.0004	N/A	N/A	N/A	0.003	0.763	0.0051	N/A	N/A	N/A
313	0.005	0.664	0.0105	N/A	N/A	N/A	0.050	0.183	-0.0023	N/A	N/A	N/A	0.034	0.273	-0.0235	N/A	N/A	N/A
314	0.038	0.248	-0.0184	N/A	N/A	N/A	0.011	0.536	0.0025	N/A	N/A	N/A	0.008	0.597	-0.0138	N/A	N/A	N/A
315	0.000	0.971	-0.0007	N/A	N/A	N/A	0.006	0.638	-0.0008	N/A	N/A	N/A	0.033	0.282	-0.0203	N/A	N/A	N/A
316	0.021	0.387	-0.0191	N/A	N/A	N/A	0.018	0.429	-0.0019	N/A	N/A	N/A	0.046	0.204	-0.0196	N/A	N/A	N/A
317	0.020	0.407	-0.0198	N/A	N/A	N/A	0.008	0.603	0.0021	N/A	N/A	N/A	0.007	0.629	-0.1010	N/A	N/A	N/A
318	0.001	0.831	0.0030	0.013	0.506	0.0104	0.020	0.411	0.0021	0.047	0.197	0.0030	0.041	0.236	-0.0181	0.001	0.842	-0.0027
319	0.007	0.619	0.0081	0.010	0.547	0.0146	0.000	0.980	-0.0001	0.008	0.596	0.0020	0.076	0.100	-0.0229	0.013	0.503	0.0106
320	0.016	0.475	0.0174	0.000	0.923	-0.0039	0.002	0.809	0.0007	0.003	0.744	-0.0032	0.038	0.264	-0.0168	0.003	0.747	-0.0054
321	0.003	0.749	0.0086	0.001	0.868	0.0040	0.006	0.669	0.0008	0.001	0.850	-0.0008	0.170	0.055	-0.0251	0.006	0.654	-0.0069
322	0.005	0.681	0.0082	0.015	0.466	0.0186	0.016	0.451	-0.0014	0.010	0.564	0.0014	0.064	0.130	-0.0266	0.012	0.521	-0.0055
323	0.018	0.435	0.0196	0.035	0.269	0.0207	0.008	0.602	0.0013	0.006	0.640	0.0015	0.015	0.470	-0.0096	0.018	0.432	-0.0120
324	0.016	0.451	0.0242	0.016	0.455	0.0235	0.010	0.564	0.0026	0.009	0.571	0.0021	0.075	0.100	-0.0198	0.014	0.480	-0.0087
325	0.004	0.708	0.0680	0.008	0.600	0.0082	0.004	0.699	-0.0006	0.014	0.485	0.0015	0.138	0.026	-0.0388	0.056	0.157	-0.0150
326	0.002	0.801	0.0027	0.000	0.972	0.0007	0.006	0.651	0.0009	0.000	0.945	0.0002	0.040	0.237	-0.0172	0.039	0.239	-0.0169
327	0.002	0.817	0.0046	0.000	0.957	0.0011	0.006	0.640	-0.0014	0.001	0.870	-0.0004	0.162	0.014	-0.0347	0.043	0.215	-0.0179
328	0.008	0.588	0.0068	0.023	0.372	0.0097	0.017	0.438	-0.0014	0.008	0.600	0.0010	0.041	0.231	-0.0162	0.023	0.374	-0.0127
329	0.010	0.340	0.0057	0.000	0.955	0.0008	0.062	0.149	0.0027	0.004	0.725	-0.0023	0.058	0.164	-0.0197	0.057	0.168	-0.0171
330	0.000	0.800	0.0004	0.016	0.457	0.0120	0.022	0.379	0.0027	0.009	0.574	0.0016	0.024	0.365	-0.0142	0.039	0.241	-0.0170
331	0.000	0.020	0.0016	0.000	0.984	-0.0003	0.046	0.204	0.0054	0.003	0.731	0.0008	0.016	0.456	-0.0146	0.085	0.080	-0.0240
332	0.062	0.142	0.0155	0.024	0.360	0.0120	0.002	0.805	-0.0004	0.025	0.355	0.0017	0.103	0.057	-0.0284	0.043	0.216	-0.0163
333	0.006	0.654	0.0064	0.054	0.167	0.0091	0.013	0.494	-0.0016	0.005	0.684	-0.0009	0.072	0.109	-0.0161	0.036	0.258	-0.0124
334	0.014	0.490	0.0068	0.006	0.650	0.0048	0.011	0.536	-0.0010	0.001	0.864	-0.0002	0.071	0.111	-0.0219	0.030	0.305	-0.0129
335	0.006	0.639	0.0044	0.040	0.233	0.0072	0.016	0.463	-0.0013	0.025	0.349	0.0014	0.076	0.099	-0.0215	0.063	0.134	-0.0172
336	0.042	0.221	0.0101	0.000	0.997	0.0001	0.001	0.873	0.0002	0.007	0.617	-0.0083	0.096	0.062	-0.0251	0.079	0.093	-0.0192
337	0.000	0.987	0.0002	0.000	0.918	0.0012	0.043	0.220	-0.0021	0.014	0.483	-0.0011	0.081	0.087	-0.0198	0.069	0.116	-0.0154
338	0.005	0.693	0.0041	0.004	0.724	0.0037	0.000	0.939	-0.0001	0.003	0.753	0.0004	0.035	0.271	-0.0215	0.004	0.729	-0.0042
339	0.025	0.349	0.0088	0.001	0.876	0.0017	0.001	0.856	0.0002	0.025	0.355	-0.0039	0.019	0.413	-0.0098	0.104	0.051	-0.0183
340	0.047	0.196	0.0100	0.017	0.440	0.0072	0.002	0.772	0.0004	0.000	0.998	0.0000	0.048	0.195	-0.0154	0.001	0.882	-0.0020
341	0.000	0.993	0.0001	0.018	0.439	0.0078	0.004	0.731	-0.0012	0.029	0.325	-0.0036	0.067	0.126	-0.0257	0.007	0.628	-0.0085
342	0.001	0.836	0.0023	0.005	0.677	-0.0177	0.001	0.893	-0.0004	0.006	0.669	-0.0084	0.044	0.221	-0.0143	0.059	0.165	-0.0242
343	0.002	0.778	-0.0039	0.000	0.991	-0.0006	0.059	0.153	-0.0019	0.004	0.711	-0.0065	0.072	0.112	-0.0167	0.010	0.570	-0.0089
344	0.001	0.840	0.0032	0.043	0.221	-0.0210	0.004	0.701	0.0006	0.009	0.570	-0.0018	0.025	0.349	-0.0137	0.024	0.360	-0.0120
345	0.030	0.316	0.0227	0.001	0.863	0.0127	0.116	0.039	0.0044	0.000	0.982	0.0002	0.016	0.460	0.0143	0.002	0.783	0.0059
346	0.002	0.809	0.003	0.019	0.424	-0.0236	0.126	0.037	0.0049	0.001	0.865	-0.0019	0.014	0.499	0.0218	0.023	0.388	0.0209
347	0.002	0.787	0.0019	0.010	0.573	-0.0156	0.106	0.056	0.0046	0.000	0.943	-0.0007	0.009	0.591	0.0114	0.034	0.289	0.0241
348	0.003	0.767	0.0018	0.000	0.997	0.0000	0.146	0.021	0.0047	0.118	0.043	0.0046	0.017	0.453	0.0153	0.032	0.304	0.0156
349	0.015	0.478	0.0054	0.003	0.739	0.0027	0.056	0.171	0.0034	0.172	0.013	0.0059	0.014	0.496	0.0141	0.045	0.220	0.0265
350	0.015	0.471	0.0045	0.001	0.851	-0.0066	0.102	0.054	0.0037	0.011	0.535	0.0035	0.001	0.847	0.0039	0.033	0.285	0.0248
400	0.002	0.816	0.0044	0.000	0.948	-0.0015	0.108	0.087	-0.0044	0.068	0.180	-0.0026	0.071	0.171	-0.0340	0.070	0.172	-0.0727
401	0.026	0.411	-0.0144	0.000	0.961	-0.0009	0.041	0.301	-0.0126	0.073	0.183	-0.0038	0.140	0.049	-0.0431	0.201	0.022	-0.0454
402	0.017	0.522	-0.0165	0.000	0.933	-0.0016	0.018	0.510	-0.0014	0.004	0.758	-0.0007	0.088	0.132	-0.0221	0.097	0.113	-0.0171
403	0.056	0.233	-0.0172	0.010	0.621	-0.0082	0.000	0.968	0.0001	0.006	0.711	-0.0011	0.032	0.375	-0.0142	0.087	0.136	-0.0492

	Total Nitrogen						Dissolved Inorganic Nitrogen						Total Organic Nitrogen					
	Surface			*Bottom*			*Surface*			*Bottom*			*Surface*			*Bottom*		
Station	R^2	p-value	slope	R^2	p-value	slope	R^2	p-value	slope	R^2	p-value	slope	R^2	p-value	slope	R^2	p-value	slope
200	0.024	0.357	0.3457	0.076	0.121	0.7385	0.000	0.934	-0.0011	0.019	0.450	-0.0146	0.025	0.355	0.3467	0.079	0.114	0.7531
201	0.006	0.648	0.1586	0.000	0.998	-0.0006	0.000	0.984	-0.0008	0.005	0.683	-0.0194	0.007	0.638	0.1594	0.009	0.602	-0.1379
202	0.005	0.668	0.1177	0.009	0.576	0.1779	0.004	0.714	0.0097	0.000	0.955	0.0014	0.005	0.689	0.1079	0.009	0.574	0.1764
203	0.032	0.290	0.3490	N/A	N/A	N/A	0.005	0.669	-0.0072	N/A	N/A	N/A	0.033	0.285	0.3520	N/A	N/A	N/A
204	0.045	0.208	0.4217	0.002	0.800	0.0748	0.003	0.729	-0.0140	0.000	0.925	0.0031	0.046	0.203	0.4357	0.002	0.821	0.0672
205	0.034	0.275	0.2804	0.058	0.153	0.3621	0.000	0.898	0.0046	0.008	0.602	0.0123	0.031	0.299	0.2758	0.053	0.169	0.3497
206	0.044	0.211	0.3324	0.075	0.100	0.4433	0.005	0.690	0.0106	0.042	0.225	0.0292	0.041	0.228	0.3217	0.065	0.128	0.414
207	0.025	0.350	0.2616	N/A	N/A	N/A	0.000	0.912	-0.0031	N/A	N/A	N/A	0.025	0.351	0.2647	N/A	N/A	N/A
208	0.037	0.253	0.3307	0.052	0.176	0.3773	0.001	0.835	0.0052	0.005	0.683	0.0103	0.034	0.271	0.3255	0.047	0.197	0.3669
209	0.003	0.768	0.1422	N/A	N/A	N/A	0.000	0.921	0.0047	N/A	N/A	N/A	0.002	0.789	0.1318	N/A	N/A	N/A
210	0.123	0.033	0.6891	0.063	0.134	0.3995	0.010	0.549	0.0165	0.002	0.787	0.0078	0.111	0.043	0.6721	0.058	0.152	0.3916
211	0.024	0.365	0.2667	0.062	0.156	0.7584	0.010	0.548	0.0573	0.010	0.570	0.0478	0.014	0.488	0.2093	0.054	0.186	0.7104
212	0.036	0.260	0.3240	0.072	0.109	0.5199	0.006	0.658	0.0122	0.002	0.802	0.0058	0.032	0.288	0.3180	0.068	0.118	0.5141
213	0.390	0.023	0.7337	0.155	0.016	0.8749	0.002	0.818	0.0052	0.005	0.687	-0.0099	0.135	0.025	0.7284	0.155	0.016	0.8847
214	0.086	0.078	0.6344	N/A	N/A	N/A	0.025	0.350	0.0530	N/A	N/A	N/A	0.071	0.111	0.5813	N/A	N/A	N/A
215	0.130	0.028	0.9032	0.211	0.436	-1.6431	0.008	0.596	0.2790	0.209	0.439	-0.0466	0.117	0.039	0.8753	0.2	0.451	-1.5965
216	0.125	0.032	0.6908	0.012	0.793	0.2374	0.010	0.551	0.1350	0.581	0.028	-0.1118	0.118	0.038	0.6773	0.027	0.699	0.3492
217	0.068	0.120	0.4568	N/A	N/A	N/A	0.005	0.684	0.0273	N/A	N/A	N/A	0.053	0.172	0.4295	N/A	N/A	N/A
218	0.100	0.056	0.5386	N/A	N/A	N/A	0.000	0.910	-0.0037	0.025	0.843	0.0205	0.092	0.068	0.5423	0.877	0.228	-3.2021
219	0.146	0.020	0.5907	0.160	0.014	0.7146	0.009	0.579	-0.0150	0.068	0.119	-0.0302	0.146	0.020	0.6057	0.166	0.012	0.7447
220	0.059	0.146	0.5523	0.066	0.123	0.4913	0.014	0.478	-0.0132	0.002	0.804	-0.0054	0.061	0.140	0.5654	0.066	0.124	0.4967
221	0.118	0.037	0.7422	0.092	0.068	0.7163	0.002	0.779	-0.0058	0.009	0.570	-0.0102	0.160	0.039	0.7479	0.093	0.067	0.7265
222	0.158	0.016	0.8853	0.171	0.011	0.8457	0.002	0.802	-0.0038	0.046	0.202	-0.0287	0.157	0.019	0.8872	0.175	0.01	0.8744
223	0.084	0.083	0.6217	N/A	N/A	N/A	0.005	0.681	-0.0950	N/A	N/A	N/A	0.084	0.082	0.6313	N/A	N/A	N/A
224	0.121	0.035	0.6113	N/A	N/A	N/A	0.023	0.369	-0.0155	0.009	0.906	0.0095	0.125	0.032	0.6268	0.977	0.096	-0.9337
225	0.201	0.005	1.0627	0.212	0.005	0.7885	0.002	0.792	-0.0053	0.007	0.628	-0.0093	0.198	0.006	1.0680	0.212	0.005	0.8029
226	0.090	0.576	0.4513	N/A	N/A	N/A	0.032	0.287	-0.0381	N/A	N/A	N/A	0.011	0.541	0.4893	N/A	N/A	N/A
227	0.044	0.214	0.4624	0.045	0.220	0.4240	0.031	0.299	-0.0189	0.040	0.244	-0.0140	0.047	0.200	0.4813	0.049	0.209	0.4418
228	0.133	0.026	0.8056	0.174	0.011	1.0702	0.066	0.126	-0.0359	0.174	0.010	-0.0503	0.141	0.022	0.8415	0.186	0.009	1.1226
229	0.032	0.290	0.4069	N/A	N/A	N/A	0.066	0.123	-0.0495	N/A	N/A	N/A	0.041	0.227	0.4563	N/A	N/A	N/A
230	0.066	0.025	0.6344	0.044	0.215	0.4781	0.066	0.125	-0.0354	0.011	0.536	-0.0163	0.073	0.107	0.6697	0.046	0.201	0.4944
231	0.114	0.041	0.8829	0.126	0.031	0.7880	0.000	0.981	-0.0006	0.009	0.573	-0.0128	0.114	0.041	0.8834	0.128	0.03	0.8007
232	0.114	0.041	0.8829	N/A	N/A	N/A	0.067	0.121	-0.0485	N/A	N/A	N/A	0.039	0.241	0.6149	N/A	N/A	N/A
233	0.134	0.026	1.1316	0.061	0.147	0.7555	0.000	0.930	0.0020	0.015	0.474	-0.0155	0.135	0.025	1.1295	0.063	0.139	0.7696
234	0.118	0.043	1.0697	0.115	0.043	1.0338	0.006	0.644	0.0074	0.014	0.479	-0.0263	0.117	0.042	1.0886	0.12	0.039	1.0581
235	0.011	0.543	-0.3363	N/A	N/A	N/A	0.060	0.158	-0.0579	N/A	N/A	N/A	0.008	0.602	-0.2785	N/A	N/A	N/A
236	0.025	0.351	0.4898	0.021	0.396	0.4285	0.005	0.694	-0.0940	0.012	0.539	-0.0108	0.021	0.402	0.4581	0.023	0.381	0.4497
237	0.046	0.202	0.5947	0.087	0.081	0.7312	0.045	0.206	-0.0220	0.031	0.300	-0.0231	0.049	0.188	0.6166	0.093	0.07	0.7543
238	0.043	0.212	-0.6681	N/A	N/A	N/A	0.073	0.106	-0.0803	N/A	N/A	N/A	0.036	0.261	-0.5878	N/A	N/A	N/A
239	0.074	0.103	0.5258	0.105	0.051	0.8880	0.030	0.304	0.0346	0.020	0.403	0.0231	0.068	0.119	0.4911	0.1	0.057	0.8648
240	0.133	0.027	0.7197	0.102	0.054	0.7859	0.002	0.779	0.0640	0.000	0.966	-0.0011	0.131	0.028	0.7133	0.101	0.056	0.7869
241	0.007	0.617	0.2201	N/A	N/A	N/A	0.000	0.952	0.0014	N/A	N/A	N/A	0.007	0.620	0.2186	N/A	N/A	N/A
242	0.016	0.467	0.3050	0.024	0.359	0.4219	0.000	0.969	0.0013	0.000	0.915	-0.0033	0.016	0.456	0.3106	0.024	0.357	0.4251
243	0.123	0.034	0.7203	0.211	0.004	0.8903	0.060	0.144	0.0433	0.005	0.669	0.0134	0.109	0.046	0.6770	0.209	0.004	0.8768
244	0.000	0.968	-0.0188	0.000	0.939	-0.0426	0.026	0.345	-0.2670	0.003	0.768	-0.0129	0.000	0.986	0.0079	0	0.96	-0.0284
245	0.042	0.233	0.5165	0.060	0.158	0.7855	0.034	0.284	-0.0301	0.006	0.653	-0.0097	0.047	0.206	0.5465	0.061	0.152	0.7952
246	0.113	0.045	0.6318	0.135	0.027	0.6221	0.010	0.569	-0.0129	0.050	0.196	-0.0216	0.112	0.049	0.6404	0.137	0.028	0.6489
247	0.002	0.799	-0.0970	N/A	N/A	N/A	0.006	0.647	-0.0206	N/A	N/A	N/A	0.003	0.767	-0.1143	N/A	N/A	N/A
248	0.037	0.259	0.4019	0.050	0.201	0.4645	0.001	0.883	-0.0027	0.006	0.660	0.0095	0.040	0.251	0.4184	0.051	0.204	0.472
249	0.108	0.051	0.8452	0.077	0.112	0.5738	0.006	0.672	-0.0075	0.021	0.403	-0.0165	0.109	0.053	0.8632	0.089	0.092	0.6236
250	0.005	0.681	-0.1311	N/A	N/A	N/A	0.011	0.552	-0.0140	N/A	N/A	N/A	0.010	0.572	-0.1887	N/A	N/A	N/A

	Total Nitrogen						Dissolved Inorganic Nitrogen						Total Organic Nitrogen					
	Surface			*Bottom*			*Surface*			*Bottom*			*Surface*			*Bottom*		
Station	R^2	p-value	slope	R^2	p-value	slope	R^2	p-value	slope	R^2	p-value	slope	R^2	p-value	slope	R^2	p-value	slope
251	0.009	0.581	0.1806	0.031	0.303	0.3442	0.105	0.057	-0.0380	0.067	0.132	-0.0265	0.018	0.441	0.2577	0.044	0.226	0.4144
252	0.051	0.185	0.6343	0.089	0.077	0.6575	0.035	0.282	-0.0175	0.004	0.726	-0.0110	0.055	0.175	0.6713	0.087	0.085	0.6683
253	0.004	0.719	0.1475	N/A	N/A	N/A	0.001	0.876	-0.0047	N/A	N/A	N/A	0.004	0.712	0.1523	N/A	N/A	N/A
254	0.004	0.713	0.1326	N/A	N/A	N/A	0.002	0.821	0.0046	N/A	N/A	N/A	0.004	0.719	0.1279	N/A	N/A	N/A
255	0.013	0.516	0.2368	0.015	0.476	0.2620	0.002	0.776	0.0058	0.009	0.582	-0.0102	0.012	0.524	0.2310	0.016	0.457	0.2722
256	0.010	0.571	0.1895	0.050	0.198	0.4673	0.016	0.464	-0.0151	0.004	0.702	-0.0112	0.011	0.543	0.2045	0.053	0.19	0.4949
257	0.015	0.472	-0.2934	N/A	N/A	N/A	0.003	0.760	-0.0750	N/A	N/A	N/A	0.014	0.486	-0.2860	N/A	N/A	N/A
258	0.005	0.690	0.1613	0.020	0.419	0.2956	0.005	0.674	-0.0089	0.107	0.052	-0.0427	0.006	0.672	0.1710	0.026	0.351	0.3393
259	0.109	0.052	1.1357	0.157	0.019	1.3737	0.029	0.321	-0.0226	0.066	0.130	-0.0299	0.113	0.049	1.1589	0.163	0.016	1.4041
260	0.035	0.290	0.5817	N/A	N/A	N/A	0.016	0.470	0.0300	N/A	N/A	N/A	0.035	0.298	0.5606	N/A	N/A	N/A
261	0.073	0.122	0.6377	0.053	0.196	0.4572	0.000	0.905	0.0440	0.008	0.604	-0.0333	0.073	0.123	0.6336	0.062	0.162	0.4955
262	0.081	0.098	0.9044	0.102	0.065	0.9001	0.001	0.891	-0.0038	0.002	0.809	0.0071	0.084	0.097	0.9145	0.103	0.069	0.9146
263	0.127	0.036	0.7953	0.210	0.006	1.0466	0.148	0.023	-0.0479	0.167	0.015	-0.0507	0.148	0.025	0.8761	0.235	0.004	1.1335
264	0.097	0.069	0.5626	0.102	0.061	0.5883	0.098	0.068	-0.0383	0.051	0.197	-0.0270	0.106	0.056	0.6009	0.116	0.048	0.6219
265	0.019	0.435	0.2701	N/A	N/A	N/A	0.008	0.612	-0.2930	N/A	N/A	N/A	0.210	0.404	0.3007	N/A	N/A	N/A
266	0.000	0.928	-0.0389	N/A	N/A	N/A	0.025	0.366	-0.0317	N/A	N/A	N/A	0.000	0.988	-0.0061	N/A	N/A	N/A
267	0.134	0.031	0.8714	0.135	0.030	1.0649	0.005	0.695	-0.0100	0.042	0.240	-0.0354	0.139	0.028	0.8813	0.145	0.024	1.1003
268	0.079	0.097	0.6578	N/A	N/A	N/A	0.017	0.447	-0.0248	0.697	0.371	-0.7586	0.090	0.075	0.6826	0.192	0.712	1.2924
269	0.042	0.231	2.4863	0.051	0.193	1.9479	0.001	0.866	-0.0040	0.035	0.272	-0.0355	0.042	0.230	2.4903	0.052	0.186	1.9833
270	0.092	0.073	1.1651	0.122	0.040	1.1955	0.001	0.878	-0.0063	0.010	0.563	-0.0137	0.091	0.074	1.1714	0.121	0.04	1.209
271	0.117	0.041	1.2391	0.122	0.037	0.7207	0.001	0.851	-0.0049	0.021	0.397	-0.0186	0.116	0.042	1.2439	0.125	0.035	0.7393
272	0.115	0.043	0.7128	0.113	0.045	1.0806	0.004	0.712	0.0071	0.002	0.799	0.0060	0.110	0.048	0.7056	0.109	0.053	1.0796
273	0.083	0.088	1.1494	0.179	0.010	1.0383	0.005	0.687	-0.0113	0.005	0.670	-0.0162	0.083	0.088	1.1606	0.174	0.011	1.0545
274	0.083	0.088	0.8506	0.087	0.081	1.0457	0.001	0.895	0.0043	0.001	0.896	0.0037	0.080	0.095	0.8462	0.084	0.086	1.042
275	0.060	0.149	0.7933	0.075	0.112	0.9005	0.000	0.902	0.0030	0.007	0.637	-0.0109	0.058	0.157	0.7899	0.074	0.113	0.9096
276	0.139	0.025	1.2611	0.129	0.032	1.7061	0.000	0.935	0.0021	0.015	0.470	-0.0168	0.136	0.027	1.2589	0.13	0.031	1.7229
277	0.046	0.218	0.8941	0.060	0.150	0.9096	0.055	0.168	-0.0395	0.041	0.234	-0.0448	0.049	0.204	0.9305	0.064	0.136	0.9544
278	0.060	0.163	1.0317	0.050	0.192	0.9909	0.012	0.524	-0.0155	0.011	0.535	-0.0149	0.057	0.161	1.0472	0.05	0.189	1.0058
279	0.074	0.108	0.8255	0.066	0.130	0.7724	0.006	0.645	-0.1000	0.016	0.463	-0.0247	0.074	0.108	0.8355	0.068	0.125	0.7971
280	0.040	0.245	0.5014	0.073	0.110	1.4468	0.006	0.647	-0.0110	0.013	0.510	-0.0337	0.041	0.237	0.5124	0.075	0.105	1.481
281	0.083	0.089	0.8038	0.177	0.011	1.4016	0.790	0.097	-0.0373	0.174	0.013	-0.0620	0.091	0.075	0.8410	0.208	0.006	1.534
282	0.001	0.869	-0.1076	N/A	N/A	N/A	0.007	0.637	0.0230	N/A	N/A	N/A	0.001	0.843	-0.1307	N/A	N/A	N/A
283	0.004	0.721	0.2348	N/A	N/A	N/A	0.010	0.577	-0.0059	N/A	N/A	N/A	0.004	0.720	0.2376	N/A	N/A	N/A
284	0.000	0.944	0.0383	N/A	N/A	N/A	0.006	0.651	-0.0065	N/A	N/A	N/A	0.000	0.934	0.0447	N/A	N/A	N/A
285	0.001	0.876	-0.0807	N/A	N/A	N/A	0.006	0.666	-0.0287	N/A	N/A	N/A	0.000	0.921	-0.0520	N/A	N/A	N/A
286	0.000	0.997	0.0020	N/A	N/A	N/A	0.002	0.781	-0.0183	N/A	N/A	N/A	0.000	0.970	0.0204	N/A	N/A	N/A
287	0.004	0.727	0.1867	N/A	N/A	N/A	0.001	0.877	-0.0020	N/A	N/A	N/A	0.004	0.725	0.1887	N/A	N/A	N/A
288	0.009	0.568	0.3436	N/A	N/A	N/A	0.009	0.575	-0.0072	N/A	N/A	N/A	0.010	0.561	0.3508	N/A	N/A	N/A
289	0.002	0.771	0.1737	N/A	N/A	N/A	0.004	0.698	0.0463	N/A	N/A	N/A	0.001	0.835	0.1273	N/A	N/A	N/A
290	0.031	0.315	0.6611	N/A	N/A	N/A	0.013	0.510	-0.0187	N/A	N/A	N/A	0.032	0.305	0.6797	N/A	N/A	N/A
291	0.015	0.467	0.5652	N/A	N/A	N/A	0.004	0.710	0.0076	N/A	N/A	N/A	0.015	0.473	0.5575	N/A	N/A	N/A
292	0.010	0.561	0.3336	N/A	N/A	N/A	0.000	0.965	-0.0023	N/A	N/A	N/A	0.010	0.561	0.3358	N/A	N/A	N/A
293	0.009	0.581	0.3449	N/A	N/A	N/A	0.007	0.634	-0.0289	N/A	N/A	N/A	0.010	0.555	0.3738	N/A	N/A	N/A
294	0.016	0.455	0.3220	N/A	N/A	N/A	0.003	0.741	0.0065	N/A	N/A	N/A	0.015	0.472	0.3155	N/A	N/A	N/A
295	0.021	0.409	0.4629	N/A	N/A	N/A	0.005	0.695	-0.0388	N/A	N/A	N/A	0.024	0.373	0.5017	N/A	N/A	N/A
296	0.012	0.529	0.3648	N/A	N/A	N/A	0.000	0.930	-0.0019	N/A	N/A	N/A	0.012	0.536	0.3607	N/A	N/A	N/A
297	0.034	0.271	0.5036	N/A	N/A	N/A	0.031	0.297	0.0298	N/A	N/A	N/A	0.029	0.311	0.4738	N/A	N/A	N/A
298	0.022	0.384	0.5842	N/A	N/A	N/A	0.019	0.420	-0.0196	N/A	N/A	N/A	0.023	0.366	0.6038	N/A	N/A	N/A
299	0.000	0.920	0.0642	N/A	N/A	N/A	0.007	0.622	0.0295	N/A	N/A	N/A	0.000	0.956	0.0346	N/A	N/A	N/A
300	0.013	0.494	0.4245	N/A	N/A	N/A	0.000	0.988	-0.0004	N/A	N/A	N/A	0.014	0.493	0.4249	N/A	N/A	N/A
301	0.012	0.521	0.4382	N/A	N/A	N/A	0.011	0.533	-0.0132	N/A	N/A	N/A	0.013	0.509	0.4513	N/A	N/A	N/A

	Total Nitrogen						Dissolved Inorganic Nitrogen						Total Organic Nitrogen					
	Surface			*Bottom*			*Surface*			*Bottom*			*Surface*			*Bottom*		
Station	R^2	p-value	slope	R^2	p-value	slope	R^2	p-value	slope	R^2	p-value	slope	R^2	p-value	slope	R^2	p-value	slope
302	0.002	0.356	0.5291	N/A	N/A	N/A	0.063	0.135	-0.0275	N/A	N/A	N/A	0.027	0.330	0.5566	N/A	N/A	N/A
303	0.001	0.855	-0.1299	N/A	N/A	N/A	0.003	0.752	-0.0202	N/A	N/A	N/A	0.001	0.874	-0.1098	N/A	N/A	N/A
304	0.004	0.713	0.2540	N/A	N/A	N/A	0.003	0.730	-0.0173	N/A	N/A	N/A	0.004	0.696	0.2713	N/A	N/A	N/A
305	0.036	0.262	0.6341	N/A	N/A	N/A	0.016	0.459	0.0172	N/A	N/A	N/A	0.034	0.276	0.6169	N/A	N/A	N/A
306	0.033	0.282	0.6083	N/A	N/A	N/A	0.002	0.812	-0.0071	N/A	N/A	N/A	0.034	0.276	0.6153	N/A	N/A	N/A
307	0.050	0.185	0.6805	N/A	N/A	N/A	0.001	0.858	0.0056	N/A	N/A	N/A	0.048	0.193	0.6748	N/A	N/A	N/A
308	0.008	0.591	0.3535	N/A	N/A	N/A	0.001	0.851	0.0062	N/A	N/A	N/A	0.008	0.598	0.3473	N/A	N/A	N/A
309	0.036	0.260	0.6251	N/A	N/A	N/A	0.017	0.441	-0.0134	N/A	N/A	N/A	0.037	0.251	0.6385	N/A	N/A	N/A
310	0.009	0.586	0.3192	N/A	N/A	N/A	0.013	0.506	0.0616	N/A	N/A	N/A	0.005	0.664	0.2574	N/A	N/A	N/A
311	0.008	0.592	0.3824	N/A	N/A	N/A	0.014	0.450	-0.0552	N/A	N/A	N/A	0.011	0.546	0.4343	N/A	N/A	N/A
312	0.037	0.251	0.7797	N/A	N/A	N/A	0.004	0.726	0.0067	N/A	N/A	N/A	0.036	0.260	0.7730	N/A	N/A	N/A
313	0.046	0.203	0.6454	N/A	N/A	N/A	0.010	0.561	-0.0152	N/A	N/A	N/A	0.048	0.195	0.6606	N/A	N/A	N/A
314	0.026	0.339	0.6779	N/A	N/A	N/A	0.025	0.346	-0.0297	N/A	N/A	N/A	0.028	0.322	0.7075	N/A	N/A	N/A
315	0.056	0.160	0.8538	N/A	N/A	N/A	0.017	0.440	-0.0218	N/A	N/A	N/A	0.058	0.151	0.8755	N/A	N/A	N/A
316	0.038	0.246	0.6572	N/A	N/A	N/A	0.061	0.140	-0.0404	N/A	N/A	N/A	0.043	0.219	0.6976	N/A	N/A	N/A
317	0.030	0.309	0.5690	N/A	N/A	N/A	0.015	0.476	-0.0277	N/A	N/A	N/A	0.032	0.286	0.5966	N/A	N/A	N/A
318	0.106	0.050	0.9608	0.134	0.028	1.9975	0.007	0.619	-0.0104	0.006	0.640	0.0105	0.061	0.148	0.6807	0.132	0.03	1.9848
319	0.073	0.105	0.7477	0.153	0.017	1.3853	0.012	0.511	-0.0147	0.018	0.431	0.0272	0.076	0.099	0.7624	0.149	0.018	1.358
320	0.030	0.322	0.4261	0.034	0.289	0.4179	0.000	0.966	0.0014	0.002	0.811	-0.0129	0.032	0.305	0.4247	0.039	0.257	0.4308
321	0.061	0.146	0.5991	0.016	0.470	0.2944	0.008	0.607	-0.0157	0.000	0.911	-0.0036	0.029	0.331	0.3777	0.018	0.446	0.2979
322	0.142	0.021	1.1219	0.174	0.010	1.3604	0.017	0.437	-0.0194	0.007	0.622	0.0147	0.150	0.018	1.1413	0.174	0.011	1.3524
323	0.900	0.058	0.7358	0.184	0.008	0.9893	0.004	0.718	0.0111	0.003	0.741	0.0102	0.099	0.580	0.7246	0.184	0.008	0.979
324	0.076	0.098	0.6330	0.137	0.024	0.8453	0.001	0.875	0.0650	0.005	0.687	0.0165	0.081	0.089	0.6264	0.139	0.023	0.8288
325	0.093	0.067	0.8405	0.158	0.015	1.1556	0.041	0.239	-0.0314	0.002	0.803	-0.0051	0.091	0.074	0.8379	0.16	0.014	1.1606
326	0.119	0.036	0.7257	0.123	0.033	0.7355	0.011	0.546	-0.0135	0.007	0.618	-0.016	0.120	0.035	0.7491	0.124	0.032	0.7514
327	0.184	0.008	0.8917	0.191	0.007	0.8869	0.040	0.234	-0.0315	0.013	0.502	-0.0173	0.193	0.007	0.9231	0.191	0.007	0.9042
328	0.235	0.002	1.0561	0.270	0.001	1.3721	0.008	0.601	-0.0107	0.000	0.924	-0.0021	0.234	0.002	1.0668	0.23	0.001	1.3741
329	0.099	0.061	0.6689	0.163	0.014	0.7474	0.006	0.663	-0.0890	0.015	0.479	-0.0185	0.042	0.235	0.3908	0.169	0.014	0.7713
330	0.125	0.032	0.7803	0.157	0.015	0.8214	0.002	0.817	-0.0072	0.000	0.900	-0.0035	0.122	0.034	0.7874	0.155	0.016	0.8248
331	0.177	0.010	1.1500	0.261	0.001	1.5981	0.004	0.727	-0.0108	0.022	0.386	-0.0235	0.177	0.009	1.1607	0.266	0.001	1.6216
332	0.199	0.006	1.1622	0.218	0.004	1.2322	0.013	0.509	-0.0131	0.000	0.902	-0.0025	0.197	0.070	1.1554	0.219	0.003	1.2347
333	0.208	0.050	0.9934	0.282	0.001	1.0952	0.009	0.586	-0.0111	0.002	0.786	-0.0037	0.210	0.004	1.0045	0.279	0.001	1.0989
334	0.131	0.028	0.9768	0.209	0.004	1.3775	0.024	0.362	-0.0160	0.006	0.648	-0.0082	0.134	0.026	0.9928	0.209	0.004	1.3856
335	0.178	0.009	1.1407	0.168	0.012	1.3203	0.028	0.327	-0.0181	0.013	0.502	-0.0087	0.183	0.008	1.1588	0.17	0.011	1.3289
336	0.199	0.006	0.9593	0.295	0.001	1.0676	0.022	0.377	-0.0148	0.010	0.547	-0.0274	0.203	0.005	0.9741	0.296	0.001	1.095
337	0.195	0.006	0.8866	0.211	0.004	1.4086	0.032	0.287	-0.0216	0.021	0.398	-0.0153	0.202	0.005	0.9082	0.214	0.004	1.4238
338	0.147	0.021	1.1989	0.168	0.016	1.1264	0.018	0.441	-0.0173	0.000	0.994	-0.0001	0.152	0.019	1.2162	0.168	0.016	1.1302
339	0.283	0.001	1.4531	0.275	0.001	1.6136	0.000	0.960	-0.0008	0.044	0.214	-0.0204	0.283	0.001	1.4539	0.279	0.001	1.634
340	0.140	0.023	1.0895	0.169	0.012	1.2358	0.003	0.745	-0.0049	0.003	0.766	0.0055	0.141	0.022	1.0943	0.167	0.012	1.2302
341	0.086	0.082	0.7878	0.144	0.025	1.0188	0.042	0.229	-0.0262	0.001	0.838	-0.0042	0.092	0.072	0.8140	0.144	0.025	1.023
342	0.145	0.022	0.9686	0.154	0.020	1.0969	0.015	0.491	-0.0127	0.015	0.487	-0.0468	0.152	0.021	1.0170	0.115	0.05	0.9196
343	0.144	0.023	1.0171	0.166	0.015	1.0823	0.036	0.268	-0.0220	0.001	0.884	-0.0108	0.147	0.021	1.0391	0.128	0.037	0.945
344	0.200	0.004	1.4489	0.226	0.003	1.4344	0.006	0.654	-0.0102	0.051	0.178	-0.0347	0.207	0.005	1.4591	0.231	0.003	1.4688
345	0.172	0.011	1.3144	0.231	0.003	1.6177	0.068	0.126	0.0442	0.001	0.823	0.0188	0.150	0.020	1.2145	0.225	0.003	1.5988
346	0.095	0.072	0.7441	0.106	0.056	0.7998	0.020	0.416	0.0293	0.000	0.929	-0.0045	0.092	0.077	0.7147	0.11	0.052	0.8043
347	0.030	0.074	0.7285	0.103	0.060	0.7109	0.018	0.442	0.0177	0.001	0.870	0.0078	0.092	0.076	0.7107	0.102	0.061	0.7031
348	0.074	0.109	0.6260	0.104	0.063	0.7145	0.027	0.341	0.0221	0.044	0.235	0.0219	0.071	0.115	0.6038	0.099	0.075	0.7063
349	0.067	0.128	0.5953	0.060	0.156	0.6057	0.046	0.207	0.0287	0.066	0.136	0.0351	0.064	0.138	0.5666	0.056	0.172	0.5705
350	0.165	0.013	1.6350	0.148	0.019	1.2038	0.008	0.594	0.0119	0.006	0.654	0.0219	0.163	0.013	1.6230	0.144	0.02	1.1817
400	0.139	0.051	1.6695	0.163	0.033	1.7748	0.036	0.337	-0.0340	0.063	0.199	-0.0767	0.144	0.047	1.7034	0.17	0.029	1.8431
401	0.219	0.012	1.9725	0.230	0.015	1.9866	0.103	0.096	-0.0702	0.132	0.068	-0.0546	0.230	0.010	2.0426	0.238	0.013	2.0407
402	0.226	0.012	1.6371	0.217	0.016	1.7044	0.067	0.192	-0.0401	0.028	0.404	-0.0194	0.230	0.011	1.6773	0.219	0.016	1.7241
403	0.143	0.052	1.5679	0.235	0.010	1.6868	0.008	0.133	-0.0313	0.080	0.153	-0.0584	0.146	0.049	1.5991	0.245	0.009	1.7452

	Total Phosphorus						Soluble Reactive Phosphate						Alkaline Phosphatase					
	Surface			*Bottom*			*Surface*			*Bottom*			*Surface*			*Bottom*		
Station	R^2	p-value	slope	R^2	p-value	slope	R^2	p-value	slope	R^2	p-value	slope	R^2	p-value	slope	R^2	p-value	slope
200	0.030	0.306	0.0059	0.002	0.818	-0.0017	0.313	0.000	0.0043	0.262	0.002	0.0055	0.042	0.229	0.0046	0.043	0.253	0.006
201	0.009	0.570	0.0042	0.001	0.866	-0.0012	0.353	0.000	0.0057	0.072	0.132	0.0047	0.210	0.005	0.0054	0.080	0.105	0.004
202	0.024	0.358	-0.0041	0.040	0.234	-0.0059	0.140	0.220	0.0043	0.199	0.006	0.0041	0.044	0.217	0.0032	0.025	0.358	0.003
203	0.030	0.305	-0.0043	N/A	N/A	N/A	0.087	0.077	0.0028	N/A	N/A	N/A	0.035	0.277	0.0030	N/A	N/A	N/A
204	0.056	0.160	0.0115	0.096	0.071	0.0135	0.095	0.064	0.0350	0.088	0.084	0.0037	0.258	0.002	0.0068	0.145	0.024	0.005
205	0.011	0.535	0.0026	0.020	0.407	-0.0042	0.260	0.001	0.0046	0.316	0.000	0.0043	0.202	0.006	0.0069	0.055	0.169	0.004
206	0.019	0.416	-0.0034	0.036	0.260	-0.0046	0.333	0.000	0.0048	0.310	0.000	0.0041	0.092	0.073	0.0036	0.049	0.197	0.003
207	0.011	0.536	-0.0027	N/A	N/A	N/A	0.369	0.000	0.0053	N/A	N/A	N/A	0.144	0.022	0.0064	N/A	N/A	N/A
208	0.010	0.552	-0.0032	0.000	0.900	0.0005	0.355	0.000	0.0044	0.334	0.000	0.0050	0.111	0.047	0.0050	0.106	0.053	0.005
209	0.117	0.038	0.0121	N/A	N/A	N/A	0.064	0.132	0.0017	N/A	N/A	N/A	0.016	0.470	0.0191	N/A	N/A	N/A
210	0.025	0.352	-0.0036	0.069	0.115	-0.0066	0.104	0.051	0.0360	0.077	0.097	0.0031	0.054	0.171	0.0032	0.049	0.194	0.003
211	0.006	0.643	-0.0030	0.012	0.525	-0.0042	0.097	0.060	0.0034	0.146	0.021	0.0028	0.002	0.796	-0.0012	0.068	0.129	0.005
212	0.094	0.065	-0.0077	0.055	0.163	-0.0068	0.081	0.088	0.0028	0.214	0.004	0.0036	0.080	0.094	0.0042	0.102	0.057	0.005
213	0.017	0.448	0.0041	0.000	0.987	0.0001	0.118	0.038	0.0045	0.033	0.285	0.0024	0.018	0.442	0.0049	0.080	0.095	0.004
214	0.014	0.485	0.0057	N/A	N/A	N/A	0.045	0.209	0.0021	N/A	N/A	N/A	0.009	0.591	0.0013	N/A	N/A	N/A
215	0.013	0.502	0.0120	0.599	0.124	0.0375	0.165	0.013	0.0034	0.694	0.039	0.0023	0.006	0.662	0.0013	0.040	0.748	-0.011
216	0.027	0.337	0.0085	0.455	0.066	0.0178	0.079	0.093	0.0031	0.005	0.859	0.0005	0.022	0.386	0.0032	0.046	0.646	0.001
217	0.068	0.125	0.0138	N/A	N/A	N/A	0.125	0.032	0.0040	N/A	N/A	N/A	0.031	0.307	0.0021	N/A	N/A	N/A
218	0.045	0.205	0.0105	0.989	0.067	-0.0414	0.080	0.095	0.0039	0.816	0.097	0.0048	0.004	0.708	0.0011	0.899	0.206	-0.004
219	0.008	0.606	0.0028	0.035	0.284	0.0071	0.107	0.052	0.0039	0.152	0.017	0.0041	0.021	0.404	0.0017	0.002	0.798	0.001
220	0.051	0.178	0.0121	0.060	0.152	0.0105	0.139	0.023	0.0044	0.119	0.039	0.0043	0.029	0.319	0.0032	0.031	0.301	0.004
221	0.013	0.502	0.0039	0.008	0.613	0.0026	0.126	0.033	0.0041	0.090	0.071	0.0028	0.006	0.658	0.0013	0.018	0.441	0.002
222	0.005	0.679	0.0027	0.003	0.763	0.0016	0.057	0.162	0.0022	0.013	0.509	0.0011	0.000	0.969	0.0001	0.020	0.414	0.002
223	0.043	0.221	0.0078	N/A	N/A	N/A	0.105	0.050	0.0033	N/A	N/A	N/A	0.016	0.451	0.0022	N/A	N/A	N/A
224	0.104	0.052	0.0126	0.740	0.341	-0.0125	0.029	0.323	0.0017	0.898	0.052	-0.0084	0.001	0.874	0.0004	0.646	0.406	-0.003
225	0.007	0.616	0.0034	0.000	0.925	-0.0006	0.034	0.282	0.0024	0.127	0.033	0.0029	0.000	0.954	-0.0002	0.004	0.728	0.001
226	0.001	0.858	0.0012	N/A	N/A	N/A	0.234	0.003	0.0036	N/A	N/A	N/A	0.019	0.412	0.0027	N/A	N/A	N/A
227	0.001	0.881	0.0010	0.000	0.904	-0.0006	0.148	0.020	0.0041	0.176	0.012	0.0032	0.051	0.181	0.0025	0.027	0.337	0.002
228	0.006	0.645	0.0031	0.040	0.237	0.0105	0.087	0.076	0.0026	0.043	0.217	0.0024	0.021	0.395	0.0012	0.081	0.087	0.007
229	0.033	0.284	0.0093	N/A	N/A	N/A	0.135	0.025	0.0021	N/A	N/A	N/A	0.040	0.234	0.0024	N/A	N/A	N/A
230	0.027	0.332	0.0095	0.016	0.453	0.0080	0.117	0.038	0.0025	0.011	0.543	0.0022	0.005	0.679	-0.0007	0.000	0.984	0.000
231	0.012	0.525	0.0069	0.008	0.596	0.0045	0.129	0.031	0.0033	0.164	0.014	0.0039	0.030	0.306	0.0012	0.004	0.718	0.000
232	0.003	0.757	0.0021	N/A	N/A	N/A	0.293	0.001	0.0033	N/A	N/A	N/A	0.010	0.547	0.0017	N/A	N/A	N/A
233	0.005	0.691	0.0027	0.009	0.569	0.0030	0.085	0.085	0.0026	0.164	0.014	0.0047	0.032	0.288	0.0026	0.009	0.574	0.002
234	0.005	0.665	-0.0019	0.000	1.000	0.0000	0.190	0.007	0.0047	0.042	0.224	0.0037	0.081	0.088	0.0037	0.125	0.032	0.004
235	0.010	0.550	-0.0035	N/A	N/A	N/A	0.098	0.059	0.0029	N/A	N/A	N/A	0.001	0.854	-0.0008	N/A	N/A	N/A
236	0.002	0.783	-0.0015	0.046	0.203	0.0072	0.271	0.001	0.0037	0.205	0.006	0.0031	0.020	0.400	0.0024	0.002	0.771	0.001
237	0.021	0.398	0.0109	0.011	0.542	0.0046	0.242	0.002	0.0041	0.299	0.000	0.0045	0.021	0.389	0.0017	0.001	0.853	0.001
238	0.017	0.435	-0.0048	N/A	N/A	N/A	0.121	0.035	0.0023	N/A	N/A	N/A	0.038	0.247	-0.0051	N/A	N/A	N/A
239	0.004	0.700	-0.0023	0.000	0.972	0.0002	0.191	0.007	0.0039	0.233	0.003	0.0050	0.039	0.242	0.0021	0.057	0.154	0.003
240	0.027	0.330	-0.0044	0.003	0.754	-0.0014	0.279	0.001	0.0055	0.146	0.020	0.0037	0.034	0.282	0.0022	0.087	0.081	0.003
241	0.020	0.400	0.0042	N/A	N/A	N/A	0.137	0.024	0.0034	N/A	N/A	N/A	0.002	0.802	-0.0008	N/A	N/A	N/A
242	0.000	0.913	0.0006	0.005	0.670	-0.0024	0.107	0.051	0.0028	0.248	0.002	0.0050	0.037	0.262	-0.0058	0.022	0.391	-0.004
243	0.000	0.965	-0.0003	0.019	0.415	-0.0039	0.226	0.003	0.0053	0.154	0.016	0.0041	0.052	0.180	0.0021	0.071	0.116	0.003
244	0.017	0.446	-0.0038	0.020	0.432	-0.0064	0.009	0.582	0.0010	0.037	0.285	0.0024	0.022	0.400	-0.0026	0.106	0.068	-0.007
245	0.091	0.074	0.0138	0.027	0.354	0.0072	0.113	0.045	0.0030	0.160	0.017	0.0030	0.078	0.104	-0.0055	0.070	0.123	-0.007
246	0.036	0.271	0.0091	0.042	0.228	0.0083	0.208	0.005	0.0045	0.225	0.004	0.0031	0.000	0.955	0.0001	0.013	0.520	0.001
247	0.014	0.493	0.0045	N/A	N/A	N/A	0.141	0.024	0.0043	N/A	N/A	N/A	0.093	0.071	0.0038	N/A	N/A	N/A
248	0.034	0.278	0.0054	0.001	0.828	-0.0009	0.151	0.019	0.0034	0.243	0.003	0.0051	0.038	0.263	0.0028	0.019	0.433	0.002
249	0.000	0.928	-0.0004	0.002	0.785	0.0014	0.109	0.049	0.0030	0.221	0.004	0.0034	0.064	0.143	0.0017	0.140	0.027	0.003
250	0.017	0.443	0.0029	N/A	N/A	N/A	0.040	0.179	0.0034	N/A	N/A	N/A	0.042	0.231	0.0024	N/A	N/A	N/A

	Total Phosphorus						Soluble Reactive Phosphate						Alkaline Phosphatase					
	Surface			*Bottom*			*Surface*			*Bottom*			*Surface*			*Bottom*		
Station	R^2	p-value	slope	R^2	p-value	slope	R^2	p-value	slope	R^2	p-value	slope	R^2	p-value	slope	R^2	p-value	slope
251	0.005	0.675	0.0019	0.017	0.453	-0.0027	0.072	0.114	0.0030	0.089	0.077	0.0038	0.034	0.284	0.0036	0.023	0.379	0.002
252	0.006	0.647	0.0051	0.005	0.671	0.0048	0.093	0.071	0.0029	0.015	0.476	0.0026	0.009	0.590	-0.0006	0.001	0.835	-0.001
253	0.007	0.639	0.0060	N/A	N/A	N/A	0.031	0.308	0.0016	N/A	N/A	N/A	0.042	0.229	0.0017	N/A	N/A	N/A
254	0.028	0.328	0.0105	N/A	N/A	N/A	0.054	0.174	0.0024	N/A	N/A	N/A	0.004	0.730	0.0005	N/A	N/A	N/A
255	0.024	0.366	0.0097	0.086	0.082	0.0146	0.163	0.014	0.0041	0.117	0.041	0.0040	0.000	0.976	-0.0001	0.006	0.659	-0.002
256	0.052	0.182	0.0085	0.029	0.325	0.0112	0.135	0.028	0.0043	0.078	0.104	0.0037	0.000	0.899	-0.0003	0.028	0.337	0.002
257	0.049	0.194	0.0119	N/A	N/A	N/A	0.164	0.014	0.0059	N/A	N/A	N/A	0.016	0.458	0.0011	N/A	N/A	N/A
258	0.025	0.361	0.0094	0.005	0.692	0.0030	0.138	0.026	0.0045	0.141	0.024	0.0035	0.001	0.854	0.0006	0.008	0.614	-0.002
259	0.041	0.238	0.0098	0.111	0.048	0.0163	0.052	0.180	0.0039	0.114	0.044	0.0045	0.005	0.700	-0.0007	0.002	0.806	-0.001
260	0.048	0.208	0.0102	N/A	N/A	N/A	0.136	0.032	0.0043	N/A	N/A	N/A	0.009	0.592	-0.0017	N/A	N/A	N/A
261	0.067	0.135	0.0128	0.010	0.572	0.0047	0.443	0.000	0.0045	0.289	0.001	0.0029	0.024	0.370	0.0039	0.019	0.435	0.003
262	0.056	0.166	0.0126	0.007	0.638	0.0038	0.089	0.077	0.0042	0.081	0.092	0.0046	0.000	0.915	-0.0003	0.000	0.967	0.000
263	0.051	0.184	0.0081	0.051	0.185	0.0100	0.120	0.038	0.0053	0.057	0.160	0.0044	0.001	0.833	0.0004	0.032	0.295	-0.002
264	0.048	0.208	0.0156	0.032	0.302	0.0099	0.193	0.008	0.0033	0.185	0.011	0.0025	0.013	0.516	0.0010	0.005	0.702	0.001
265	0.000	0.908	-0.0007	N/A	N/A	N/A	0.018	0.439	0.0021	N/A	N/A	N/A	0.000	0.949	0.0002	N/A	N/A	N/A
266	0.006	0.661	0.0032	N/A	N/A	N/A	0.257	0.002	0.0038	N/A	N/A	N/A	0.005	0.691	-0.0013	N/A	N/A	N/A
267	0.001	0.835	-0.0010	0.001	0.868	-0.0010	0.197	0.008	0.0038	0.099	0.065	0.0019	0.005	0.693	-0.0017	0.003	0.761	-0.001
268	0.029	0.317	0.0060	0.795	0.299	0.0177	0.068	0.126	0.0026	N/A	N/A	N/A	0.042	0.229	0.0021	0.952	0.140	0.031
269	0.056	0.163	0.0065	0.025	0.359	0.0040	0.069	0.122	0.0039	0.040	0.248	0.0019	0.000	0.927	0.0004	0.013	0.501	-0.003
270	0.001	0.875	-0.0010	0.002	0.817	-0.0011	0.021	0.398	0.0017	0.024	0.367	0.0020	0.001	0.842	-0.0007	0.028	0.326	-0.004
271	0.010	0.559	0.0038	0.023	0.376	0.0064	0.068	0.124	0.0024	0.058	0.156	0.0028	0.026	0.348	0.0037	0.030	0.310	0.004
272	0.000	0.973	-0.0002	0.001	0.856	-0.0009	0.115	0.043	0.0036	0.056	0.171	0.0027	0.070	0.120	0.0044	0.064	0.136	0.006
273	0.081	0.092	0.0083	0.004	0.704	0.0016	0.129	0.032	0.0041	0.089	0.077	0.0037	0.021	0.404	0.0018	0.100	0.060	0.004
274	0.000	0.910	0.0006	0.002	0.795	0.0014	0.146	0.022	0.0038	0.149	0.020	0.0047	0.000	0.944	0.0001	0.001	0.892	0.000
275	0.058	0.158	0.0073	0.023	0.377	0.0057	0.184	0.009	0.0044	0.173	0.012	0.0044	0.029	0.324	0.0032	0.007	0.635	0.002
276	0.096	0.066	0.0115	0.009	0.579	0.0037	0.114	0.044	0.0044	0.185	0.009	0.0048	0.013	0.507	0.0015	0.014	0.496	0.002
277	0.003	0.767	0.0030	0.006	0.655	0.0019	0.149	0.020	0.0003	0.093	0.071	0.0030	0.028	0.328	0.0021	0.096	0.066	0.005
278	0.020	0.412	0.0037	0.003	0.770	0.0015	0.085	0.084	0.0025	0.128	0.032	0.0037	0.005	0.673	0.0016	0.016	0.457	0.003
279	0.038	0.254	0.0054	0.008	0.615	0.0078	0.145	0.022	0.0029	0.096	0.066	0.0039	0.091	0.073	0.0029	0.091	0.075	0.002
280	0.091	0.074	0.0096	0.012	0.517	0.0047	0.050	0.168	0.0034	0.070	0.119	0.0043	0.022	0.393	0.0016	0.050	0.190	0.002
281	0.000	0.901	-0.0008	0.030	0.314	-0.0054	0.113	0.045	0.0022	0.092	0.077	0.0018	0.025	0.373	-0.0082	0.016	0.483	0.003
282	0.330	0.000	-0.0200	N/A	N/A	N/A	0.050	0.678	0.0015	N/A	N/A	N/A	0.054	0.173	-0.0064	N/A	N/A	N/A
283	0.071	0.115	-0.0140	N/A	N/A	N/A	0.045	0.221	0.0028	N/A	N/A	N/A	0.014	0.485	0.0035	N/A	N/A	N/A
284	0.162	0.014	-0.0115	N/A	N/A	N/A	0.018	0.434	0.0021	N/A	N/A	N/A	0.012	0.511	-0.0023	N/A	N/A	N/A
285	0.080	0.079	-0.0097	N/A	N/A	N/A	0.037	0.264	0.0032	N/A	N/A	N/A	0.046	0.210	0.0119	N/A	N/A	N/A
286	0.032	0.296	-0.0061	N/A	N/A	N/A	0.022	0.390	0.0019	N/A	N/A	N/A	0.034	0.285	-0.0031	N/A	N/A	N/A
287	0.002	0.798	0.0015	N/A	N/A	N/A	0.033	0.285	0.0022	N/A	N/A	N/A	0.006	0.653	0.0011	N/A	N/A	N/A
288	0.002	0.459	-0.0054	N/A	N/A	N/A	0.081	0.088	0.0049	N/A	N/A	N/A	0.003	0.757	0.0016	N/A	N/A	N/A
289	0.025	0.348	-0.0051	N/A	N/A	N/A	0.022	0.384	0.0020	N/A	N/A	N/A	0.003	0.748	-0.0018	N/A	N/A	N/A
290	0.099	0.066	-0.0141	N/A	N/A	N/A	0.061	0.153	0.0032	N/A	N/A	N/A	0.046	0.217	0.0070	N/A	N/A	N/A
291	0.182	0.008	-0.0130	N/A	N/A	N/A	0.042	0.221	0.0022	N/A	N/A	N/A	0.000	0.966	0.0002	N/A	N/A	N/A
292	0.174	0.010	-0.0111	N/A	N/A	N/A	0.019	0.410	0.0180	N/A	N/A	N/A	0.031	0.299	-0.0031	N/A	N/A	N/A
293	0.192	0.007	-0.0109	N/A	N/A	N/A	0.049	0.188	0.0027	N/A	N/A	N/A	0.010	0.551	-0.0013	N/A	N/A	N/A
294	0.005	0.672	-0.0019	N/A	N/A	N/A	0.001	0.821	-0.0005	N/A	N/A	N/A	0.054	0.166	-0.0064	N/A	N/A	N/A
295	0.000	0.979	0.0002	N/A	N/A	N/A	0.001	0.890	0.0003	N/A	N/A	N/A	0.030	0.316	0.0062	N/A	N/A	N/A
296	0.008	0.613	0.0033	N/A	N/A	N/A	0.024	0.371	0.0019	N/A	N/A	N/A	0.007	0.622	0.0021	N/A	N/A	N/A
297	0.020	0.404	0.0046	N/A	N/A	N/A	0.058	0.151	0.0078	N/A	N/A	N/A	0.015	0.476	-0.0015	N/A	N/A	N/A
298	0.025	0.353	0.0099	N/A	N/A	N/A	0.007	0.630	0.0010	N/A	N/A	N/A	0.020	0.407	0.0044	N/A	N/A	N/A
299	0.005	0.692	0.0028	N/A	N/A	N/A	0.011	0.539	0.0012	N/A	N/A	N/A	0.001	0.836	0.0009	N/A	N/A	N/A
300	0.005	0.665	-0.0023	N/A	N/A	N/A	0.048	0.192	0.0270	N/A	N/A	N/A	0.002	0.818	-0.0020	N/A	N/A	N/A
301	0.038	0.248	0.0084	N/A	N/A	N/A	0.007	0.616	0.0010	N/A	N/A	N/A	0.002	0.796	0.0025	N/A	N/A	N/A

	Total Phosphorus						Soluble Reactive Phosphate						Alkaline Phosphatase					
	Surface			*Bottom*			*Surface*			*Bottom*			*Surface*			*Bottom*		
Station	R^2	p-value	slope	R^2	p-value	slope	R^2	p-value	slope	R^2	p-value	slope	R^2	p-value	slope	R^2	p-value	slope
302	0.017	0.444	0.0056	N/A	N/A	N/A	0.045	0.280	0.0029	N/A	N/A	N/A	0.034	0.274	0.0081	N/A	N/A	N/A
303	0.017	0.442	0.0063	N/A	N/A	N/A	0.030	0.306	0.0024	N/A	N/A	N/A	0.024	0.360	-0.0059	N/A	N/A	N/A
304	0.016	0.461	0.0052	N/A	N/A	N/A	0.000	0.930	0.0001	N/A	N/A	N/A	0.005	0.693	0.0023	N/A	N/A	N/A
305	0.053	0.172	0.0126	N/A	N/A	N/A	0.065	0.128	0.0043	N/A	N/A	N/A	0.016	0.459	0.0068	N/A	N/A	N/A
306	0.087	0.077	0.0145	N/A	N/A	N/A	0.060	0.144	0.0033	N/A	N/A	N/A	0.003	0.759	0.0034	N/A	N/A	N/A
307	0.055	0.164	0.0122	N/A	N/A	N/A	0.023	0.144	0.0033	N/A	N/A	N/A	0.009	0.567	0.0078	N/A	N/A	N/A
308	0.053	0.178	0.0083	N/A	N/A	N/A	0.027	0.331	0.0019	N/A	N/A	N/A	0.041	0.227	0.0162	N/A	N/A	N/A
309	0.000	0.912	0.0008	N/A	N/A	N/A	0.028	0.233	0.0022	N/A	N/A	N/A	0.007	0.624	0.0115	N/A	N/A	N/A
310	0.022	0.380	0.0059	N/A	N/A	N/A	0.036	0.226	0.0034	N/A	N/A	N/A	0.015	0.477	0.0396	N/A	N/A	N/A
311	0.016	0.457	0.0036	N/A	N/A	N/A	0.048	0.201	0.0026	N/A	N/A	N/A	0.072	0.108	0.0162	N/A	N/A	N/A
312	0.018	0.430	-0.0052	N/A	N/A	N/A	0.033	0.279	0.0022	N/A	N/A	N/A	0.016	0.458	0.0226	N/A	N/A	N/A
313	0.002	0.810	0.0022	N/A	N/A	N/A	0.055	0.164	0.0036	N/A	N/A	N/A	0.020	0.408	0.0296	N/A	N/A	N/A
314	0.019	0.421	0.0068	N/A	N/A	N/A	0.042	0.225	0.0030	N/A	N/A	N/A	0.001	0.885	0.0018	N/A	N/A	N/A
315	0.033	0.280	0.0068	N/A	N/A	N/A	0.014	0.481	0.0026	N/A	N/A	N/A	0.016	0.460	0.0208	N/A	N/A	N/A
316	0.044	0.212	0.0093	N/A	N/A	N/A	0.108	0.047	0.0024	N/A	N/A	N/A	0.033	0.281	0.0108	N/A	N/A	N/A
317	0.013	0.501	0.0039	N/A	N/A	N/A	0.047	0.197	0.0024	N/A	N/A	N/A	0.036	0.259	0.0151	N/A	N/A	N/A
318	0.005	0.667	0.0027	0.043	0.218	-0.0087	0.011	0.543	0.0010	0.078	0.093	0.0023	0.035	0.296	-0.0045	0.020	0.427	-0.0039
319	0.038	0.246	-0.0063	0.080	0.091	-0.0097	0.043	0.218	0.0013	0.297	0.000	0.0057	0.001	0.889	0.0005	0.000	0.977	-0.0001
320	0.015	0.489	-0.0034	0.000	0.911	0.0011	0.247	0.002	0.0063	0.020	0.419	0.0038	0.025	0.391	-0.0023	0.011	0.581	0.0009
321	0.001	0.876	0.0008	0.019	0.432	-0.0047	0.092	0.077	0.0037	0.090	0.080	0.0042	0.001	0.877	0.0005	0.001	0.904	0.0002
322	0.003	0.761	-0.0016	0.035	0.273	-0.0046	0.122	0.034	0.0037	0.071	0.111	0.0036	0.057	0.183	0.0103	0.014	0.505	0.0024
323	0.028	0.329	-0.0048	0.018	0.439	-0.0045	0.130	0.028	0.0048	0.202	0.005	0.0051	0.003	0.757	-0.0007	0.000	0.906	-0.0003
324	0.003	0.734	-0.0043	0.072	0.114	0.0085	0.114	0.004	0.0046	0.073	0.105	0.0024	0.006	0.667	0.0012	0.001	0.889	0.0004
325	0.086	0.082	-0.0122	0.057	0.161	-0.0083	0.002	0.779	0.0005	0.026	0.341	0.0020	0.009	0.607	-0.0029	0.020	0.437	-0.0051
326	0.002	0.788	-0.0019	0.038	0.249	-0.0084	0.012	0.516	0.0010	0.050	0.182	0.0026	0.016	0.478	-0.0014	0.011	0.568	-0.0014
327	0.039	0.238	-0.0067	0.020	0.408	-0.0045	0.016	0.450	0.0012	0.006	0.650	0.0007	0.000	0.945	-0.0002	0.007	0.651	-0.0016
328	0.024	0.358	0.0094	0.034	0.273	0.0132	0.067	0.123	0.0023	0.129	0.029	0.0022	0.048	0.219	0.0016	0.054	0.193	0.0030
329	0.030	0.310	0.0082	0.053	0.176	0.0137	0.015	0.468	0.0010	0.005	0.690	0.0009	0.008	0.627	-0.0011	0.000	0.981	0.0000
330	0.008	0.605	0.0048	0.006	0.661	0.0030	0.006	0.644	0.0005	0.061	0.140	0.0019	0.005	0.692	-0.0010	0.002	0.794	-0.0008
331	0.004	0.716	0.0020	0.043	0.218	0.0071	0.026	0.343	0.0020	0.030	0.306	0.0019	0.000	0.911	-0.0003	0.000	0.932	-0.0002
332	0.017	0.442	0.0067	0.016	0.457	0.0071	0.007	0.111	0.0021	0.037	0.255	0.0017	0.005	0.688	-0.0018	0.001	0.851	-0.0009
333	0.002	0.130	-0.0017	0.000	0.924	0.0010	0.076	0.098	0.0032	0.082	0.086	0.0028	0.001	0.857	0.0006	0.008	0.632	-0.0018
334	0.003	0.729	0.0026	0.000	0.902	0.0007	0.035	0.266	0.0019	0.031	0.296	0.0021	0.000	0.977	-0.0002	0.003	0.748	-0.0014
335	0.000	0.998	0.0002	0.074	0.102	0.0123	0.039	0.240	0.0018	0.155	0.016	0.0038	0.005	0.684	-0.0007	0.008	0.617	0.0012
336	0.009	0.582	0.0036	0.002	0.820	-0.0016	0.120	0.036	0.0270	0.019	0.414	0.0021	0.004	0.722	-0.0008	0.000	0.988	0.0000
337	0.001	0.844	-0.0011	0.000	0.916	0.0007	0.220	0.030	0.0035	0.153	0.018	0.0032	0.040	0.262	-0.0021	0.022	0.414	-0.0015
338	0.008	0.607	0.0037	0.011	0.552	0.0041	0.350	0.028	0.0033	0.110	0.052	0.0022	0.007	0.652	0.0046	0.010	0.590	0.0012
339	0.030	0.309	0.0093	0.009	0.569	0.0037	0.088	0.075	0.0023	0.072	0.107	0.0029	0.011	0.565	-0.0012	0.000	0.966	0.0001
340	0.024	0.362	0.0073	0.002	0.771	-0.0018	0.074	0.103	0.0024	0.148	0.019	0.0033	0.038	0.279	-0.0026	0.007	0.646	0.0008
341	0.001	0.880	0.0009	0.009	0.588	0.0029	0.051	0.193	0.0026	0.089	0.086	0.0029	0.058	0.185	-0.0032	0.005	0.697	-0.0007
342	0.002	0.822	0.0012	0.022	0.396	0.0067	0.278	0.010	0.0047	0.007	0.645	0.0017	0.020	0.438	-0.0011	0.007	0.658	-0.0007
343	0.061	0.145	0.0015	0.051	0.194	0.0140	0.123	0.039	0.0030	0.007	0.644	0.0018	0.022	0.419	-0.0010	0.006	0.680	-0.0005
344	0.041	0.228	0.0070	0.001	0.844	0.0011	0.084	0.082	0.0029	0.060	0.143	0.0022	0.045	0.234	0.0019	0.023	0.395	0.0032
345	0.003	0.380	0.0021	0.003	0.756	-0.0019	0.129	0.029	0.0041	0.000	0.918	0.0004	0.004	0.712	0.0005	0.004	0.715	0.0012
346	0.016	0.471	0.0044	0.080	0.100	0.0169	0.101	0.620	0.0025	0.002	0.792	0.0008	0.001	0.878	0.0003	0.001	0.890	0.0004
347	0.030	0.320	0.0068	0.026	0.359	0.0069	0.150	0.477	0.0012	0.005	0.689	0.0010	0.000	0.914	0.0003	0.004	0.722	0.0008
348	0.001	0.826	0.0015	0.007	0.636	0.0056	0.169	0.013	0.0048	0.235	0.003	0.0037	0.008	0.625	0.0022	0.006	0.693	0.0013
349	0.000	0.978	-0.0003	0.004	0.717	0.0023	0.085	0.089	0.0025	0.085	0.089	0.0017	0.000	0.996	0.0000	0.004	0.744	0.0005
350	0.001	0.870	0.0010	0.000	0.991	-0.0001	0.106	0.049	0.0023	0.026	0.338	0.0021	0.032	0.323	0.0030	0.003	0.755	0.0004
400	0.004	0.736	0.0052	0.009	0.624	0.0081	0.046	0.275	0.0026	0.011	0.595	0.0017	0.022	0.447	-0.0033	0.020	0.468	-0.0034
401	0.012	0.582	0.0067	0.002	0.837	0.0027	0.086	0.130	0.0038	0.134	0.066	0.0042	0.011	0.589	-0.0015	0.068	0.197	-0.0036
402	0.021	0.474	-0.0062	0.013	0.573	0.0053	0.055	0.238	0.0035	0.115	0.084	0.0063	0.096	0.116	-0.0038	0.063	0.206	-0.0031
403	0.034	0.356	0.0087	0.002	0.819	0.0020	0.075	0.168	0.0043	0.031	0.383	0.0022	0.002	0.845	0.0007	0.008	0.651	0.0016

	Total Organic Carbon						Silicate						Turbidity					
	Surface			*Bottom*			*Surface*			*Bottom*			*Surface*			*Bottom*		
Station	R^2	p-value	slope	R^2	p-value	slope	R^2	p-value	slope	R^2	p-value	slope	R^2	p-value	slope	R^2	p-value	slope
200	0.413	0.000	-12.5710	0.448	0.000	-12.7790	0.010	0.574	-0.0159	0.002	0.804	-0.0048	0.027	0.328	-0.0218	0.000	0.933	0.0014
201	0.333	0.000	-10.6110	0.554	0.000	-13.7950	0.002	0.797	0.0243	0.002	0.809	-0.0144	0.056	0.159	-0.0775	0.113	0.052	-0.1553
202	0.559	0.000	-13.1540	0.330	0.000	-10.4900	0.006	0.646	0.0186	0.012	0.529	-0.0260	0.011	0.536	-0.0334	0.011	0.529	-0.0407
203	0.382	0.000	-10.2210	N/A	N/A	N/A	0.005	0.683	-0.0059	N/A	N/A	N/A	0.011	0.544	-0.0118	N/A	N/A	N/A
204	0.434	0.000	-11.6590	0.301	0.001	-8.9208	0.000	0.916	0.0055	0.004	0.726	0.0168	0.059	0.147	-0.0732	0.108	0.054	-0.1043
205	0.421	0.000	-11.5540	0.467	0.000	-15.1480	0.010	0.561	0.0251	0.009	0.583	0.0242	0.034	0.271	-0.0579	0.057	0.155	-0.0758
206	0.465	0.000	-12.1100	0.434	0.000	-11.2620	0.001	0.867	-0.0038	0.021	0.408	0.0152	0.020	0.408	-0.0304	0.016	0.460	-0.0276
207	0.472	0.000	-13.4630	N/A	N/A	N/A	0.003	0.763	0.0329	N/A	N/A	N/A	0.036	0.259	-0.0448	N/A	N/A	N/A
208	0.101	0.056	-6.9517	0.140	0.023	-8.3663	0.001	0.860	-0.0055	0.008	0.622	0.0284	0.056	0.157	-0.0622	0.045	0.205	-0.0539
209	0.227	0.003	-12.8750	N/A	N/A	N/A	0.022	0.391	-0.1479	N/A	N/A	N/A	0.012	0.523	-0.0385	N/A	N/A	N/A
210	0.208	0.005	-8.2989	0.302	0.001	-11.3420	0.001	0.876	0.0042	0.012	0.523	0.0248	0.039	0.244	-0.0291	0.078	0.093	-0.0515
211	0.339	0.000	-12.3250	0.225	0.004	-10.0960	0.002	0.781	-0.0234	0.000	0.983	-0.0021	0.011	0.544	0.0179	0.020	0.417	0.0272
212	0.182	0.009	-7.5164	0.286	0.001	-11.7230	0.018	0.439	0.0252	0.032	0.300	-0.0601	0.000	0.914	-0.0032	0.000	0.979	-0.0008
213	0.375	0.000	-13.4230	0.356	0.000	-10.6880	0.001	0.866	-0.0019	0.097	0.069	-0.0466	0.055	0.162	0.1407	0.005	0.692	0.0068
214	0.325	0.000	-11.8180	N/A	N/A	N/A	0.000	0.956	0.0028	N/A	N/A	N/A	0.004	0.709	-0.0225	N/A	N/A	N/A
215	0.250	0.002	-10.6550	0.099	0.606	25.9050	0.006	0.656	0.0181	0.799	0.296	-0.3608	0.001	0.865	-0.0047	0.164	0.499	-0.2713
216	0.209	0.004	-10.2470	0.001	0.940	-1.2425	0.004	0.726	0.0047	0.090	0.471	-0.0398	0.001	0.889	-0.0013	0.564	0.020	0.0992
217	0.327	0.000	-12.7680	N/A	N/A	N/A	0.009	0.583	0.0228	N/A	N/A	N/A	0.001	0.847	-0.0145	N/A	N/A	N/A
218	0.153	0.017	-7.1853	0.986	0.075	103.7600	0.015	0.492	0.0159	N/A	N/A	N/A	0.000	0.925	-0.0042	0.551	0.151	-0.2528
219	0.088	0.074	-6.0937	0.110	0.045	-7.5459	0.078	0.111	-0.0682	0.016	0.479	0.0193	0.034	0.271	0.0233	0.002	0.789	0.0036
220	0.154	0.016	-6.7092	0.110	0.045	-6.9728	0.048	0.206	-0.0549	0.001	0.869	-0.0075	0.011	0.546	-0.0518	0.031	0.300	-0.0793
221	0.273	0.001	-10.7530	0.235	0.002	-10.0620	0.115	0.047	-0.0925	0.038	0.264	-0.0423	0.017	0.447	-0.0577	0.032	0.293	-0.0674
222	0.285	0.001	-10.3840	0.248	0.002	-9.5122	0.011	0.542	0.0072	0.013	0.520	-0.0134	0.022	0.391	-0.0145	0.006	0.643	-0.0056
223	0.103	0.053	-6.2484	N/A	N/A	N/A	0.105	0.058	-0.0972	N/A	N/A	N/A	0.004	0.696	-0.0176	0.439	0.539	-0.0706
224	0.295	0.001	-11.3220	0.179	0.722	7.0564	0.006	0.666	0.0092	0.009	0.904	0.0060	0.004	0.722	0.0167	0.199	0.554	-0.0724
225	0.414	0.000	-10.8990	0.399	0.000	-10.5270	0.011	0.544	-0.0090	0.043	0.241	-0.0283	0.022	0.386	0.0157	0.043	0.226	0.0240
226	0.215	0.004	-11.1590	N/A	N/A	N/A	0.094	0.074	-0.2289	N/A	N/A	N/A	0.015	0.473	-0.0285	N/A	N/A	N/A
227	0.232	0.003	-9.2703	0.257	0.001	-9.4980	0.003	0.775	-0.0148	0.044	0.225	-0.0630	0.001	0.824	-0.0191	0.002	0.809	-0.0190
228	0.367	0.000	-12.8290	0.445	0.000	-11.3690	0.027	0.348	-0.0253	0.087	0.085	-0.0240	0.004	0.694	0.0085	0.000	0.969	0.0008
229	0.347	0.000	19.0850	N/A	N/A	N/A	0.036	0.278	-0.1619	N/A	N/A	N/A	0.002	0.789	-0.0249	N/A	N/A	N/A
230	0.222	0.003	-13.4240	0.310	0.000	-17.9560	0.042	0.235	-0.1460	0.040	0.249	-0.1491	0.000	0.962	-0.0023	0.000	0.933	0.0052
231	0.276	0.001	-12.0070	0.260	0.001	-12.1230	0.040	0.247	-0.0335	0.039	0.257	-0.0323	0.158	0.015	0.0298	0.086	0.079	0.0171
232	0.186	0.008	-15.5230	N/A	N/A	N/A	0.114	0.047	-0.2731	N/A	N/A	N/A	0.050	0.184	-0.1163	N/A	N/A	N/A
233	0.209	0.004	-21.4160	0.232	0.003	-21.8040	0.053	0.181	-0.1109	0.075	0.112	-0.1513	0.014	0.489	-0.0288	0.033	0.280	-0.0422
234	0.226	0.003	-10.6690	0.187	0.008	-8.3857	0.035	0.280	-0.0239	0.127	0.039	-0.0485	0.020	0.407	0.0075	0.003	0.768	-0.0044
235	0.242	0.002	-20.7250	N/A	N/A	N/A	0.082	0.096	-0.7106	N/A	N/A	N/A	0.042	0.225	-0.1048	N/A	N/A	N/A
236	0.224	0.003	-11.6530	0.189	0.008	-13.2220	0.073	0.117	-0.1856	0.009	0.581	-0.1588	0.000	0.975	0.0017	0.001	0.822	-0.0148
237	0.276	0.001	-10.2420	0.280	0.001	-11.7600	0.118	0.043	-0.0778	0.031	0.312	-0.1107	0.005	0.678	-0.0208	0.000	0.956	0.0016
238	0.377	0.000	-23.3260	N/A	N/A	N/A	0.086	0.087	-0.8674	N/A	N/A	N/A	0.045	0.206	-0.2184	0.472	0.518	-0.6290
239	0.141	0.024	-9.0906	0.032	0.300	-4.5583	0.045	0.231	-0.2553	0.032	0.308	-0.2119	0.012	0.525	-0.0591	0.000	0.904	-0.0036
240	0.065	0.127	-6.3545	0.157	0.015	-13.5980	0.033	0.297	0.1958	0.014	0.493	-0.0454	0.005	0.692	-0.0170	0.001	0.883	-0.0037
241	0.288	0.001	-19.8380	N/A	N/A	N/A	0.059	0.159	-0.4713	N/A	N/A	N/A	0.039	0.238	-0.1261	N/A	N/A	N/A
242	0.293	0.001	-13.8480	0.220	0.003	-10.9660	0.017	0.462	-0.2372	0.005	0.680	-0.1603	0.007	0.633	-0.0525	0.008	0.590	-0.0921
243	0.195	0.006	-7.5288	0.251	0.002	-7.9906	0.031	0.311	-0.1132	0.001	0.894	-0.0030	0.007	0.623	-0.0227	0.000	0.978	0.0005
244	0.123	0.036	-7.8214	0.250	0.003	-13.0210	0.029	0.339	-0.4011	0.038	0.274	-0.4688	0.025	0.353	-0.1518	0.054	0.188	-0.2013
245	0.367	0.000	-13.5740	0.179	0.010	-8.5716	0.061	0.159	-0.4744	0.014	0.512	-0.0987	0.023	0.379	-0.0674	0.003	0.770	-0.0220
246	0.166	0.014	-5.8173	0.154	0.020	-5.8803	0.093	0.080	-0.1880	0.096	0.075	-0.1096	0.018	0.430	-0.0275	0.000	0.970	-0.0006
247	0.512	0.000	-17.8740	N/A	N/A	N/A	0.105	0.061	-0.3520	0.084	0.812	0.8241	0.036	0.270	-0.1075	0.525	0.276	-0.4000
248	0.510	0.000	12.4250	0.336	0.000	-8.5602	0.084	0.096	-0.1622	0.127	0.045	-0.1723	0.042	0.231	-0.0203	0.080	0.101	-0.0460
249	0.454	0.000	-11.2920	0.380	0.000	-10.5730	0.008	0.623	-0.0303	0.006	0.654	-0.0358	0.054	0.173	-0.0175	0.013	0.515	-0.0078
250	0.415	0.000	12.1410	N/A	N/A	N/A	0.004	0.720	-0.1034	N/A	N/A	N/A	0.013	0.516	0.0393	N/A	N/A	N/A

	Total Organic Carbon						Silicate						Turbidity					
	Surface			*Bottom*			*Surface*			*Bottom*			*Surface*			*Bottom*		
Station	R^2	p-value	slope	R^2	p-value	slope	R^2	p-value	slope	R^2	p-value	slope	R^2	p-value	slope	R^2	p-value	slope
251	0.476	0.000	-14.6620	0.315	0.000	-10.2730	0.137	0.031	-0.2908	0.038	0.268	-0.1546	0.001	0.838	0.0075	0.008	0.610	-0.0221
252	0.307	0.000	-9.1222	0.333	0.000	-8.9887	0.011	0.550	-0.0448	0.100	0.073	-0.0375	0.009	0.573	0.0113	0.002	0.779	0.0057
253	0.252	0.002	-9.8987	N/A	N/A	N/A	0.052	0.194	-0.1067	N/A	N/A	N/A	0.000	0.958	-0.0018	N/A	N/A	N/A
254	0.422	0.000	-15.5240	N/A	N/A	N/A	0.004	0.716	-0.0421	N/A	N/A	N/A	0.022	0.383	0.0301	0.813	0.285	-0.2678
255	0.413	0.000	-13.2480	0.318	0.000	-11.0390	0.148	0.025	-0.2475	0.241	0.003	-0.2562	0.033	0.289	-0.0286	0.031	0.303	-0.0304
256	0.319	0.000	-1.4040	0.236	0.003	-7.9222	0.181	0.012	-0.1114	0.007	0.636	-0.0276	0.009	0.590	-0.0051	0.008	0.604	-0.0089
257	0.170	0.014	-7.1929	N/A	N/A	N/A	0.008	0.609	0.0505	N/A	N/A	N/A	0.000	0.913	-0.0047	N/A	N/A	N/A
258	0.189	0.009	-6.7843	0.258	0.002	-8.3342	0.007	0.638	-0.1050	0.186	0.012	-0.1847	0.003	0.741	0.0098	0.038	0.254	-0.0410
259	0.191	0.008	-6.4528	0.239	0.003	-7.7728	0.040	0.259	-0.1194	0.140	0.029	-0.1455	0.029	0.321	-0.0150	0.056	0.166	-0.0203
260	0.132	0.032	-6.2498	N/A	N/A	N/A	0.016	0.479	-0.0526	N/A	N/A	N/A	0.016	0.472	-0.0383	N/A	N/A	N/A
261	0.198	0.008	-7.7251	0.257	0.002	-8.5562	0.023	0.398	-0.0787	0.015	0.492	-0.0611	0.005	0.680	0.0140	0.000	0.929	-0.0033
262	0.325	0.000	-11.2450	0.260	0.002	-10.5200	0.009	0.600	-0.0612	0.095	0.076	-0.1542	0.010	0.556	0.0199	0.001	0.888	-0.0040
263	0.259	0.002	-7.9987	0.285	0.001	-9.2175	0.000	0.988	0.0011	0.001	0.895	-0.0111	0.036	0.266	0.0512	0.004	0.700	0.0102
264	0.227	0.004	-9.5361	0.243	0.003	-8.7273	0.047	0.224	-0.0370	0.003	0.757	-0.0337	0.042	0.247	0.0110	0.024	0.381	0.0094
265	0.108	3.990	-8.2819	N/A	N/A	N/A	0.054	0.195	-1.9314	N/A	N/A	N/A	0.175	0.012	0.0413	N/A	N/A	N/A
266	0.372	0.000	-14.8530	N/A	N/A	N/A	0.088	0.093	-0.1819	N/A	N/A	N/A	0.010	0.559	0.0481	0.970	0.110	-1.4964
267	0.210	0.006	-9.1379	0.323	0.000	-10.3160	0.001	0.856	-0.0122	0.001	0.837	-0.0307	0.030	0.317	0.0241	0.004	0.720	-0.0059
268	0.279	0.001	-10.5130	0.442	0.537	-20.0470	0.008	0.608	0.0816	N/A	N/A	N/A	0.115	0.043	0.0776	0.326	0.429	-0.2036
269	0.206	0.005	-7.9338	0.302	0.001	-11.5430	0.004	0.714	0.0432	0.014	0.507	-0.0694	0.024	0.366	0.0286	0.012	0.518	-0.0241
270	0.256	0.002	-17.3400	0.372	0.000	-11.9900	0.007	0.630	-0.0220	0.019	0.440	-0.0555	0.014	0.494	-0.0213	0.016	0.460	-0.0217
271	0.122	0.037	-0.6128	0.188	0.008	-8.2426	0.015	0.492	-0.0589	0.074	0.120	-0.1241	0.007	0.616	0.0138	0.081	0.093	0.0671
272	0.000	0.972	-0.1972	0.003	0.752	-1.7408	0.030	0.326	-0.0567	0.024	0.384	-0.0509	0.009	0.579	0.0160	0.030	0.313	0.0309
273	0.386	0.000	-12.5780	0.351	0.000	-11.7440	0.138	0.030	-0.0872	0.008	0.604	-0.0374	0.042	0.229	0.0283	0.021	0.400	0.0246
274	0.213	0.005	-8.6483	0.211	0.005	-8.6088	0.107	0.058	-0.1337	0.113	0.052	-0.1217	0.000	0.939	-0.0020	0.034	0.279	0.0251
275	0.172	0.012	-7.8399	0.189	0.008	-8.2814	0.024	0.385	-0.0707	0.070	0.131	-0.1390	0.043	0.223	0.0617	0.016	0.462	-0.0380
276	0.248	0.002	-18.2580	0.064	0.142	-7.6588	0.041	0.254	-0.0497	0.092	0.087	-0.1276	0.002	0.796	-0.0051	0.000	0.961	0.0010
277	0.357	0.000	-11.7110	0.280	0.001	-10.3810	0.002	0.796	0.0406	0.031	0.318	-0.1201	0.004	0.702	0.0188	0.013	0.503	-0.0314
278	0.348	0.000	-13.9900	0.330	0.000	-13.6440	0.035	0.291	-0.0837	0.022	0.401	-0.0708	0.003	0.737	0.0187	0.000	0.922	-0.0049
279	0.309	0.000	-11.4620	0.244	0.002	-10.3200	0.016	0.472	-0.0337	0.047	0.226	0.0800	0.000	0.952	-0.0023	0.025	0.354	0.0194
280	0.352	0.000	-13.9630	0.330	0.000	-11.6090	0.039	0.261	-0.0484	0.027	0.359	-0.0466	0.070	0.119	0.0188	0.009	0.582	-0.0084
281	0.330	0.000	-13.3130	0.442	0.000	-17.8170	0.072	0.126	-0.1115	0.053	0.199	-0.1082	0.001	0.854	-0.0130	0.018	0.436	0.0537
282	0.254	0.002	-13.2450	N/A	N/A	N/A	0.001	0.842	-0.0974	N/A	N/A	N/A	0.343	0.000	-0.2111	N/A	N/A	N/A
283	0.264	0.001	-15.4080	N/A	N/A	N/A	0.009	0.595	-0.5377	N/A	N/A	N/A	0.028	0.333	-0.3601	N/A	N/A	N/A
284	0.141	0.022	-8.5058	N/A	N/A	N/A	0.007	0.643	0.4937	N/A	N/A	N/A	0.014	0.483	-0.0542	N/A	N/A	N/A
285	0.497	0.000	-18.9470	N/A	N/A	N/A	0.024	0.377	-0.4239	N/A	N/A	N/A	0.000	0.979	0.0015	N/A	N/A	N/A
286	0.497	0.000	-18.4070	N/A	N/A	N/A	0.000	0.963	0.0145	N/A	N/A	N/A	0.050	0.189	-0.0715	N/A	N/A	N/A
287	0.229	0.003	-10.2630	N/A	N/A	N/A	0.015	0.489	-0.7373	N/A	N/A	N/A	0.216	0.004	0.0718	N/A	N/A	N/A
288	0.141	0.022	-13.6040	N/A	N/A	N/A	0.066	0.135	-0.6262	N/A	N/A	N/A	0.006	0.657	-0.0436	N/A	N/A	N/A
289	0.124	0.032	-7.7350	N/A	N/A	N/A	0.031	0.313	-0.7815	N/A	N/A	N/A	0.036	0.258	0.0418	N/A	N/A	N/A
290	0.169	0.014	-16.2670	N/A	N/A	N/A	0.001	0.899	-0.0401	N/A	N/A	N/A	0.039	0.257	-0.1183	N/A	N/A	N/A
291	0.140	0.022	-13.5950	N/A	N/A	N/A	0.001	0.839	0.0667	N/A	N/A	N/A	0.037	0.252	0.0348	N/A	N/A	N/A
292	0.135	0.025	-13.5510	N/A	N/A	N/A	0.009	0.597	-0.1767	N/A	N/A	N/A	0.024	0.355	0.0257	N/A	N/A	N/A
293	0.102	0.054	-15.8560	N/A	N/A	N/A	0.056	0.173	-0.2611	N/A	N/A	N/A	0.002	0.789	0.0073	N/A	N/A	N/A
294	0.095	0.063	-10.9740	N/A	N/A	N/A	0.005	0.682	-0.1214	N/A	N/A	N/A	0.002	0.797	-0.0063	N/A	N/A	N/A
295	0.085	0.090	-7.0454	N/A	N/A	N/A	0.028	0.356	0.2242	N/A	N/A	N/A	0.000	0.959	-0.0036	N/A	N/A	N/A
296	0.185	0.009	-15.1660	N/A	N/A	N/A	0.008	0.616	-0.1627	N/A	N/A	N/A	0.005	0.683	0.0086	N/A	N/A	N/A
297	0.117	0.039	-11.5740	N/A	N/A	N/A	0.009	0.596	0.1893	N/A	N/A	N/A	0.247	0.002	0.1641	N/A	N/A	N/A
298	0.010	0.565	1.8717	N/A	N/A	N/A	0.013	0.507	0.1370	N/A	N/A	N/A	0.054	0.164	-0.2111	N/A	N/A	N/A
299	0.086	0.079	-6.0997	N/A	N/A	N/A	0.006	0.651	0.0534	N/A	N/A	N/A	0.007	0.635	0.0155	N/A	N/A	N/A
300	0.203	0.005	-11.6540	N/A	N/A	N/A	0.026	0.351	-0.1261	N/A	N/A	N/A	0.002	0.799	-0.0157	N/A	N/A	N/A
301	0.006	0.655	1.5610	N/A	N/A	N/A	0.012	0.525	0.0982	N/A	N/A	N/A	0.019	0.421	0.0623	N/A	N/A	N/A

	Total Organic Carbon						Silicate						Turbidity					
	Surface			*Bottom*			*Surface*			*Bottom*			*Surface*			*Bottom*		
Station	R^2	p-value	slope	R^2	p-value	slope	R^2	p-value	slope	R^2	p-value	slope	R^2	p-value	slope	R^2	p-value	slope
302	0.008	0.593	1.7866	N/A	N/A	N/A	0.005	0.699	-0.0296	N/A	N/A	N/A	0.000	0.959	-0.0041	N/A	N/A	N/A
303	0.048	0.197	-8.6555	N/A	N/A	N/A	0.002	0.821	0.0562	N/A	N/A	N/A	0.058	0.150	0.0390	N/A	N/A	N/A
304	0.025	0.351	-5.5649	N/A	N/A	N/A	0.012	0.544	0.1708	N/A	N/A	N/A	0.012	0.514	0.0381	N/A	N/A	N/A
305	0.000	0.968	0.1359	N/A	N/A	N/A	0.037	0.267	0.0650	N/A	N/A	N/A	0.002	0.789	0.0214	N/A	N/A	N/A
306	0.032	0.287	3.8086	N/A	N/A	N/A	0.003	0.738	-0.0226	N/A	N/A	N/A	0.002	0.795	0.0218	N/A	N/A	N/A
307	0.024	0.364	-5.3247	N/A	N/A	N/A	0.001	0.880	-0.0232	N/A	N/A	N/A	0.000	0.949	0.0051	N/A	N/A	N/A
308	0.027	0.333	-9.1990	N/A	N/A	N/A	0.038	0.268	-0.1217	N/A	N/A	N/A	0.009	0.581	0.0451	N/A	N/A	N/A
309	0.050	0.184	-4.5484	N/A	N/A	N/A	0.026	0.356	0.0428	N/A	N/A	N/A	0.008	0.602	-0.0542	N/A	N/A	N/A
310	0.052	0.175	-15.9380	N/A	N/A	N/A	0.002	0.821	-0.0320	N/A	N/A	N/A	0.038	0.255	0.0811	N/A	N/A	N/A
311	0.115	0.040	-28.9270	N/A	N/A	N/A	0.049	0.201	-0.1018	N/A	N/A	N/A	0.001	0.831	-0.0095	N/A	N/A	N/A
312	0.136	0.025	-17.3870	N/A	N/A	N/A	0.003	0.737	0.0369	N/A	N/A	N/A	0.002	0.817	-0.0184	N/A	N/A	N/A
313	0.097	0.060	-24.5410	N/A	N/A	N/A	0.000	0.922	-0.0117	N/A	N/A	N/A	0.020	0.415	-0.0668	N/A	N/A	N/A
314	0.058	0.151	-11.6800	N/A	N/A	N/A	0.004	0.705	-0.0461	N/A	N/A	N/A	0.006	0.646	0.0230	N/A	N/A	N/A
315	0.105	0.050	-5.4785	N/A	N/A	N/A	0.000	0.910	0.0128	N/A	N/A	N/A	0.006	0.660	0.0532	N/A	N/A	N/A
316	0.211	0.004	-8.8867	N/A	N/A	N/A	0.020	0.414	-0.0818	N/A	N/A	N/A	0.006	0.651	0.0160	N/A	N/A	N/A
317	0.100	0.057	-6.8706	N/A	N/A	N/A	0.012	0.531	-0.0701	N/A	N/A	N/A	0.091	0.074	0.0411	N/A	N/A	N/A
318	0.385	0.000	-14.4290	0.333	0.000	-13.1570	0.004	0.719	0.0391	0.007	0.621	0.0515	0.008	0.613	0.0604	0.000	0.921	-0.0150
319	0.414	0.000	-13.9970	0.368	0.000	-12.1470	0.004	0.715	-0.0276	0.006	0.646	0.0406	0.007	0.639	0.0597	0.019	0.428	0.0920
320	0.415	0.000	-13.5130	0.419	0.000	-13.2240	0.007	0.640	0.0156	0.036	0.289	-0.0818	0.020	0.435	0.0206	0.026	0.369	0.0234
321	0.477	0.000	-15.0150	0.426	0.000	-13.9560	0.031	0.317	-0.0320	0.004	0.742	-0.0107	0.004	0.731	0.0092	0.023	0.402	0.0183
322	0.371	0.000	-12.1460	0.324	0.000	-11.4120	0.007	0.641	0.0162	0.001	0.839	-0.0249	0.013	0.500	-0.0318	0.010	0.555	-0.0248
323	0.307	0.000	-12.9200	0.287	0.001	-12.6460	0.036	0.273	-0.1002	0.030	0.319	-0.1117	0.019	0.417	0.0894	0.056	0.165	0.2327
324	0.360	0.000	-13.0510	0.454	0.000	-15.6690	0.007	0.623	0.0390	0.004	0.732	0.0261	0.019	0.426	0.0802	0.011	0.550	0.0615
325	0.349	0.000	-13.8450	0.438	0.000	-15.5410	0.000	0.959	-0.0032	0.000	0.997	0.0003	0.021	0.398	-0.1980	0.018	0.441	-0.1033
326	0.409	0.000	-13.5040	0.502	0.000	-16.4240	0.015	0.481	-0.0615	0.007	0.633	-0.0487	0.033	0.292	0.1281	0.038	0.255	0.1563
327	0.471	0.000	-14.8840	0.399	0.000	-13.4660	0.014	0.496	0.0467	0.017	0.453	0.0499	0.006	0.642	0.0655	0.003	0.766	0.0528
328	0.393	0.000	-18.3150	0.353	0.000	-12.4070	0.003	0.774	0.0067	0.009	0.590	-0.0127	0.048	0.199	0.0366	0.019	0.422	0.0168
329	0.309	0.000	-13.3030	0.304	0.000	-12.7640	0.015	0.484	-0.0386	0.014	0.501	-0.0732	0.046	0.215	0.0897	0.073	0.117	0.1409
330	0.378	0.000	-17.2460	0.321	0.000	-27.7390	0.002	0.822	0.0183	0.038	0.262	0.1441	0.043	0.227	0.1437	0.072	0.114	0.1553
331	0.279	0.001	-13.2460	0.203	0.005	-10.6020	0.001	0.852	0.0084	0.004	0.715	-0.0179	0.008	0.614	0.0380	0.001	0.867	0.0099
332	0.213	0.004	-10.0950	0.228	0.003	-11.1520	0.001	0.826	-0.0125	0.014	0.505	-0.0425	0.004	0.716	0.0284	0.013	0.510	0.0450
333	0.280	0.001	-11.7040	0.269	0.001	-11.2480	0.021	0.406	0.0444	0.016	0.475	0.0384	0.036	0.272	0.0595	0.000	0.925	-0.0124
334	0.174	0.010	-8.8002	0.207	0.005	-16.0290	0.008	0.605	0.0215	0.018	0.446	0.0523	0.013	0.509	0.0257	0.001	0.896	-0.0062
335	0.111	0.044	-7.8151	0.127	0.031	-7.6355	0.012	0.524	0.0202	0.002	0.780	0.0121	0.037	0.259	0.0245	0.022	0.384	0.0312
336	0.193	0.007	-8.3483	0.171	0.011	-8.1259	0.089	0.081	0.2235	0.039	0.255	-0.1117	0.080	0.095	0.0876	0.080	0.095	0.0709
337	0.150	0.018	-7.4548	0.210	0.004	-9.2316	0.027	0.350	0.0432	0.046	0.216	0.0544	0.051	0.184	0.0556	0.042	0.231	0.0448
338	0.362	0.000	-9.2089	0.231	0.004	-7.7931	0.006	0.667	0.0122	0.037	0.281	0.1378	0.051	0.191	0.0303	0.052	0.193	0.0317
339	0.123	0.033	-5.1568	0.172	0.011	-5.4482	0.000	0.930	-0.0034	0.001	0.893	-0.0043	0.002	0.787	0.0086	0.004	0.725	0.0120
340	0.268	0.001	-12.4260	0.179	0.009	-9.0668	0.006	0.658	0.0135	0.001	0.890	-0.0041	0.011	0.548	0.0306	0.033	0.292	0.0529
341	0.176	0.011	-9.5985	0.092	0.076	-6.7906	0.001	0.857	-0.0074	0.020	0.431	0.0824	0.013	0.511	-0.0232	0.003	0.775	-0.0106
342	0.129	0.031	-13.4340	0.143	0.025	-11.0530	0.055	0.181	-0.0642	0.078	0.116	-0.1252	0.045	0.224	0.0531	0.175	0.014	0.1166
343	0.145	0.024	-9.2916	0.056	0.180	-4.9778	0.005	0.679	0.0124	0.068	0.143	-0.1299	0.058	0.171	0.0453	0.345	0.000	0.1713
344	0.297	0.000	-11.7820	0.248	0.002	-11.2670	0.088	0.083	0.0459	0.070	0.130	-0.0423	0.021	0.398	0.0304	0.025	0.357	0.0306
345	0.159	0.014	-8.8932	0.207	0.005	-9.1711	0.004	0.718	0.0095	0.010	0.563	-0.0305	0.010	0.564	-0.0184	0.023	0.377	0.0353
346	0.156	0.019	-9.0195	0.216	0.005	-18.0100	0.004	0.738	-0.0105	0.043	0.249	-0.0417	0.056	0.176	0.0180	0.143	0.027	0.0267
347	0.186	0.010	-27.2350	0.167	0.016	-21.6240	0.009	0.601	0.0270	0.020	0.432	-0.0305	0.131	0.035	0.0511	0.214	0.006	0.0538
348	0.272	0.001	-24.5000	0.269	0.001	-18.6200	0.029	0.334	-0.0327	0.001	0.843	-0.0073	0.120	0.042	0.0539	0.081	0.104	0.0564
349	0.302	0.001	-15.0300	0.281	0.001	-16.5610	0.001	0.889	-0.0032	0.010	0.575	-0.0135	0.004	0.723	0.0168	0.077	0.112	0.0329
350	0.338	0.000	-14.0090	0.278	0.001	-12.5830	0.000	0.920	0.0024	0.005	0.694	-0.0148	0.056	0.166	0.0240	0.103	0.057	0.0600
400	-0.835	0.069	-8.8973	0.131	0.058	-9.4421	0.025	0.426	0.0106	0.019	0.483	0.0077	0.001	0.906	-0.0040	0.002	0.830	-0.0085
401	0.142	0.048	-11.3990	0.090	0.145	-9.3061	0.134	0.055	-0.1079	0.107	0.103	-0.1213	0.072	0.176	-0.0724	0.130	0.077	-0.2243
402	0.262	0.006	-12.9750	0.232	0.013	-12.1720	0.024	0.438	-0.1022	0.028	0.405	-0.1134	0.003	0.779	0.0132	0.018	0.507	0.0335
403	0.310	0.003	-14.4830	0.302	0.004	-13.9230	0.001	0.876	0.0120	0.011	0.608	-0.0308	0.016	0.539	0.0216	0.037	0.343	0.0342

	Dissolved Oxygen						Salinity						Temperature					
	Surface			*Bottom*			*Surface*			*Bottom*			*Surface*			*Bottom*		
Station	R^2	p-value	slope	R^2	p-value	slope	R^2	p-value	slope	R^2	p-value	slope	R^2	p-value	slope	R^2	p-value	slope
200	0.120	0.036	-0.1690	0.137	0.026	-0.0988	0.098	0.060	0.0491	0.100	0.060	0.0455	0.005	0.675	0.0737	0.018	0.433	0.1395
201	0.201	0.050	-0.1610	0.202	0.006	-0.1607	0.039	0.240	0.0854	0.048	0.197	0.0959	0.008	0.594	0.1432	0.017	0.449	0.2076
202	0.202	0.050	-0.1315	0.188	0.008	-0.1947	0.067	0.122	0.0788	0.076	0.104	0.0754	0.009	0.570	0.1369	0.021	0.397	0.2059
203	0.210	0.004	-0.1440	0.057	0.162	-0.1083	0.052	0.173	0.0289	0.043	0.225	0.0307	0.004	0.715	0.0660	0.014	0.485	0.1279
204	0.170	0.011	-0.1430	0.237	0.003	-0.1725	0.051	0.180	0.0941	0.059	0.155	0.1017	0.010	0.547	0.1616	0.022	0.390	0.2368
205	0.298	0.000	-0.1759	0.263	0.001	-0.1802	0.032	0.291	0.0597	0.033	0.286	0.0615	0.011	0.542	0.1533	0.024	0.366	0.2322
206	0.097	0.065	-0.1034	0.188	0.009	-0.1270	0.032	0.299	0.0292	0.033	0.298	0.0279	0.001	0.871	0.0323	0.007	0.627	0.1006
207	0.233	0.002	-0.1385	0.223	0.004	-0.1701	0.067	0.123	0.1005	0.056	0.163	0.0858	0.008	0.604	0.1428	0.021	0.402	0.2337
208	0.209	0.007	-0.1305	0.216	0.006	-0.1546	0.034	0.294	0.0500	0.027	0.356	0.0430	0.009	0.597	0.1391	0.022	0.399	0.2269
209	0.013	0.503	-0.0462	0.018	0.432	-0.0549	0.051	0.180	0.1096	0.051	0.178	0.1098	0.015	0.465	-0.1559	0.014	0.478	-0.1506
210	0.297	0.001	-0.2390	0.150	0.021	-0.1201	0.009	0.577	0.0155	0.003	0.752	0.0093	0.007	0.617	0.0828	0.030	0.311	0.1784
211	0.202	0.006	-0.1790	0.325	0.000	-0.2216	0.002	0.782	0.0313	0.029	0.325	0.0799	0.006	0.650	0.1341	0.017	0.458	0.2208
212	0.096	0.065	-0.1308	0.253	0.002	-0.1786	0.010	0.556	0.0278	0.004	0.713	0.0152	0.018	0.435	0.1949	0.032	0.298	0.2637
213	0.045	0.212	-0.0912	0.124	0.038	-0.1063	0.012	0.512	0.0184	0.000	0.920	0.0028	0.007	0.618	0.0870	0.038	0.252	0.1839
214	0.225	0.004	-0.2005	0.146	0.026	-0.1542	0.000	0.901	0.0128	0.003	0.776	0.0305	0.012	0.520	0.1791	0.023	0.383	0.2469
215	0.279	0.001	-0.1731	0.268	0.002	-0.1670	0.001	0.870	0.0124	0.002	0.800	0.0175	0.008	0.602	0.1431	0.021	0.416	0.2270
216	0.204	0.006	-0.1581	0.161	0.015	-0.1285	0.025	0.348	0.0268	0.001	0.826	0.0062	0.013	0.509	0.1209	0.037	0.258	0.2064
217	0.294	0.001	-0.1890	0.325	0.000	-0.1809	0.000	0.907	0.0097	0.038	0.263	0.0916	0.005	0.695	0.1105	0.011	0.544	0.1661
218	0.070	0.123	-0.1008	0.053	0.190	-0.1072	0.024	0.365	0.0320	0.028	0.338	0.0357	0.010	0.556	0.1387	0.028	0.338	0.2296
219	0.161	0.014	-0.1018	0.038	0.253	-0.0696	0.000	0.923	-0.0021	0.042	0.229	0.0460	0.012	0.513	0.1089	0.023	0.381	0.1378
220	0.069	0.006	-0.0918	0.265	0.001	-0.1663	0.014	0.482	0.0361	0.014	0.493	0.0374	0.016	0.453	0.1893	0.038	0.252	0.2937
221	0.055	0.162	-0.0904	0.176	0.011	-0.1355	0.003	0.737	0.0139	0.001	0.844	0.0079	0.017	0.442	0.1853	0.036	0.270	0.2707
222	0.257	0.001	-0.1183	0.010	0.555	-0.0539	0.016	0.452	0.0235	0.006	0.658	0.0092	0.004	0.706	0.0608	0.056	0.165	0.2284
223	0.291	0.001	-0.1731	0.181	0.009	-0.1308	0.009	0.567	0.0380	0.010	0.558	0.0397	0.120	0.525	0.1475	0.011	0.542	0.1415
224	0.207	0.005	-0.2028	0.090	0.076	-0.0832	0.001	0.895	0.0042	0.001	0.878	-0.0048	0.014	0.489	0.1524	0.018	0.441	0.1718
225	0.015	0.467	-0.0416	0.076	0.098	-0.0715	0.006	0.654	0.0140	0.002	0.805	0.0071	0.021	0.397	0.1485	0.056	0.160	0.2460
226	0.180	0.050	-0.1220	0.124	0.041	-0.1134	0.058	0.171	0.1014	0.076	0.108	0.1144	0.015	0.490	0.1951	0.006	0.649	0.1280
227	0.053	0.177	-0.1085	0.185	0.009	-0.1294	0.003	0.746	0.0156	0.003	0.753	0.0145	0.010	0.564	0.1415	0.010	0.567	0.1433
228	0.248	0.002	-0.1134	0.066	0.130	-0.0924	0.000	0.921	0.0026	0.000	0.961	-0.0010	0.013	0.509	0.1181	0.013	0.504	0.1203
229	0.159	0.016	-0.1488	0.123	0.039	-0.1265	0.050	0.182	0.0853	0.017	0.452	0.0507	0.017	0.442	0.1819	0.011	0.540	0.1533
230	0.127	0.036	-0.1067	0.205	0.006	-0.1180	0.002	0.798	0.0123	0.000	0.922	-0.0047	0.001	0.881	0.0340	0.010		0.0417
231	0.120	0.040	-0.0854	0.055	0.182	-0.0621	0.011	0.535	-0.0144	0.024	0.372	-0.0203	0.007	0.638	0.0798	0.013	0.512	0.1145
232	0.122	0.039	-0.1533	0.222	0.004	-0.1873	0.026	0.352	-0.0926	0.002	0.791	0.0171	0.012	0.531	0.1551	0.004	0.721	0.0897
233	0.150	0.020	-0.1162	0.171	0.012	-0.1208	0.001	0.870	0.0067	0.003	0.760	-0.0128	0.008	0.598	0.1096	0.009	0.582	0.1153
234	0.004	0.699	-0.0218	0.020	0.408	-0.0452	0.004	0.721	0.0098	0.046	0.209	0.0162	0.003	0.767	0.0498	0.057	0.160	0.2357
235	0.046	0.211	-0.0658	0.023	0.376	-0.0518	0.000	0.964	0.0026	0.001	0.856	-0.0111	0.005	0.660	0.0960	0.005	0.671	0.1055
236	0.117	0.041	-0.1034	0.059	0.155	-0.0895	0.007	0.639	0.0219	0.000	0.944	0.0030	0.007	0.634	0.1049	0.009	0.581	0.1259
237	0.186	0.009	-0.1184	0.060	0.156	-0.0595	0.026	0.350	0.0345	0.001	0.879	0.0040	0.007	0.629	0.0903	0.007	0.629	0.0900
238	0.024	0.375	-0.0601	0.024	0.370	-0.0506	0.006	0.646	0.0296	0.004	0.732	0.0214	0.001	0.780	0.0375	0.001	0.877	0.0380
239	0.027	0.340	-0.0647	0.074	0.108	-0.0758	0.016	0.469	0.0220	0.000	0.984	-0.0004	0.000	0.603	0.0974	0.017	0.436	0.1397
240	0.089	0.078	-0.0720	0.030	0.310	-0.0420	0.027	0.342	0.0280	0.024	0.362	0.0150	0.090	0.581	0.0980	0.022	0.384	0.1476
241	0.043	0.231	-0.9505	0.041	0.244	-0.0862	0.026	0.345	0.0692	0.006	0.652	0.0307	0.007	0.625	0.1201	0.006	0.657	0.1114
242	0.086	0.082	-0.0953	0.039	0.246	-0.0598	0.020	0.414	0.0512	0.014	0.495	0.0384	0.001	0.887	0.0386	0.010	0.555	0.1428
243	0.120	0.039	-0.0815	0.027	0.338	-0.0375	0.042	0.225	0.0359	0.002	0.812	0.0048	0.016	0.462	0.1222	0.056	0.157	0.2357
244	0.044	0.235	-0.0740	0.069	0.132	-0.1020	0.043	0.238	0.1010	0.044	0.234	0.1105	0.035	0.293	0.2536	0.035	0.288	0.2555
245	0.004	0.728	-0.0168	0.008	0.614	-0.0280	0.008	0.611	0.0311	0.000	0.918	0.0062	0.007	0.636	0.1109	0.006	0.653	0.1035
246	0.002	0.824	-0.0154	0.011	0.552	-0.0216	0.007	0.627	0.0175	0.002	0.784	-0.0073	0.009	0.593	0.1005	0.011	0.546	0.1115
247	0.004	0.729	-0.0240	0.042	0.236	-0.0681	0.032	0.304	0.0790	0.036	0.278	0.0793	0.017	0.462	0.1714	0.017	0.452	0.1747
248	0.002	0.810	0.0105	0.012	0.538	-0.0258	0.001	0.846	0.0080	0.006	0.667	-0.0159	0.004	0.060	0.0708	0.005	0.701	0.0708
249	0.167	0.016	-0.0917	0.045	0.228	-0.0540	0.002	0.807	0.0087	0.001	0.855	-0.0059	0.004	0.728	0.0607	0.009	0.584	0.0949
250	0.056	0.169	-0.0732	0.100	0.064	-0.0868	0.020	0.421	0.0632	0.024	0.384	0.0701	0.010	0.563	0.1163	0.009	0.585	0.1098

	Dissolved Oxygen						Salinity						Temperature					
	Surface			*Bottom*			*Surface*			*Bottom*			*Surface*			*Bottom*		
Station	R^2	p-value	slope	R^2	p-value	slope	R^2	p-value	slope	R^2	p-value	slope	R^2	p-value	slope	R^2	p-value	slope
251	0.017	0.453	-0.0363	0.001	0.883	-0.0079	0.026	0.352	0.0553	0.017	0.450	0.0312	0.007	0.637	0.0905	0.007	0.639	0.0891
252	0.084	0.096	-0.0762	0.001	0.880	-0.0058	0.138	0.028	0.0679	0.049	0.203	0.0316	0.022	0.400	0.1335	0.012	0.537	0.1076
253	0.110	0.060	-0.1978	0.065	0.158	-0.1442	0.019	0.441	0.0669	0.000	0.937	-0.0064	0.003	0.773	0.0578	0.000	0.926	-0.0191
254	0.287	0.002	-0.1969	0.277	0.002	-0.1896	0.018	0.450	0.0589	0.011	0.552	0.0464	0.004	0.714	0.0691	0.003	0.740	0.0623
255	0.177	0.012	-0.1230	0.013	0.513	-0.0257	0.052	0.187	0.0667	0.049	0.203	0.0608	0.007	0.627	0.0910	0.008	0.618	0.0948
256	0.042	0.239	-0.0566	0.049	0.200	-0.0629	0.098	0.066	0.0542	0.038	0.262	0.0311	0.014	0.505	0.1079	0.025	0.367	0.1646
257	0.212	0.007	-0.2529	0.187	0.014	-0.1936	0.002	0.788	0.0189	0.014	0.516	0.0463	0.007	0.636	-0.0916	0.004	0.722	-0.0684
258	0.004	0.731	0.0148	0.028	0.340	-0.0357	0.001	0.836	0.0072	0.010	0.577	0.0183	0.001	0.876	-0.0262	0.000	0.899	-0.0216
259	0.013	0.513	-0.0341	0.006	0.661	-0.0164	0.000	0.970	-0.0010	0.000	0.968	0.0011	0.000	0.996	0.0009	0.000	0.985	-0.0030
260	0.249	0.003	-0.1646	0.250	0.003	-0.1724	0.016	0.476	0.0477	0.017	0.465	0.0483	0.015	0.494	0.1319	0.017	0.464	0.1414
261	0.032	0.307	-0.0757	0.165	0.015	-0.1343	0.001	0.855	0.0098	0.004	0.730	0.0185	0.007	0.643	-0.0927	0.003	0.752	-0.0614
262	0.039	0.251	-0.0428	0.023	0.381	-0.0435	0.004	0.711	0.0186	0.001	0.861	0.0070	0.005	0.695	-0.0700	0.000	0.913	-0.0202
263	0.033	0.293	-0.0445	0.011	0.545	-0.0276	0.009	0.594	0.0134	0.000	0.962	-0.0012	0.000	0.799	-0.0418	0.000	0.972	0.0059
264	0.172	0.013	-0.0868	0.071	0.122	-0.0626	0.000	0.971	-0.0011	0.000	0.997	-0.0001	0.000	0.925	0.0158	0.001	0.860	0.0295
265	0.004	0.723	-0.0228	0.000	0.937	-0.0050	0.001	0.861	0.0232	0.000	0.920	0.0135	0.004	0.725	-0.0692	0.003	0.769	-0.0582
266	0.229	0.006	-0.1657	0.084	0.114	-0.1088	0.021	0.423	-0.0574	0.005	0.701	-0.0305	0.006	0.681	-0.0905	0.002	0.832	-0.0517
267	0.094	0.068	-0.0691	0.024	0.369	-0.0532	0.000	0.970	-0.0010	0.002	0.775	0.0075	0.005	0.680	-0.0689	0.001	0.880	-0.0256
268	0.004	0.721	-0.0185	0.145	0.029	-0.1221	0.002	0.780	0.0165	0.001	0.864	0.0106	0.001	0.853	-0.0391	0.002	0.817	-0.0500
269	0.095	0.072	-0.0726	0.047	0.213	-0.0579	0.000	0.966	0.0020	0.001	0.837	0.0099	0.002	0.775	-0.0552	0.000	0.934	-0.0161
270	0.073	0.111	-0.0752	0.062	0.144	-0.0525	0.011	0.542	0.0193	0.007	0.618	0.0139	0.003	0.771	-0.0500	0.000	0.949	-0.0112
271	0.003	0.748	-0.0214	0.048	0.212	-0.0635	0.000	0.952	0.0030	0.000	0.964	0.0022	0.001	0.864	-0.0324	0.000	0.960	-0.0093
272	0.014	0.485	-0.0414	0.113	0.045	-0.0835	0.000	0.935	-0.0028	0.000	0.975	0.0011	0.001	0.883	0.0258	0.000	0.985	0.0032
273	0.225	0.004	-0.1084	0.082	0.096	-0.0753	0.000	0.958	-0.0015	0.003	0.753	0.0085	0.000	0.964	0.0074	0.018	0.429	0.1285
274	0.182	0.011	-0.1248	0.142	0.031	-0.1193	0.025	0.367	-0.0733	0.022	0.406	-0.0552	0.001	0.866	-0.0323	0.005	0.677	-0.0800
275	0.071	0.122	-0.0552	0.040	0.243	-0.0564	0.000	0.937	0.0032	0.026	0.345	-0.0616	0.001	0.847	-0.0363	0.002	0.782	0.0510
276	0.020	0.423	-0.0503	0.037	0.270	-0.0479	0.003	0.739	0.0092	0.000	0.932	-0.0023	0.000	0.963	0.0074	0.000	0.933	0.0138
277	0.019	0.434	-0.0335	0.000	0.914	-0.0055	0.006	0.662	-0.0196	0.009	0.587	-0.0228	0.004	0.714	0.0695	0.008	0.614	0.0976
278	0.173	0.150	-0.1383	0.002	0.779	-0.0138	0.000	0.978	-0.0012	0.003	0.751	-0.0117	0.000	0.943	0.0140	0.004	0.735	0.0652
279	0.035	0.283	-0.4120	0.002	0.785	-0.0100	0.000	0.998	-0.0001	0.012	0.534	-0.0082	0.010	0.575	0.0930	0.034	0.287	0.1827
280	0.123	0.039	-0.1221	0.064	0.143	-0.0594	0.003	0.758	0.0214	0.002	0.788	-0.0043	0.000	0.925	-0.0170	0.014	0.501	0.1233
281	0.026	0.372	0.0423	0.011	0.569	0.0238	0.038	0.277	-0.0556	0.004	0.723	-0.0126	0.006	0.677	-0.1015	0.005	0.683	-0.1051
282	0.103	0.057	-0.1173	0.061	0.148	-0.0937	0.058	0.157	0.2470	0.060	0.152	0.2492	0.000	0.963	0.0087	0.000	0.949	0.0121
283	0.194	0.007	-0.2239	0.099	0.062	-0.1336	0.023	0.377	0.1236	0.023	0.382	0.1228	0.000	0.982	0.0042	0.000	0.993	0.0016
284	0.060	0.146	-0.1069	0.064	0.129	-0.1131	0.031	0.295	0.1491	0.037	0.252	0.1619	0.000	0.996	-0.0009	0.000	0.996	0.0009
285	0.183	0.009	-0.2027	0.041	0.234	-0.0654	0.056	0.163	0.1813	0.053	0.177	0.1745	0.000	0.980	-0.0046	0.000	0.992	-0.0020
286	0.020	0.405	-0.0496	0.014	0.498	-0.0360	0.033	0.286	0.0946	0.031	0.305	0.0911	0.000	0.965	0.0083	0.000	0.987	0.0030
287	0.132	0.029	-0.1895	0.063	0.139	-0.1139	0.028	0.327	0.1417	0.027	0.341	0.1400	0.001	0.891	-0.0250	0.001	0.893	-0.0245
288	0.220	0.005	-0.2105	0.074	0.103	-0.1038	0.017	0.440	0.0985	0.016	0.462	0.0937	0.000	0.997	0.0008	0.000	0.999	0.0001
289	0.049	0.190	-0.0604	0.002	0.788	-0.0134	0.005	0.664	0.0579	0.018	0.434	0.1010	0.030	0.744	0.0615	0.006	0.653	0.0863
290	0.049	0.202	-0.0655	0.088	0.084	-0.0947	0.013	0.514	0.0661	0.013	0.513	0.0662	0.001	0.882	0.0291	0.001	0.859	0.0349
291	0.162	0.014	-0.1600	0.090	0.071	-0.1178	0.015	0.467	0.0921	0.016	0.460	0.0935	0.000	0.995	0.0011	0.000	0.977	0.0056
292	0.025	0.355	-0.0548	0.000	0.986	0.0009	0.018	0.429	0.0881	0.017	0.448	0.0847	0.004	0.731	0.0651	0.004	0.704	0.0720
293	0.007	0.647	-0.0238	0.005	0.694	-0.0214	0.040	0.257	0.1065	0.049	0.217	0.1192	0.000	0.758	-0.0562	0.007	0.639	0.0915
294	0.013	0.550	-0.0433	0.006	0.657	-0.0309	0.044	0.212	0.1401	0.042	0.226	0.1363	0.004	0.699	0.0742	0.005	0.665	0.0842
295	0.145	0.240	-0.1301	0.110	0.052	-0.1191	0.020	0.420	0.0614	0.021	0.403	0.0647	0.006	0.661	0.0860	0.006	0.652	0.0881
296	0.181	0.011	-0.2321	0.148	0.022	-0.1593	0.001	0.831	-0.0189	0.002	0.796	-0.0230	0.000	0.996	0.0011	0.000	0.998	-0.0005
297	0.078	0.098	-0.1211	0.065	0.134	-0.1265	0.013	0.515	0.0711	0.013	0.511	0.0714	0.000	0.999	-0.0001	0.000	0.995	0.0013
298	0.002	0.797	-0.0124	0.012	0.512	-0.3650	0.063	0.133	0.0924	0.068	0.120	0.0960	0.000	0.964	-0.0101	0.000	0.972	-0.0079
299	0.000	0.928	-0.0080	0.022	0.385	-0.0959	0.022	0.393	0.0778	0.003	0.778	0.0237	0.024	0.320	0.1942	0.021	0.415	0.1850
300	0.017	0.436	-0.0520	0.022	0.385	-0.0594	0.027	0.331	0.0717	0.026	0.339	0.0693	0.003	0.752	0.0655	0.003	0.747	0.0673
301	0.002	0.817	-0.0172	0.020	0.414	-0.0593	0.051	0.180	0.0959	0.070	0.119	0.1112	0.000	0.948	-0.0143	0.000	0.940	-0.0169

	Dissolved Oxygen						Salinity						Temperature					
	Surface			*Bottom*			*Surface*			*Bottom*			*Surface*			*Bottom*		
Station	R^2	p-value	slope	R^2	p-value	slope	R^2	p-value	slope	R^2	p-value	slope	R^2	p-value	slope	R^2	p-value	slope
302	0.018	0.423	-0.0581	0.042	0.222	-0.0943	0.040	0.237	0.0704	0.042	0.224	0.0714	0.010	0.826	-0.0513	0.003	0.728	-0.0827
303	0.100	0.056	-0.1601	0.126	0.031	-0.1813	0.056	0.157	0.1210	0.050	0.183	0.1052	0.013	0.508	-0.1504	0.011	0.541	-0.1363
304	0.021	0.391	-0.0608	0.033	0.282	-0.0766	0.071	0.111	0.1353	0.056	0.157	0.0979	0.003	0.733	-0.0796	0.003	0.735	-0.0827
305	0.091	0.070	-0.0925	0.098	0.060	-0.1009	0.025	0.351	0.0555	0.028	0.324	0.0583	0.002	0.795	-0.0599	0.002	0.800	-0.0584
306	0.014	0.492	0.0376	0.000	0.986	0.0010	0.077	0.096	0.1356	0.050	0.185	0.0815	0.010	0.552	-0.1423	0.007	0.625	-0.1093
307	0.065	0.128	-0.0910	0.075	0.101	-0.1021	0.051	0.181	0.1018	0.033	0.281	0.0667	0.008	0.610	-0.1210	0.005	0.671	-0.0968
308	0.007	0.690	-0.0311	0.020	0.404	-0.0509	0.022	0.376	0.0781	0.021	0.392	0.0752	0.003	0.600	-0.0673	0.002	0.796	-0.0568
309	0.003	0.738	-0.0228	0.002	0.775	-0.0201	0.034	0.275	0.0595	0.034	0.273	0.0626	0.001	0.824	-0.0497	0.002	0.805	-0.0555
310	0.000	0.918	-0.0072	0.003	0.758	-0.0215	0.013	0.509	0.0471	0.002	0.818	0.0164	0.013	0.501	-0.1382	0.013	0.499	-0.1388
311	0.006	0.647	-0.0291	0.014	0.480	-0.0475	0.021	0.388	0.0809	0.025	0.354	0.0872	0.010	0.433	-0.1678	0.018	0.430	-0.1682
312	0.008	0.592	-0.0361	0.009	0.581	-0.0397	0.049	0.186	0.0747	0.057	0.160	0.0831	0.006	0.658	-0.0974	0.002	0.780	-0.0624
313	0.060	0.144	-0.1288	0.063	0.133	-0.1278	0.039	0.241	0.0689	0.040	0.233	0.0699	0.200	0.407	-0.1855	0.019	0.418	-0.1779
314	0.100	0.056	-0.1376	0.100	0.056	-0.1564	0.071	0.111	0.1335	0.060	0.143	0.1005	0.010	0.220	-0.1454	0.005	0.682	-0.0948
315	0.043	0.220	-0.0987	0.048	0.194	-0.1088	0.082	0.086	0.1132	0.086	0.079	0.1152	0.003	0.757	-0.0687	0.004	0.707	-0.0834
316	0.021	0.388	0.0571	0.018	0.435	0.0584	0.032	0.287	0.0572	0.037	0.254	0.0617	0.001	0.851	-0.0388	0.000	0.905	-0.0249
317	0.000	0.910	0.0055	0.001	0.880	-0.0071	0.028	0.319	0.0632	0.036	0.262	0.0726	0.003	0.754	-0.0668	0.003	0.747	-0.0704
318	0.010	0.566	-0.0291	0.000	0.980	-0.0013	0.007	0.626	0.0234	0.001	0.828	0.0101	0.050	0.600	-0.1122	0.002	0.775	-0.0757
319	0.013	0.515	-0.0288	0.003	0.756	0.0136	0.001	0.850	0.0088	0.005	0.672	0.0181	0.006	0.667	-0.1115	0.004	0.728	-0.0907
320	0.000	0.936	0.0052	0.000	0.941	-0.0034	0.001	0.845	-0.0221	0.001	0.826	-0.0040	0.005	0.699	-0.0773	0.005	0.678	0.0854
321	0.079	0.101	-0.1010	0.012	0.547	-0.0271	0.002	0.804	-0.0092	0.002	0.804	0.0065	0.001	0.829	-0.0425	0.004	0.703	-0.0828
322	0.010	0.892	-0.0073	0.005	0.671	-0.0159	0.040	0.235	-0.0478	0.009	0.572	0.0133	0.004	0.707	-0.0677	0.002	0.769	-0.0553
323	0.000	0.962	0.0018	0.005	0.695	0.0140	0.002	0.782	0.0105	0.002	0.810	0.0082	0.002	0.817	-0.0549	0.000	0.919	-0.0236
324	0.086	0.078	-0.0896	0.006	0.660	-0.0175	0.005	0.674	0.0169	0.001	0.828	0.0087	0.000	0.917	-0.0255	0.000	0.944	-0.0172
325	0.003	0.771	0.0159	0.008	0.606	0.0262	0.009	0.598	-0.0275	0.008	0.601	-0.0259	0.015	0.477	-0.1841	0.014	0.489	-0.1795
326	0.036	0.273	-0.0739	0.000	0.945	-0.0025	0.006	0.659	0.0157	0.001	0.857	0.0055	0.000	0.989	-0.0034	0.000	0.934	0.0184
327	0.022	0.385	-0.0355	0.000	0.912	-0.0051	0.004	0.726	0.0135	0.004	0.731	0.0132	0.003	0.739	-0.0781	0.001	0.836	-0.0491
328	0.003	0.742	-0.0202	0.004	0.708	-0.0120	0.004	0.717	-0.0116	0.024	0.355	-0.0222	0.003	0.758	-0.0523	0.003	0.744	-0.0559
329	0.018	0.452	-0.0804	0.001	0.890	0.0115	0.012	0.530	0.0233	0.003	0.758	0.0070	0.001	0.874	0.0354	0.002	0.816	0.0463
330	0.000	0.940	-0.0033	0.000	0.939	0.0028	0.005	0.700	0.0136	0.004	0.727	0.0114	0.000	0.915	-0.0241	0.000	0.933	-0.0187
331	0.006	0.644	0.0171	0.000	0.985	0.0007	0.001	0.823	-0.0075	0.005	0.682	-0.0133	0.007	0.621	-0.0968	0.007	0.631	-0.0968
332	0.062	0.150	-0.0767	0.001	0.837	0.0080	0.000	1.000	0.0000	0.000	0.932	-0.0030	0.006	0.652	-0.0982	0.006	0.649	-0.0989
333	0.001	0.843	-0.0077	0.000	0.945	0.0023	0.004	0.718	0.0105	0.004	0.705	0.0095	0.001	0.858	-0.0351	0.000	0.921	0.0197
334	0.010	0.569	-0.0232	0.007	0.633	-0.0175	0.001	0.855	0.0058	0.000	0.919	0.0030	0.003	0.759	-0.0571	0.010	0.564	-0.1086
335	0.002	0.783	0.0097	0.022	0.379	-0.0277	0.000	0.973	-0.0009	0.042	0.224	-0.0272	0.005	0.677	-0.0675	0.001	0.838	-0.0355
336	0.075	0.101	-0.1034	0.000	0.972	0.0013	0.014	0.483	0.0227	0.000	0.942	0.0013	0.003	0.630	-0.0587	0.003	0.748	0.0601
337	0.002	0.820	0.0213	0.000	0.953	-0.0021	0.034	0.275	0.0286	0.015	0.469	0.0152	0.000	0.906	-0.0228	0.000	0.993	0.0016
338	0.057	0.175	-0.0490	0.007	0.648	-0.0173	0.003	0.760	0.0121	0.015	0.498	0.0200	0.001	0.829	-0.0454	0.007	0.632	-0.1054
339	0.001	0.833	0.0101	0.007	0.618	-0.0169	0.000	0.951	-0.0016	0.001	0.821	-0.0044	0.008	0.595	-0.0913	0.005	0.690	-0.0601
340	0.017	0.444	-0.0454	0.007	0.637	-0.0146	0.000	1.000	0.0000	0.007	0.635	-0.0080	0.010	0.549	-0.1065	0.001	0.832	-0.0361
341	0.061	0.158	-0.0713	0.006	0.667	-0.0245	0.017	0.453	0.0231	0.020	0.427	0.0256	0.000	0.960	0.0098	0.004	0.713	-0.0770
342	0.063	0.140	-0.0967	0.003	0.765	-0.0133	0.011	0.547	0.0216	0.018	0.449	0.0136	0.000	0.995	0.0013	0.016	0.468	0.1390
343	0.011	0.555	-0.0334	0.051	0.208	-0.0467	0.020	0.407	0.0282	0.011	0.551	0.0116	0.001	0.856	-0.0350	0.011	0.554	0.1006
344	0.123	0.033	-0.0929	0.022	0.393	-0.0247	0.001	0.848	-0.0059	0.006	0.636	-0.0070	0.008	0.591	-0.0946	0.000	0.933	0.0145
345	0.042	0.232	-0.0523	0.000	0.900	-0.0049	0.056	0.166	-0.1172	0.011	0.537	-0.0078	0.001	0.836	-0.0310	0.014	0.496	0.1091
346	0.056	0.170	-0.0550	0.005	0.688	-0.0161	0.015	0.487	0.0232	0.006	0.670	0.0081	0.011	0.542	-0.1165	0.006	0.659	0.0833
347	0.162	0.016	-0.0935	0.029	0.338	-0.0362	0.082	0.096	0.0896	0.007	0.641	0.0089	0.012	0.523	-0.1228	0.003	0.765	0.0575
348	0.055	0.175	-0.0606	0.025	0.379	-0.0345	0.035	0.283	0.0307	0.001	0.830	0.0058	0.002	0.803	-0.0488	0.004	0.723	-0.0711
349	0.085	0.085	-0.0704	0.033	0.301	-0.0422	0.031	0.303	0.0280	0.011	0.550	0.0163	0.001	0.830	-0.0425	0.003	0.770	-0.0598
350	0.009	0.592	0.0287	0.005	0.691	0.0126	0.004	0.707	0.0117	0.001	0.845	0.0032	0.008	0.596	-0.0876	0.005	0.682	-0.0512
400	0.078	0.510	-0.0820	0.034	0.345	-0.0718	0.054	0.233	0.0443	0.086	0.131	0.0501	0.060	0.210	0.3526	0.072	0.167	0.3815
401	0.056	0.223	-0.0885	0.101	0.099	-0.1240	0.042	0.294	0.0499	0.021	0.466	0.0344	0.050	0.255	0.3341	0.048	0.265	0.3272
402	0.000	0.948	-0.0035	0.000	0.962	0.0044	0.058	0.225	0.0523	0.035	0.353	0.0406	0.017	0.518	0.1564	0.013	0.575	0.1371
403	0.015	0.545	-0.0427	0.006	0.712	-0.0241	0.021	0.474	0.0331	0.017	0.511	0.0301	0.019	0.494	0.1736	0.011	0.610	0.1300